ISSN 1407-6160

TRANSPORT AND TELECOMMUNICATION

Volume 11. No 4

2010

Transporta un sakaru institūts
(Transport and Telecommunication Institute)

Transport and Telecommunication

Volume 11, No 4 - 2010

ISSN 1407-6160
ISSN 1407-6179
(On-line: www.tsi.lv)

Riga – 2010

05/J80

All articles are reviewed.
Articles can be presented in the journal in English.

EDITORIAL CORRESPONDENCE

Transporta un sakaru institūts (Transport and Telecommunication Institute)
Lomonosova iela 1, LV-1019, Riga, Latvia. Phone: (+371)67100594. Fax: (+371)67100535.
E-mail: kiv@tsi.lv, http:// www.tsi.lv

TRANSPORT and TELECOMMUNICATION, 2010, Vol. 11, No 4
ISSN 1407-6160
The journal of Transport and Telecommunication Institute (Riga, Latvia).
The journal is being published since 2000.

The papers published in Journal "Transport and Telecommunication" are included in **SCOPUS** (since 2008, Vol. 9, No 1), **Elsevier Database**
www.info.scopus.com
www.elsevier.com

CONTENTS

Transport and Telecommunication, 2010, Volume 11, No 4, 4–13
Transport and Telecommunication Institute, Lomonosova 1, Riga, LV-1019, Latvia

NEW METHODS OF CALCULATING THE GENOME OF STRUCTURE AND THE FAILURE CRITICALITY OF THE COMPLEX OBJECTS' ELEMENTS

E. A. Kopytov [1], A. N. Pavlov [2], V. A. Zelentsov [3]

[1]Transport and Telecommunication Institute
Lomonosova 1, Riga, LV-1019, Latvia
Ph.: +371 67100669. E-mail: kopitov@tsi.lv

[2]St. Petersburg Institute for Informatics and Automation of Russian Academy of Science
14th Line 39, St. Petersburg, 199178, Russia
Ph.: +7(812)3280103. E-mail: pavlov62@list.ru

[3]St. Petersburg State University of Aerospace Instrumentation
Bolshaya Morskaya, 67, St. Petersburg, 190000, Russia
Ph.: +7(812)3280103. E-mail: zvarambler@rambler.ru

There are considered two new methods of analysing the contribution of separate elements into the efficiency of a complex object. The first one is based on the introduction of a new notion – "the genome of structure" applied for calculating the structural significance of the monotonous and non-monotonous systems. The second method allows estimation of a more general indicator – failure criticality of the element. This method is based on a combined method of a fuzzy logic conclusion and on the methods of the experiment planning theory. The failure criticality of the complex objects' elements is expressed by a vector property for which evaluating there is used a number of partial indicators, which may have both quantitative and qualitative character and for their measurement there may be used different types of scales. The resulting indicator of the element failure criticality is presented in the form of a polynomial which accounts both the influence of the separately taken indicators and the influence of the indicators' aggregations (of 2, 3, etc.). Calculation of the polynomial coefficients is made on the basis of processing the expert information and the corresponding linguistic variables quantitatively measured by fuzzy numbers.

Keywords: genome of structure, failure criticality, complex object, multi-criteria analysis, theory of experiment planning, linguistic variable

1. Introduction

Due to the increase of the structural and functional complexity of the analysed objects and systems in the theory of reliability in recent time, ever growing popularity is given to the methods, which account not only the numeric values of the indicators of the constituent elements' reliability but also more general evaluations of the elements' failures influence on the objects' functioning. There are two the most recognised indicators: the structural significance of the element and the failure criticality of the elements [1]. Both these elements cannot be fully determined by the element's properties only and must be determined in the frame of the complex object (CO) containing the given object. Ranging the elements according to these indicators makes possible to concentrate efforts on perfecting of the assemblies which play a key role in supporting the complex objects functioning.

2. The Genome of Structure and Its Application for Determining the Structural Significance of the Element

To research the reliability of the CO connected with its structural formation, we use the following structural functions: the function of reliability, safety, vitality, minimum failures' sections obtained by orthogonalising the monotonous and non-monotonous functions of the algebra of logic (FAL), replacing the logical arguments in FAL for the probabilities of their verity and the corresponding logic operations for the arithmetic ones.

In papers [2-4] there is introduced the notion of *the genome of structure*, presenting by itself the vector $\chi = (\chi_0, \chi_1, \chi_2, \ldots, \chi_n)$, which components are the coefficients of the polynomial of the function of the minimum sections of failure of the structure containing homogenous elements. And if $\chi_0 = 0$ and the sum component of the vector equal 1, the polynomial of failure $T(Q)=\chi_0+\chi_1 Q+\chi_2 Q^2+\ldots+\chi_n Q^n$ describes the structure of the monotonous CO. If $\chi_0 = 0$ and the sum component of the vector equals 0, the CO is a non-monotonous one and the polynomial of failure does not retain «1» (i.e. $T(Q) = 0$). If $\chi_0 = 1$, the CO is non-monotonous and the polynomial of failure does not retain «0» (i.e. $T(Q) = 1$). Besides, the genome of structure of the monotonous systems holds different topological properties of the structure: the degree of

the junior polynomial member equals the smallest power among the minimum sections of the structure failures; the coefficient with the junior polynomial member is always positive and equals the number of the minimum sections of the failures of the smallest power; the degree of the polynomial senior member equals the number of connections within the structure; the number of alternations of the signs «+» and «-» in the polynomial is bigger or equals the number of the structure internal knots.

With the help of the genome of structure we can calculate the integral evaluations of the significance and contribution of separate elements into the structural reliability of the CO employing the probability and fuzzy-possibility approaches for both the monotonous and non-monotonous structures.

While employing the probability approach, for the case of a homogenous structure (with the same probability of the CO elements' failures) calculation is performed under the formula $F_{\text{hom}ogen}(\chi) = (\chi_0, \chi_1, \chi_2, ..., \chi_n) \cdot (1, \frac{1}{2}, \frac{1}{3}, ..., \frac{1}{n+1})^T$, for the case of a non-homogenous structure (with different probabilities of the systems elements' failures) calculation is performed under the formula $F_{non-\text{hom}ogen}(\chi) = (\chi_0, \chi_1, \chi_2, ..., \chi_n) \cdot (1, \frac{1}{2}, \frac{1}{2^2}, ..., \frac{1}{2^n})^T$.

In case of a fuzzy-possibility description of the system elements' failures [2-4], to calculate the indicator of possibility of the structure failure we must integrate the polynomial of the failure possibility $T(\mu)=\chi_0+\chi_1\mu+\chi_2\mu^2+...+\chi_n\mu^n$ as much as possible

$$F_{possib}(\chi) = \sup_{\mu\in[0,1]} \min\{T(\mu), g(\mu)\} = \sup_{\alpha\in[0,1]} \min\{\alpha, P(\{\mu \,|\, T(\mu) \geq \alpha\})\}.$$

Before calculating we should define the degree of the possibility and, desirably, its distribution function $g(\mu)$. In case of the monotonous homogenous structures, the function of the possibility degree distribution is $g(\mu) = 1 - \mu$.

For the non-monotonous homogenous structures, when the polynomial of the failure possibility does not retain «0» and «1» ($T(0) = 1$, $T(1) = 0$), the function of the possibility degree distribution is $g(\mu) = \mu$.

If the polynomial of the possibility of the non-monotonous structure failure does not retain «1» ($T(1)=0$), the possibility degree is $P(\{\mu \,|\, T(\mu) \geq \alpha\}) = P(H_\alpha) = \sup_{A\subseteq H_\alpha} |A| = \sup\{\mu^{\max} - \mu^{\min}\}$, where $\mu^{\max} = \sup\{\mu \,|\, T(\mu) \geq \alpha\}$ and $\mu^{\min} = \inf\{\mu \,|\, T(\mu) \geq \alpha\}$.

If the polynomial of the possibility of the non-monotonous structure failure does not retain «0» ($T(0)=1$), the possibility degree is $P(\{\mu \,|\, T(\mu) \geq \alpha\}) = P(H_\alpha) = \sup_{A\subseteq H_\alpha} |A| = \sup\{1 - (\mu^{\max} - \mu^{\min})\}$, where $\mu^{\max} = \sup\{\mu \,|\, T(\mu) \leq \alpha\}$ and $\mu^{\min} = \inf\{\mu \,|\, T(\mu) \leq \alpha\}$.

Graphical interpretation of defining the integral indicator of the failure possibility for the described cases is given in figure 1, 2.

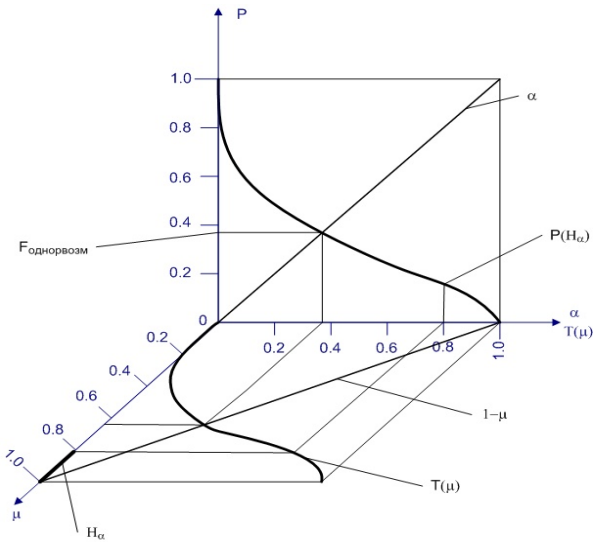

Figure 1. Graphical interpretation of defining the integral indicator of the possibility of failure of the monotonous and non-monotonous ($T(0) = 1$, $T(1) = 0$) homogenous structures

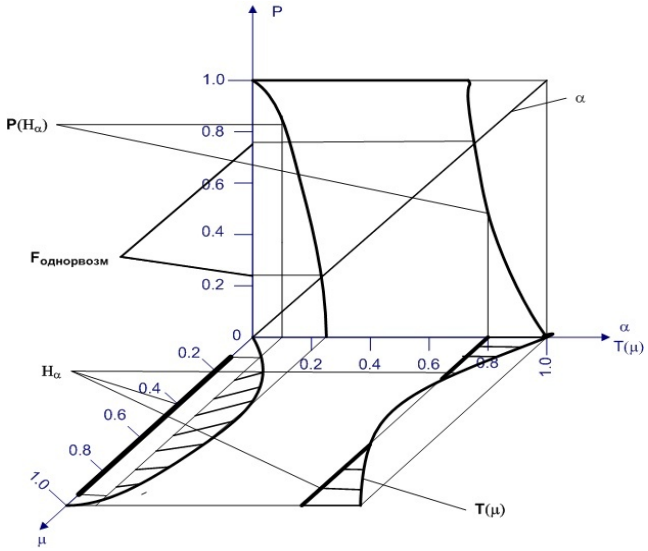

Figure 2. Graphical interpretation of defining the integral indicator of the possibility of failure of the non-monotonous (either $T(1) = 0$, or $T(1) = 0$) homogenous structures

The suggested method may be used for calculating the significance of the positive and negative elements' contributions into the structural failure of the CO. To calculate the degree of significance of the *i*-th element in the structural construction, the following polynomial should be employed:

$$\xi_i(Q_1,Q_2,...,Q_n) = T(Q_1,Q_2,...,Q_n)\big|_{Q_i=1} - T(Q_1,Q_2,...,Q_n)\big|_{Q_i=0},$$

where $T(Q_1,Q_2,...,Q_n)\big|_{Q_i=1}$ is the polynomial of failure in the case of the *i*-th element coming out of order, $T(Q_1,Q_2,...,Q_n)\big|_{Q_i=0}$ is the polynomial of failure in the case of the *i*-th element running smoothly.

The polynomials for calculating the positive and negative elements' contributions have the following form:

$$B_i^+(Q_1,Q_2,...,Q_n) = T(Q_1,Q_2,...,Q_n)\big|_{Q_i=1} - T(Q_1,Q_2,...,Q_n),$$
$$B_i^-(Q_1,Q_2,...,Q_n) = -(T(Q_1,Q_2,...,Q_n) - T(Q_1,Q_2,...,Q_n)\big|_{Q_i=0}).$$

Each of the considered polynomials $\xi_i(Q_1,Q_2,...,Q_n)$, $B_i^+(Q_1,Q_2,...,Q_n)$, $B_i^-(Q_1,Q_2,...,Q_n)$ may be confronted to a corresponding genome χ_ξ^i, χ_+^i, χ_-^i, by which employment we can calculate the elements' significance and contributions into the structural formation according to the above formulae, for example, non-homogenous probability estimations: $\alpha_i = \chi_\xi^i \cdot (1, \frac{1}{2}, \frac{1}{2^2}, ..., \frac{1}{2^n})^T$, $\beta_i^+ = \chi_\xi^i \cdot (1, \frac{1}{2}, \frac{1}{2^2}, ..., \frac{1}{2^n})^T$, $\beta_i^- = \chi_-^i \cdot (1, \frac{1}{2}, \frac{1}{2^2}, ..., \frac{1}{2^n})^T$.

Thus, with the help of the genomes χ_ξ^i, χ_+^i, χ_-^i, we can calculate the elements' significance and contribution into the CO structural formation by using both the possibility and the probability estimations.

The calculated characteristics of the CO elements' significance and contributions into the structural failure (reliability) have independent value and, moreover, they may be considered as one of the indicators of the elements' failure criticality. And, as the above analysis has shown [2-4], the given indicator takes interval values.

3. Determining the Failures Criticality: Problem Definition

The failure criticality of the complex objects' elements is a vector property for which evaluating there is used a number of partial indicators, such as [1]: degree of damage of the failure consequences; probability of failure; resistance of the element to the external unfavourable factors; degree of reserving;

controllability of the element state; length of the failure risk probability period; possibility of the failure localization.

The above indicators may have both quantitative and qualitative character and for their measurement there may be used different types of scales [1]. In the most general case, the failure criticality of the CO elements is estimated by the set of indicators $F = \{f_i,\ i = 1,...,m\}$, each of which presents a linguistic variable. An example of a linguistic scale conformably to one of the partial indicators is given in the second column of Table 1.

Table 1. A linguistic scale conformably to the indicator "Control of the element state"

Indicator	Scale	Terms
Controllability of the element state	1. The element state is not controlled 2. Periodic control is performed 3. Constant control without prediction is performed 4. Periodic control with prediction is performed 5. Constant control with prediction is performed	1. Low 2. Less than average 3. Average 4. Higher than average 5. High

Detecting critical elements on the basis of their ranging according to the degree of the failures' criticality, presents a task of a multi-criteria choice. For resolving such tasks there have been developed different methods [2-6] usually connected with the scaling of the vector criterion and with convolutions of different types. It is using of convolutions that conditions the main disadvantages of the given methods, namely:

- determining of the used in the convolutions weight coefficients of partial elements, is attended by serious difficulties of getting and processing of expert information; as a result, weight coefficients are badly connected with the real role of partial indicators of criticality at the generalized estimate of the object elements' criticality property;
- there is not accounted the non-linear character of the indicators' influence on each other and on the generalized indicator of the failure criticality of the CO element;
- in building the integral indicator there occurs smoothing of the partial indicators values of the elements' failure criticality.

4. Method of Calculating the Failures' Criticality: Problem Solution

The given paper suggests a combined method solving the task of the multi-criteria failure criticality analysis of the CO elements' failure under the condition of substantial uncertainty, based on a combined method of a fuzzy logic conclusion and of the methods of the experiment planning theory [10-14]. The essence of the suggested method lies in the following.

Let us consider a linguistic variable $f_i =$ "controllability of the element state". It may take value from a set of simple and composite terms $T(f_i) = \{$"*Low*", "*Less than average*", "*Average*", "*Higher than average*", "*High*"$\}$ (see Table1). For formal presentation of the linguistic variables' terms we can use fuzzy numbers of the (L-R) type. Then, the values of the indicator "controllability of the element state" can be presented at a certain 100 points scale (see Figure 3).

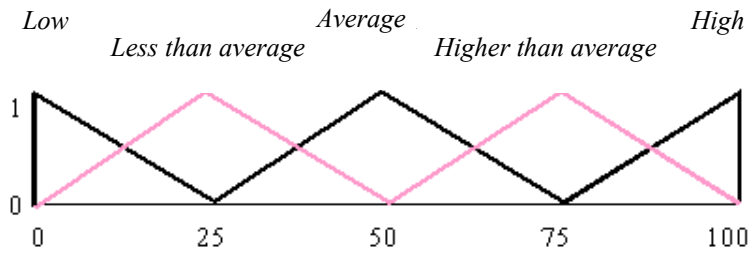

Figure 3. Indicator's presentation at a certain 100 points scale

Similarly, we can describe possible values of other partial indicators.

A generalized view of a decision-maker at the estimated failure criticality of the CO element is formed on the basis of the simultaneous analysis of several indicators with the corresponding values of terms.

Let us introduce for the resulting indicator a linguistic variable "Failure criticality of the CO element" which may take the following values $T(f^{\text{res}}) = \{$"*Low*", "*Less than average*", "*Average*", "*Higher than average*", "*High*"$\}$. The experts' opinions about the influence of the partial indicators of the element failure criticality on the resulting estimate of criticality, in the general form are described by the following production rules: P_j: "If $f_1 = A_{1j}$ and $f_2 = A_{2j}$ and … and $f_m = A_{mj}$, then $f^{\text{res}} = A_j^{\text{res}}$", where $A_{ij} \in T(f_i)$, $A_j^{\text{res}} \in T(f^{\text{res}})$.

The resulting indicator of the element failure criticality can be presented in the form of the polynomial $f^{res} = \lambda_0 + \sum_{i=1}^{m} \lambda_i f_i + \sum_{i=1}^{m} \sum_{j=1}^{m} \lambda_{ij} f_i f_j + \ldots + \lambda_{12\ldots m} f_1 f_2 \ldots f_m$, which takes in account both the influence of the separately taken indicators (through the values of the coefficients λ_i) and the influence of the indicators' aggregations of two (λ_{ij}), three (λ_{ijk}), etc.

To build the resulting indicator, it is necessary to transfer the values of all partial indicators f_i to the scale [-1, +1]. With this purpose, possible boundary values of the linguistic variable f_i are marked as -1 и +1; with this, point "0" corresponds to the middle of the scale (in conformity to the physical meaning of the given indicator). Coding of the current value of the linguistic variable f_i is performed by $\breve{f}_i = (f_i - \overline{f})/h$, where f_i is the value of the indicator at the scale of the linguistic variable; $\overline{f} = (f_i^{\max} + f_i^{\min})/2$ is the middle point of the variable scale; $h = (f_i^{\max} - f_i^{\min})/2$ is the interval of varying; $f_i^{\max}, f_i^{\min}$ are the boundary values of the variable. The result of coding is presented on Figure 4.

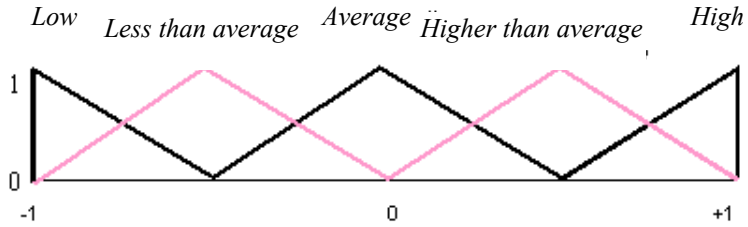

Figure 4. The result of indicator coding

Further, it is necessary to build a matrix of questioning in the expert's professional language at the boundary values of the indicators f_i. In case $m = 3$ the questioning matrix has the form presented in Table 2.

Table 2. The questioning matrix in case $m = 3$

Statement	f_1	f_2	f_3	f^{res}
1	*Low*	*Low*	*Low*	*Bad (B)*
2	*High*	*Low*	*Low*	*Less than average (LA)*
3	*Low*	*High*	*Low*	*Bad (B)*
4	*High*	*High*	*Low*	*Average (A)*
5	*Low*	*Low*	*High*	*Less than average (LA)*
6	*High*	*Low*	*High*	*Higher than average (HA)*
7	*Low*	*High*	*High*	*Average (A)*
8	*High*	*High*	*High*	*Good (G)*

Thus, for example, the second line of the table presents the following expert's judgment: 'If the indicator f_1 has the value "*High*", the indicator f_2 has the value "*Low*", the indicator f_3 has the value "*Low*" then the resulting indicator f^{res} is estimated as "*Less than average*".

Then, we form an orthogonal plan of the expert questioning [10-13], which for the case $m = 3$ is presented in Table 3.

Table 3. The orthogonal plan of the expert questioning for the case $m = 3$

	f_0	f_1	f_2	f_3	f_1f_2	f_1f_3	f_2f_3	$f_1f_2f_3$	f^{res}
1.	1	-1	-1	-1	1	1	1	-1	*B*
2.	1	1	-1	-1	-1	-1	1	1	*LA*
3.	1	-1	1	-1	-1	1	-1	1	*B*
4.	1	1	1	-1	1	-1	-1	-1	*A*
5.	1	-1	-1	1	1	-1	-1	1	*LA*
6.	1	1	-1	1	-1	1	-1	-1	*HA*
7.	1	-1	1	1	-1	-1	1	-1	*A*
8.	1	1	1	1	1	1	1	1	*G*

Let f^{res} may take the values presented on Figure 5. For building an integral indicator with substance coefficients we'll perform an operation of dephasification of the linguistic values of the variable f^{res}, for which we shall put each term in correspondence with its fuzzy number mode ("*Bad*" – 0,2; "*Less than average*" – 0,45; "*Average*" – 0,55; "*Higher than average*" – 0,75; "*Good*" – 1).

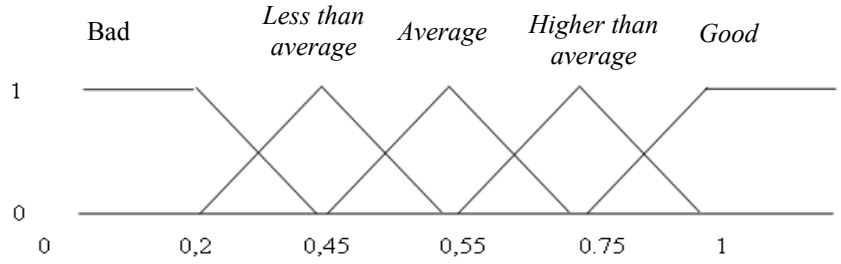

Figure 5. Values of f^{res}

Calculation of the polynomial coefficients is performed according to the rules adopted in the theory of experiment planning [10-13], for which we calculate the average scale products of the corresponding columns of the orthogonal matrix by the vector of the diphase values of the resulting indicator. The received results are given below in Table 4.

Table 4. The results of the average scale products calculation

$f_0 \times f^{\text{res}}$	$f_1 \times f^{\text{res}}$	$f_2 \times f^{\text{res}}$	$f_3 \times f^{\text{res}}$	$f_1 \times f_2 \times f^{\text{res}}$	$f_1 \times f_3 \times f^{\text{re}}$	$f_2 \times f_3 \times f^{\text{res}}$	$f_1 \times f_2 \times f_3 \times f^{\text{re}}$	*Polynomial values*
0,2	-0,2	-0,2	-0,2	0,2	0,2	0,2	-0,2	0,20
0,45	0,45	-0,45	-0,45	-0,45	-0,45	0,45	0,45	0,45
0,2	-0,2	0,2	-0,2	-0,2	0,2	-0,2	0,2	0,20
0,55	0,55	0,55	-0,55	0,55	-0,55	-0,55	-0,55	0,55
0,4	-0,4	-0,4	0,4	0,4	-0,4	-0,4	0,4	0,40
0,75	0,75	-0,75	0,75	-0,75	0,75	-0,75	-0,75	0,75
0,55	-0,55	0,55	0,55	-0,55	-0,55	0,55	-0,55	0,55
1	1	1	1	1	1	1	1	1,00
Polynomial coefficients	λ_0	λ_1	λ_2	λ_3	λ_{12}	λ_{13}	λ_{23}	λ_{123}
Polynomial values	0,5125	0,175	0,0625	0,1625	0,025	0,025	0,0375	0

Thus, the convolution of the indicators in our case has the following form:

$$f^{\text{res}} = 0,5125 + 0,175 f_1 + 0,0625 f_2 + 0,1625 f_3 + 0,025 f_1 f_2 + 0,025 f_1 f_3 + 0,0375 f_2 f_3 .$$

If we do not perform the dephasification of the resulting indicator values, the suggested method allows building a functional dependence of the failure criticality indicator on f_i with fuzzy coefficients $\lambda_0, \lambda_1, \lambda_2, ..., \lambda_{12...m}$. Though, in the given case it is reasonable to use arithmetic operations on the fuzzy trapeziform numbers introduced in the paper [13].

5. Example of Calculating the Failure Criticality

To examine the suggested approach, let us consider an example made in paper [1] and compare the results of ranging the CO elements according to the degree of criticality by the suggested method with the method of marking out Pareto layers presented in paper [1].

As a vector of criticality, we'll take a two-component vector $\vec{f} = (f_1, f_2)$. We need to range 10 elements $X = \{x_i, i = 1,...,10\}$, having the following criticality estimates: $\vec{f}(x_1) = (0.1, 0.1)$, $\vec{f}(x_2) = (0.6, 0.1)$, $\vec{f}(x_3) = (0.8, 0.1)$, $\vec{f}(x_4) = (1, 0.1)$, $\vec{f}(x_5) = (0.1, 0.4)$, $\vec{f}(x_6) = (0.4, 0.4)$, $\vec{f}(x_7) = (0.6, 0.4)$, $\vec{f}(x_8) = (0.1, 0.6)$, $\vec{f}(x_9) = (0.8, 0.6)$, $\vec{f}(x_{10}) = (0.1, 0.8)$. The results of marking out Pareto layers with the use of the classic relation of domination by Pareto on the set $X = \{x_i, i = 1,...,10\}$ are presented on Figure 6.

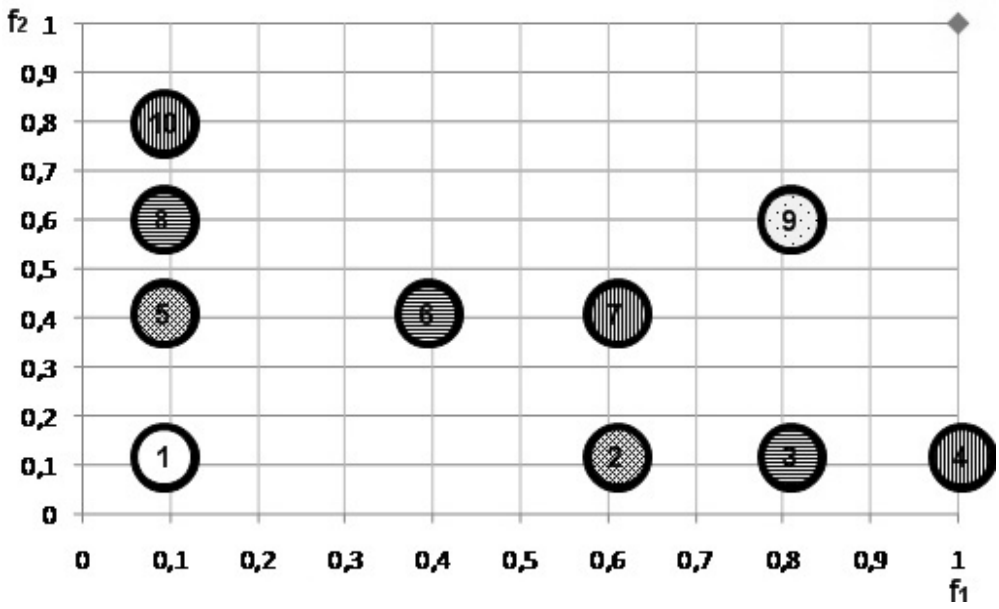

Figure 6. The results of marking out Pareto layers

Here, Pareto layers consist of the following elements: $X_1^{nd} = \{x_1\}$, $X_2^{nd} = \{x_2, x_5\}$, $X_3^{nd} = \{x_3, x_6, x_8\}$, $X_4^{nd} = \{x_4, x_7, x_{10}\}$, $X_5^{nd} = \{x_9\}$. For ranging the elements according to the criticality degree, we have used in each layer [1] a linear indicators' convolution of the type $f^{\text{res}}(x_i) = \lambda_1 f_1(x_i) + \lambda_2 f_2(x_i)$. Let the coefficients of the criticality indicators' significance be of the same value $\lambda_1 = \lambda_2 = 0.5$. Then, the result of ranging of the set $X = \{x_i, i = 1,...,10\}$ is as follows: $x_1 \prec x_5 \prec x_2 \prec x_8 \prec x_6 \prec x_3 \prec x_{10} \prec x_7 \prec x_4 \prec x_9$, which is presented on Figure 7.

It is easy to note that in case of using the suggested method, the elements x_6, x_7 in the corresponding Pareto layers $X_3^{nd} = \{x_3, x_6, x_8\}$, $X_4^{nd} = \{x_4, x_7, x_{10}\}$ at different combinations of the significance coefficients λ_1, λ_2, as the result of their ranging, will be always dominated by the given layers' elements. It means that in solving the tasks of ranging and determining the critical elements in Pareto layers, the elements x_6, x_7 will under no condition be admitted as most critical or less critical.

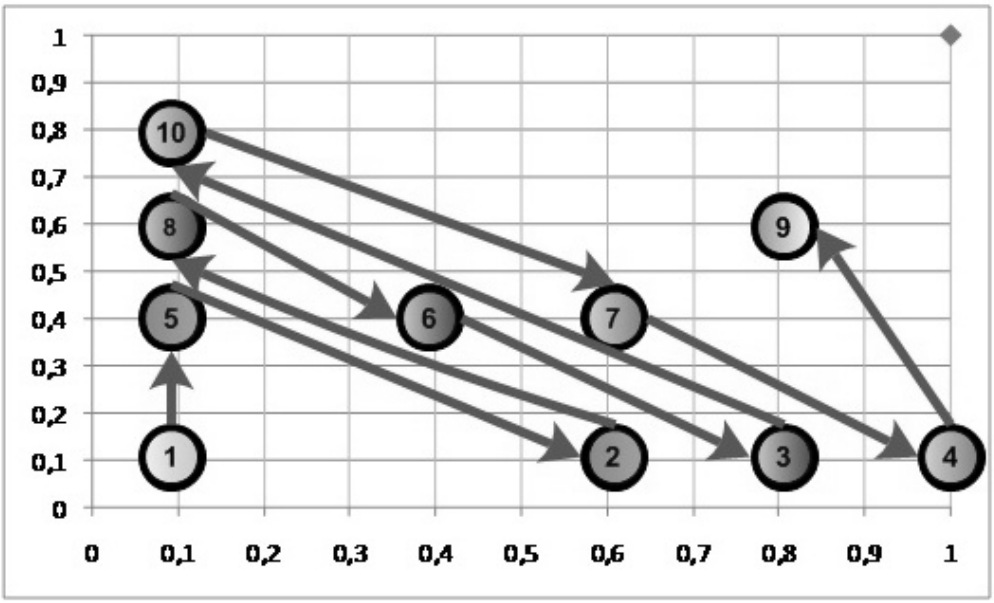

Figure 7. The result of ranging of the set $X = \{x_i, i = 1,...,10\}$

Let us perform the ranging of the CO elements according to their criticality degree by the suggested combined method. We'll show that we can mark out from the Pareto layers the elements x_6, x_7 as well as any others. Let the orthogonal plan of the expert questioning be presented in Table 5.

Table 5. The orthogonal plan of the expert questioning

f_0	f_1	f_2	f^{res}	$f_1 \times f_2$
1	-1	-1	0,1	1
1	1	-1	0,9	-1
1	-1	1	1	-1
1	1	1	1	1
$f_0 \times f^{\text{res}}$	$f_1 \times f^{\text{res}}$	$f_2 \times f^{\text{res}}$	$f_1 \times f_2 \times f^{\text{res}}$	*Polynomial values*
0,1	-0,1	-0,1	0,1	0,100
0,9	0,9	-0,9	-0,9	0,900
1	-1	1	-1	1,000
1	1	1	1	1,000
Polynomial coefficients	λ_0	λ_1	λ_2	λ_{12}
Coefficients' values	0,75	0,2	0,25	-0,2

Having processed the data of the expert questioning according to the above method we'll get the following equation describing the expert's judgment: $f^{\text{res}} = 0,75 + 0,2 f_1 + 0,25 f_2 - 0,2 f_1 f_2$. The results of calculating the integral indicator of the elements' failure criticality are shown on Figures 8 and 9.

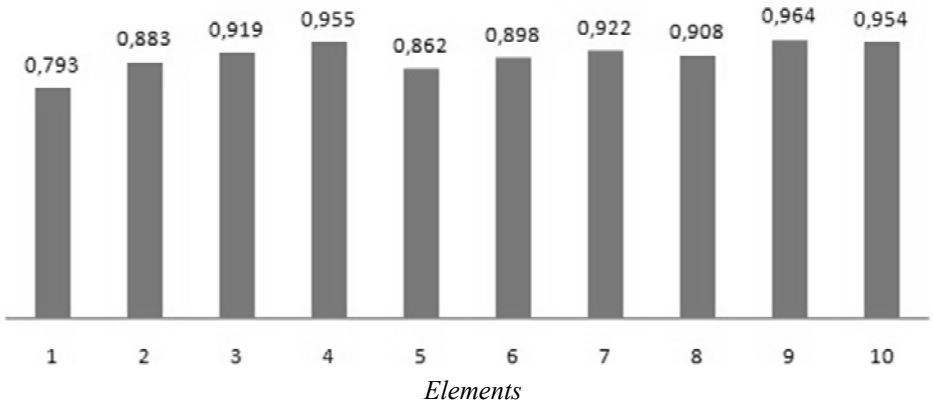

Figure 8. The results of calculating the integral indicator of the elements' failure criticality

The received results of ranging the CO elements according to the criticality degree are similar to the above ranging, shown on Figure 7. Here, the elements x_6, x_7 in the corresponding Pareto layers $X_3^{nd} = \{x_3, x_6, x_8\}$, $X_4^{nd} = \{x_4, x_7, x_{10}\}$ have turned out the least critical by the expert's opinion.

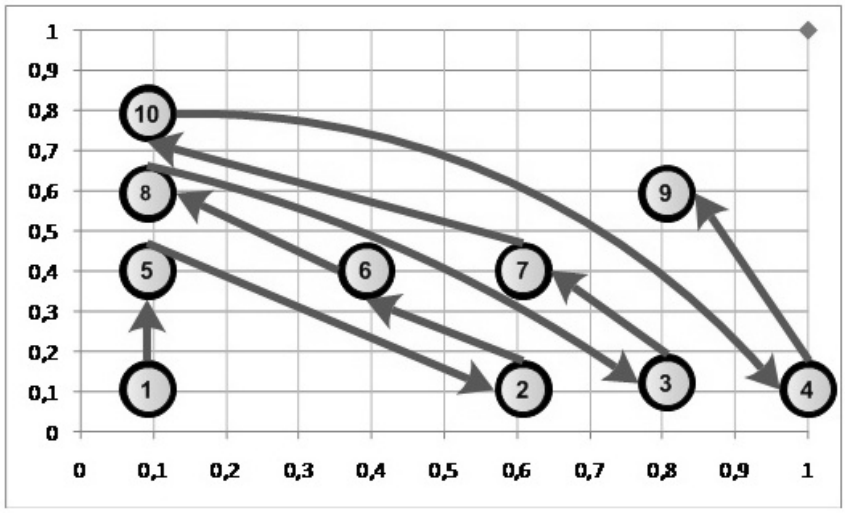

Figure 9. The results of ranging the CO elements according to the criticality degree

6. Conclusions

Advantages of the suggested approach to the analysis of the elements' contribution into the CO efficiency:

1. Introduction of the notion of the genome of structure allows evaluation of the elements' structural significance for both the monotonous and non-monotonous systems.

2. Using both quantitative and qualitative (fuzzy, inexact, interval) information about the elements' failure influence on the CO functioning substantially increases the trustworthiness the conclusions and decisions made in the CO design and management.

3. In the frame of the suggested method, there is performed formalization of the expert information, presented in the natural for the expert language, by means of introducing linguistic variables, which allow adequate reflecting of an approximate word description of objects and phenomena even in those cases when a determined description is either lacking or impossible in principle.

4. The suggested method of the failures' criticality analysis allows formalizing the expert's (group of experts') experience in the form of prediction models in a multi-dimension space and taking into account complex simultaneous influence of several factors on the resulting criticality indicator of the CO.

Due to this, there is revealed the non-linear character of the particular indicators' influence on the integral indicator of the failures' criticality and there is increased the trustworthiness of the decision-making results.

Acknowledgments

The research on the given theme has been performed with the financial support of Russian Foundation for Basic Research (grants 08–08–00346, 08–08–00403, 09–08–00259, 10-08-90027), Department of Nanotechnology and Information Technologies of Russian Academy of Science (project №O–2.3/03).

References

1. Afanasjev, V.G., Zelentsov, V.A., Mironov, A.N. *Methods of analysis of reliability and failure criticality of the complex systems.* St. Petersburg: MD, 1992. 99 p. (In Russian)
2. Pavlov, A.N., Sokolov, B.V., Sorokin, M.V. Analysis of the structural dynamics of the complex system of the information defense, *Information and Security*, Vol. 12, No 3, 2009, pp. 389-396. (In Russian)
3. Pavlov, A.N. Logic-probability and fuzzy-possibility approaches to researching the monotonous and non-monotonous structures. In: *The XI International Scientific-Technical Conference "Cybernetics and Advanced Technologies of the XXI Century", May 12-14, 2010: theses of the reports*. Voronezh: SIF «SAKVOEE», 2010, pp. 483-492. (In Russian)
4. Pavlov, A.N. Research of the non-monotonous systems: analysis of the "bridge" structure. In: *Works of the X International Scientific School MA SR-2010 "Modelling and Analysis of Security and Risks in Complex Systems", Saint-Petersburg, July 6-10, 2010*. St. Petersburg: SUAI, 2010, pp. 85-93. (In Russian)
5. Sokolov, B.V., Pavlov, A.N. et al. *Military systems engineering and systems analysis.* St. Petersburg: MD, 1999. 408 p. (In Russian)
6. *Fuzzy sets in the models of management and artificial intelligence / Edited by D.A. Pospelov*. Moscow: Nauka, 1986. 312 p. (In Russian)
7. Borisov, A.N., Krumberg, O.A., Fedorov, I.P. *Decision making on the basis of fuzzy models*. Riga: Zinatne, 1990. 184 p. (In Russian)
8. Pavlov, A.N., Sokolov, B.V. *Decision making under the condition of fuzzy information. Tutorial*. St. Petersburg: SUAI, 2006. 72 p. (In Russian)
9. Andrejchikov, A.V., Andrejchikova, O.N. *Analysis, synthesis, decision planning in economics*: *Textbook.* Moscow: Finansy i Statistika, 2000. 368 p. (In Russian)
10. Nalimov, V. V., Chernova, N. A. *Statistic models of extreme experiments planning*. Moscow: Nauka, 1965. 382 p. (In Russian)
11. Nalimov, V.V. *Experiment Theory*. Moscow: Nauka, 1971, 208 p. (In Russian)
12. Adler, J.P., Markova, E.V., Granovsky, J.V. *Experiment planning in the search of optimal conditions*. Moscow: Nauka, 1976. 280 p. (In Russian)
13. Spesivtsev, A.V. *Managing the risks of extraordinary situations on the basis of the expert information formalization*. St. Petersburg: Edition of the Polytechnic University, 2004. 238 p. (In Russian)
14. Pavlov, A.N. Methodology of building pseudo-universal convolutions of linguistic indicators on the basis of the experiment planning theory. In: *Proceedings of the XI International Conference on Soft Computations and Measurements (SCM'2008), St. Petersburg, 23-25 June 2008*. St. Petersburg, 2008. Vol.1, pp. 169-172. (In Russian)

Transport and Telecommunication, 2010, Volume 11, No 4, 14–28
Transport and Telecommunication Institute, Lomonosova 1, Riga, LV-1019, Latvia

APPROACH TO HARDWARE IMPLEMENTATION OF GENETIC ALGORITHM FOR INVERSE PROBLEM OF ROADWAY COVERAGE SUBSURFACE PROBING SOLUTION

A. Krainyukov, V. Kutev, D. Opolchenov

Transport and Telecommunications Institute
Lomonosova str. 1, Riga, LV-1019, Latvia
Ph.: +371 67100634. Fax: +371 67100660
E-mail: Aleksandrs.Krainukovs@tsi.lv, Valerijs.Kutev@tsi.lv, Daniil.Opolchenov@tsi.lv

This work has focused on the problem of approach to hardware implementation of genetic algorithm for inverse problem of roadway coverage subsurface radar probing solution. Iterative procedure to solve the inverse problem in frequency domain is used on base of aim function minimization. Genetic algorithm is used for search of global minimum of aim function.
For hardware implementation of genetic algorithm it is necessary correctly to choose the values of arguments for aim function and parameters of genetic algorithm. The authors investigated two different kinds of aim functions. Estimation of possibility for genetic algorithm hardware implementation on base of field-programmable gate array (FPGA) is discussed.

Keywords: roadway radar monitoring, inverse problem, genetic algorithm, field-programmable devices, hardware implementation

1. Introduction

Roadway structure is a complex multi-layered construction, various layers of which consist of materials of different durability. It is well-known that in different times of the year and in different environmental conditions the preservation of road cover depends not only on its usage but also on different climate-related factors.

For optimisation of exploitation, upkeep and reconstruction of road cover certain information is crucial, such as condition of its internal layers and the processes taking place within them: the appearance of potholes, changes in dampness of the soil, changes in the ability of the soil to filter water, etc. Timely identification of these processes allows one to make an informed decision about the necessary actions. This is why it is necessary to constantly monitor the condition of the inner layers of the road structure, in order to act in time in response to the changes the state of its layers.

In present time to research the inner structure of objects, of both artificial and natural origin, subsurface radar probing methods are widely used [1, 2]. The latter allows one to ascertain the thickness of the inner layers of the road structure, the degree and quality of compactness of various road components, as well as to identify areas of excessive dampness, potholes and sources of water penetration. Determining pavement thickness, detected voids beneath pavement and measuring the moisture content in pavement layers are examples of such using. However, traditional methods of interpretation of the results of the subsurface radar probing of roadways do not provide the required precision and effectiveness of the road monitoring. Transportation departments need better methods for measuring near-surface and subsurface conditions of their transportation facilities [2]. It is possible to increase the precision of diagnosis and identification of inner zones and objects based on the results of radar subsurface probing through reconstruction of the geometrical and electro-physical characteristics, which leads to the necessity to solve the inverse problem of radar subsurface probing. Reconstruction of electro-physical characteristics of the road structure is in essence identification of electro-physical parameters of the layers of the road structure, which can be achieved by solving the inverse structure problem of subsurface radar probing.

In [3,4] we will look at the specifics of solving the inverse structure problem of subsurface radar probing in the frequency domain with through using a generic algorithm for search of global minimum of aim function.. Block diagram of iterative procedure to solve radar inverse problem is shown on Figure 1.

The initial stage of the iterative procedure is concerned with calculating of module spectral density $\left|\dot{S}_e\left(\omega_i, \vec{P}\right)\right|$ for reflected signal $U_{ref}(t)$. Further, in order to solve the inverse problem of subsurface radar probing, we introduce vector of parameters:

$$\vec{P} = \{p_1, p_2, ..., p_n\} \in \vec{P}_{POS}, \tag{1}$$

where $\vec{P}_{POS}$ – is a set of possible (allowed) values for parameters of probed area. The set of allowed values for parameters is determined on the basis of pre-existing hypotheses about internal structure of probed medium.

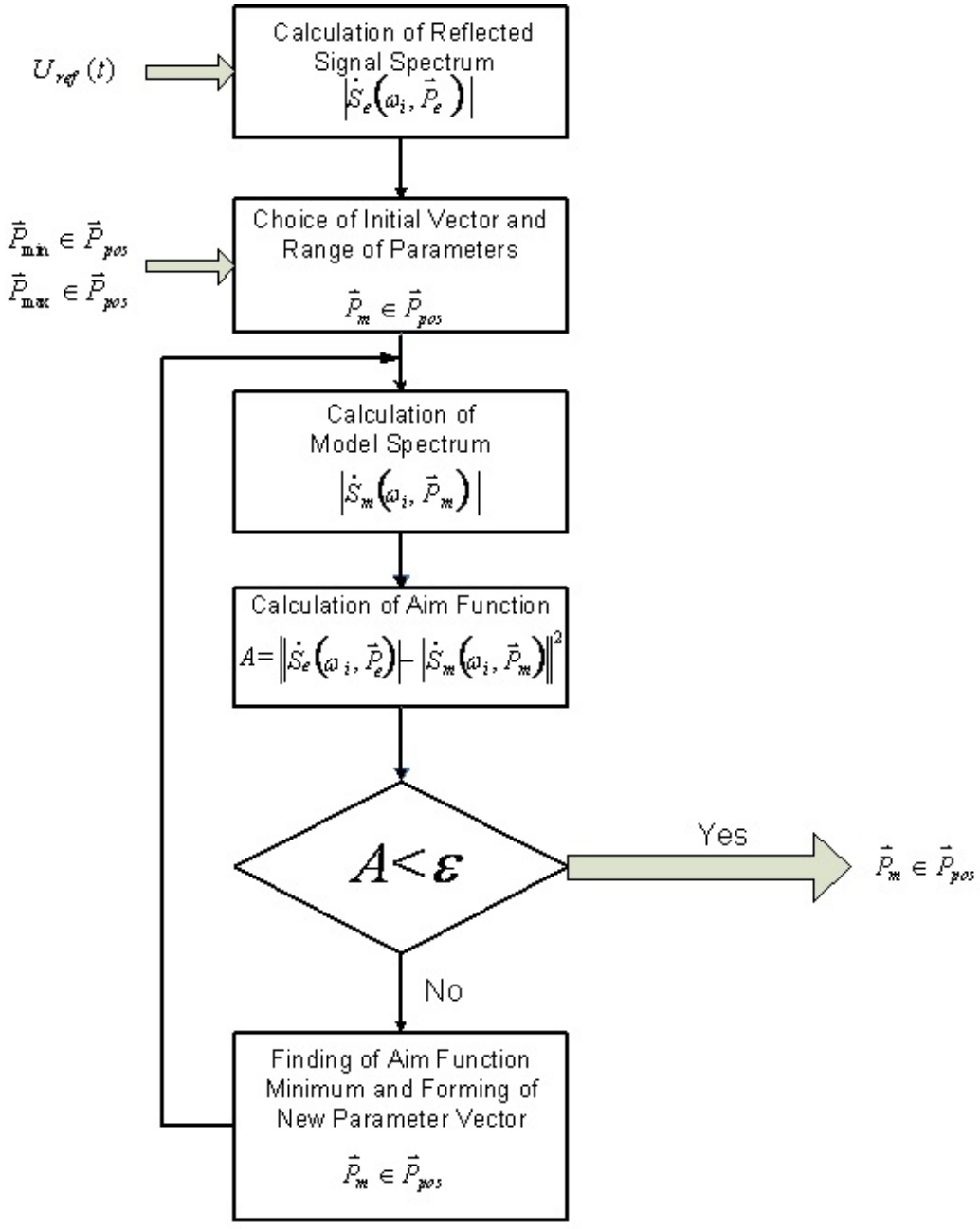

Figure 1. Block diagram of iterative procedure to solve radar inverse problem in frequency domain

Calculating of theoretical spectral density $\dot{S}_T(\omega_i, \vec{P})$ equates to the solving of the direct problem of subsurface radar probing. To calculate $\dot{S}_T(\omega_i, \vec{P})$ we chose the starting vector of parameters $\vec{P}_M$ belonging to the set of allowed values of parameters $\vec{P}_{POS}$.

The choice of the starting vector of parameters is also determined on the basis of pre-existing hypotheses about the object of probing.

Values of the modules of experimental and theoretical spectral densities are used to calculate aim function Φ_1:

$$\Phi_1 = \left\| \left| \dot{S}_e\left(\omega_i, \vec{P}\right) \right| - \left| \dot{S}_T\left(\omega_i, \vec{P}_M\right) \right| \right\|^2 = \frac{1}{n_{\max}} \sum_{i=0}^{n_{\max}} \left\| \left| \dot{S}_Э\left(\omega_i, \vec{P}\right) \right| - \left| \dot{S}_T\left(\omega_i, \vec{P}_M^j\right) \right| \right\|^2, \quad (2)$$

where n_{max} – index of the spectral component with frequency f_{max}.

If the value of the aim function Φ_1 is not more than the value of a threshold α, then solving the inverse structure problem is finished. The solution (pseudo-solution) is the vector of parameters $\vec{P}_M$. If the value of the aim function Φ_1 is greater than the value of α, then taking into account the current values of the vector $\vec{P}_M$ we formulate a new vector of parameters $\vec{P}_M$, which is used to calculate new values of the aim function Φ_1. This means, that finding a solution to the inverse problem in the form of the vector $\vec{P}_M$ is performed by iteration with the sequential improvement of accuracy of the parameters $\vec{P}_M$.

It has been suggested [4] that the value of α is set as follows:

$$\alpha = \frac{P_{av}}{K}, \quad (3)$$

where P_{av} – the averaged mean power of those spectral components $\dot{S}_e\left(\omega_i, \vec{P}\right)$, which are used for calculating of aim function Φ_1, and K – dimensionless coefficient, set by the user.

In [3,4] we researched the effect of the conditions of solving the inverse problem and parameters of generic algorithm on the error of restoration of electro-physical parameters of the modelled three-layered medium. The value of the electro-physical parameters of the layers of the two-layered medium being modelled (layer thickness h, electrical conductivity σ and the relative dielectric permittivity ε) corresponded to the electro-physical parameters of the materials of the layers road structure. It was determined that the error of restoration of electro-physical parameters can reach up to 10% and the results of restoration depends significantly on the assumptions about the parameters of the modelled two-layered medium. Optimal values of the coefficient K from the point of view of restoration of the parameters of the road surface and iteration of the algorithm lie within range from 1000 to 3000.

When solving the inverse problem of sub-layer probing it is very important to rationally select the original inputs, which are determined by various informational characteristics, scope of their existence and their quantities.

In aim function (2), used in [3, 4], informational characteristic used was the spectral density of the reflected signal is in the form of its modular values ($\left|\dot{S}_e\left(\omega_i, \vec{P}\right)\right|$ and $\left|\dot{S}_T\left(\omega_i, \vec{P}_M\right)\right|$). However, this informational characteristic can also be used in the form of complex values. In this case the expression for calculation of aim function Φ_2 is as follows:

$$\Phi_2 = \left\| \dot{S}_e\left(\omega_i, \vec{P}\right) - \dot{S}_T\left(\omega_i, \vec{P}_M\right) \right\|^2 = \frac{1}{n_{\max}} \sum_{i=0}^{n_{\max}} \left| \dot{S}_e\left(\omega_i, \vec{P}\right) - \dot{S}\left(\omega_i, \vec{P}_M^j\right) \right|^2, \quad (4)$$

and the algorithm of solving the inverse structural problem of subsurface probing stays the same (Fig. 1).

Irrespective of the form of the informational characteristic aim functions Φ_1 and Φ_2 greatly depend on the parameters of the probing medium and frequency range, in which the inverse structure problem of subsurface probing is being solved. Apart from the global minimum aim functions Φ_1 and Φ_2 have numerous false local minimums, which give possible incorrect solutions to the inverse problem.

In this work we research the effect of electro-physical parameters of the three-layer modelled medium on the behaviour of aim functions Φ_1 and Φ_2.For the chosen model of the probed medium, probing signal and aim functions Φ_1 and Φ_2, we solve the inverse problem using, according to the block diagram of iterative procedure shown on Figure 1, we research the effect of GA characteristics on the time for solving the of inverse problem, we research the hardware implementation of genetic algorithm on FPGA.

2. Analysis of Aim Functions for the Inverse Problem of Roadway Coverage Radar Subsurface Probing

2.1. Models of the roadway coverage and of the probe signal

The model of roadway coverage may be conceived as homogeneous horizontal layers: first layer-pavement and second layer -base, which are placed between two semi-infinite spaces: upper-air and lower-sub grade. Used model of probe signal was the same as in [3].

Calculation of theoretical spectral density is performed by multiplying of the spectrum of the probe signal and the theoretical coefficient of reflection of the medium $\dot{R}_T\left(\omega_i, \vec{P}_M\right)$ [3,4], which is described by the vector $\vec{P}_M$:

$$\dot{S}_T\left(\omega_i, \vec{P}\right) = \dot{S}\left(\omega_i\right) \cdot \dot{R}_T\left(\omega_i, \vec{P}_M\right). \quad (5)$$

2.2. Influence of electro-physical parameters of the medium on aim functions

Aim functions Φ_1 and Φ_2 of the inverse problem of radar subsurface probing being solved are functions of parameter vector $\vec{P}$ and used frequency spectrum of reflected signal which has maximal frequency f_{max}. For the studied model of the probed medium the number of arguments of aim functions Φ_1 and Φ_2 equals 9, i.e. 8 electro physical parameters of the model medium [4] and maximal frequency f_{max}.

In order to demonstrate the dependency of the aim functions on electro physical parameters in three-dimensional form we selected two partial arguments for calculations of them.

To calculate the value of the theoretical spectral density $\dot{S}_T\left(\omega_i, \vec{P}\right)$ we were changing the values of two of the electro physical parameters of one of the layers of the medium while keeping the remaining 6 constant and equal to the modelled ones. The range of changes of the chosen parameters was symmetrical to the modelled values and equal to them.

2.2.1. Dependence of aim functions on dielectric permittivity and thickness of the layers

Dependencies of aim functions Φ_1 and Φ_2 on dielectric permittivity ε' of the layers and their thickness *h* are shown on Figures 2 and 3.

In the upper part of each figure there is a three-dimensional view of the dependence of the aim function on two parameters calculated for f_{max} = 300 MHz, and in the bottom part – the level of the functions depends on two parameters for three values of maximal frequency f_{max} =100, 300 and 500 MHz. For the minimal level the threshold value α was used. In all of the diagrams for aim functions the value α was used, calculated using K = 2000.

The areas of aim functions Φ_1 and Φ_2 with values less than α, are shown in the centre of the diagrams and highlighted in white. The geometric form of these areas allows us to judge the degree of the effect of each parameter on the aim function.

The geometric forms of the white areas show on Figure 2 and Figure 3 are ellipses, but of different sizes. Comparative analysis of these areas allows us to make the following:

- dielectric permittivity and thickness of layers heavily affect the values of aim functions Φ_1 and Φ_2;
- calculation of the aim functions for $f_{\max} > 300$ MHz increases the size and compression of the ellipses, which means that in order to calculate aim functions it is crucial, that $f_{\max}$ is less than 300 MHz;
- aim function Φ_2 with a complex spectral density is more informative, because areas taking values less than α are smaller in size, i.e. corresponding ranges of h_1 and ε_1' on the diagrams for Φ_2 are less than those for Φ_1;
- values of aim functions Φ_1 and Φ_2 less than α, are obtainable under multidirectional changes of dielectric permittivity and thickness of the layers against the modelled values of the parameters of the layers, which can lead to errors of reconstruction of parameters of the probed medium.

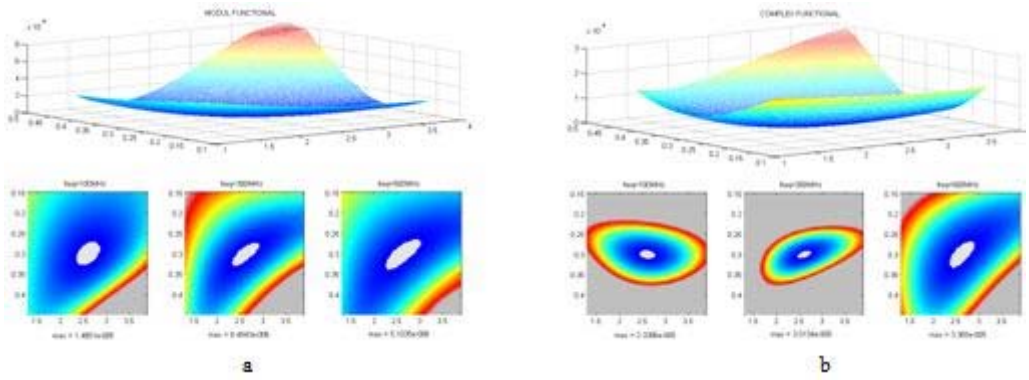

Figure 2. Influence of dielectric permittivity ε_1' and thickness h_1 of the first layer (pavement) on the aim functions Φ_1(a) and Φ_2(b)

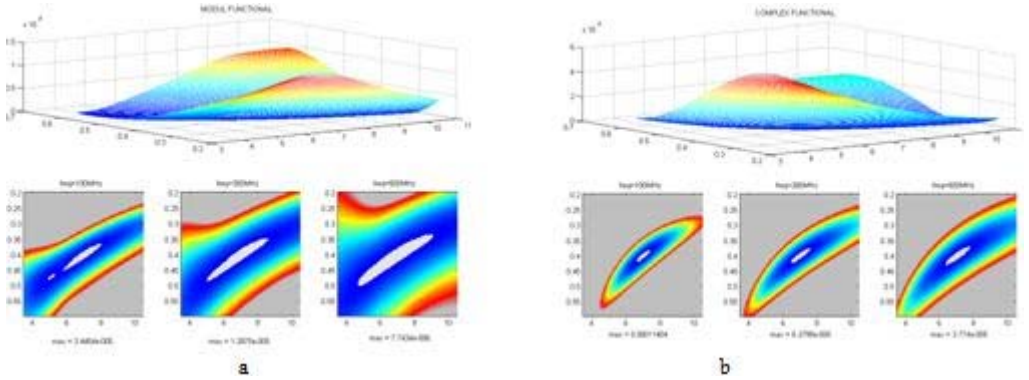

Figure 3. Influence of dielectric permittivity ε_2' and thickness h_2 of the second layer (base) on the aim functions Φ_1 (a) and Φ_2 (b)

2.2.2. Dependencies of aim functions on the electrical conductivity of the layers

Dependencies of aim functions Φ_1 and Φ_2 on the electrical conductivity of the first layer σ and on two other parameters are shown in the Figure 4. Conditions of calculations, representations and values of f_{max} are the same as those shown in the Figure 2 and Figure 3.

The geometrical form of the white areas is close to a rectangle, the length of which is equal to the range of changes of electrical conductivity of the layer, and the width depends on the second electro-physical parameter of the layer or the width of the frequency range (value f_{max}). This means that the influence of the electrical conductivity of the layers on the values of the aim functions is negligible. Electrical conductivity σ_2 and σ_3 affect aim functions similarly.

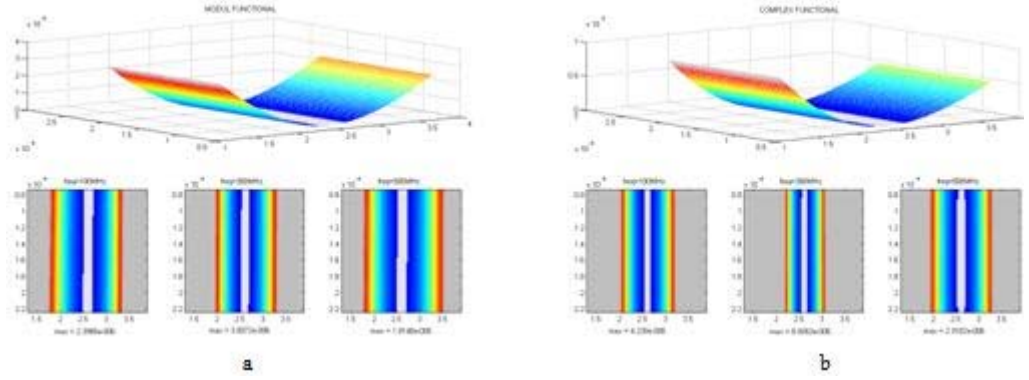

Figure 4. Influence of dielectric permittivity ε_1' and electrical conductivity σ_1 of the first layer (pavement) on the aim functions Φ_1 (a) and Φ_2 (b)

2.2.3. Influence of the parameters of lower semi-infinite space (sub grade) *on the aim functions*

On Figure 5 we have shown the influence of dielectric permittivity $\varepsilon_3^{'}$ and electrical conductivity σ_3 of lower semi-infinite space (sub grade) on the aim functions Φ_1 and Φ_2. The affect of these parameters is quite significant: the shape of the areas corresponding to the minimal values of the aim functions (less than α) is close to a circle and their sizes are minimal compared to the similar areas in previous figures. Therefore, the aim functions Φ_1 and Φ_2 are very sensitive to changes in $\varepsilon_3^{'}$ and σ_3, particularly the function Φ_2. The increase of f_{max} leads to increase of these areas, hence for the solution of the inverse problem it is crucial that f_{max} does not exceed 300 MHz

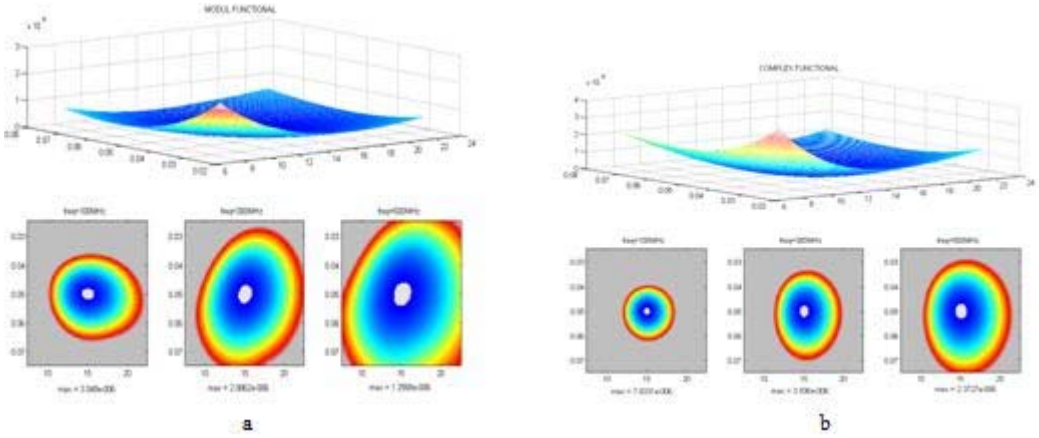

Figure 5. Influence of dielectric permittivity $\varepsilon_3^{'}$ and electrical conductivity σ_3 of lower semi-infinite space (sub grade) on the aim functions Φ_1 (a) and Φ_2 (b)

3. Results of Roadway Coverage Parameters Reconstruction with Using Aim Functions Φ_1 and Φ_2

For the chosen model of roadway coverage, probing signal and the aim functions Φ_1 and Φ_2 the solution of the inverse structural problem was carried out using generic algorithm (GA). In order to find the global minimal values generic algorithm was used with the same parameters as in [3-5].

The solution of the above problem – vector $\vec{P}_M$ was used to access the relative error of reconstruction of each of the parameters of the modelled medium. At the same time the mean number of repetitions, necessary to finish the generic algorithm, was accessed.

In order to define the optimal conditions for the generic algorithm (GA) used to solve the inverse problem of radar `subsurface probing we researched how these values are influenced by the following factors:

- coefficient K, defining the threshold of the acceptable solution α;
- frequency range of used reflected signal spectrum, limited by its maximal frequency f_{max}.

To obtain statistical assessment about 100 solutions of the inverse problem for two layer model of roadway structure were used.

3.1. Influence of value coefficient κ on the errors of roadway model parameters reconstruction

The value of K in our calculations was changed within the range of 100 to 5000 with fixed $f_{max} = 300$ MHz.

Influence of value K on first layer (pavement) parameters reconstruction On Figures 6 and 7 we show dependencies of the relative error (upper figures) and relative root-mean-square (SMR) error (lower figures) of the results of reconstruction of electro-physical parameters of the first layer (pavement) on value coefficient K.

When using the aim function Φ_2 the relative errors of reconstruction ε_1 and h_1 are less than when using aim function Φ_1, and are, in fact, close to 0 (this is clearly illustrated on Figure 2). When $K \geq 1000$ ε_1 and h_1 slightly decrease.

Dependencies of relative RMS error for the first layer parameters show that the increase of K will result in a smaller range of possible values of ε_1 and h_1 (Figure 2).

Dependencies of relative RMS error for the first layer parameters show that the increase of K will result in a smaller range of possible values of ε_1 and h_1 (Figure 2). The range of possible values of σ_1 remains unchanged with the increase of K (Figure 4); therefore the values of relative RMS error for σ_1 are stable and significant. For this reason dependencies of σ_1 have a chaotic character.

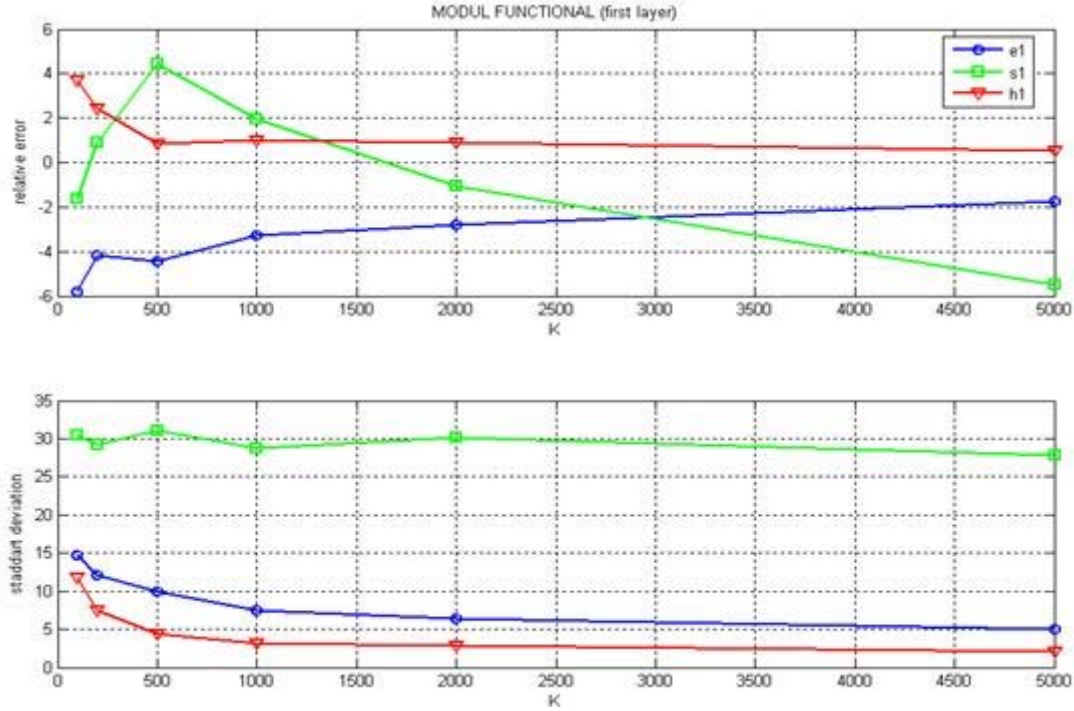

Figure 6. Influence of value K on accuracy reconstruction of first layer (pavement) parameters for using aim function Φ_1

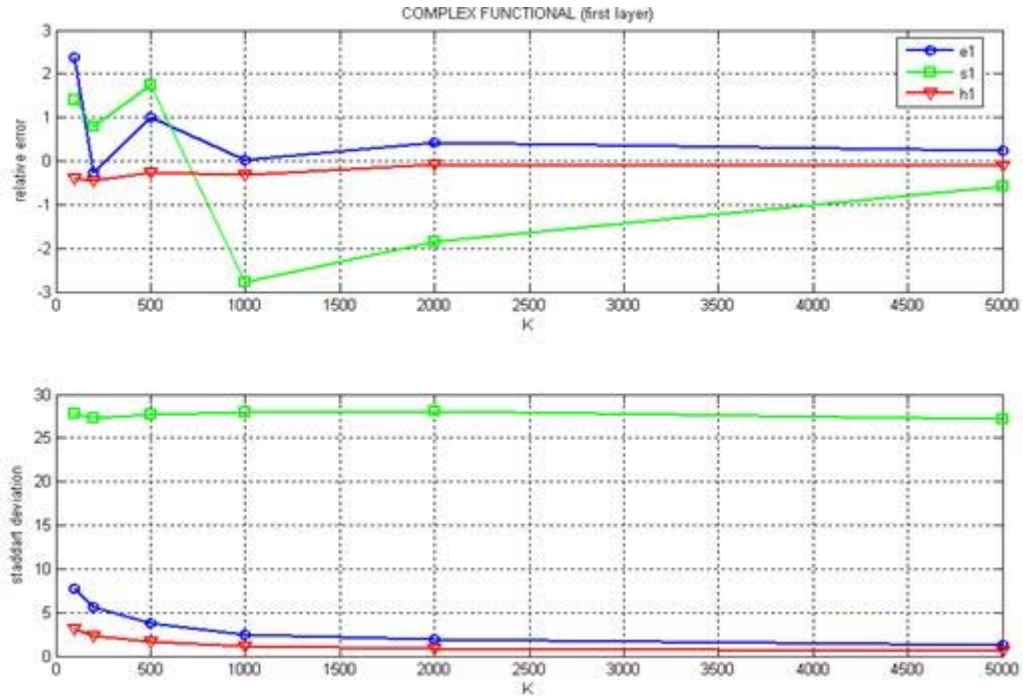

Figure 7. Influence of value K on accuracy reconstruction of first layer (base) parameters for using aim function Φ_2

Influence of value K on second layer (base) parameters reconstruction (Figure 8). Influence of value K on of relative RMS errors of second layer parameters reconstruction is similar to those of the first layer's. The difference is in higher values of relative RMS errors for ε_2 and h_2, as it is shown on Figure 2 and Figure 3. Correspondingly the values of ε_2 and h_2 are higher although they decrease with the increase of K when using the aim function Φ_1 (Figure 8,a). When using the aim function Φ_2 ε_2 and h_2 are less than 1% already when K = 1000 (Figure 8,b). Dependence of σ_2 has also a chaotic character as for σ_2 RMS error is independent of K (Figure 4).

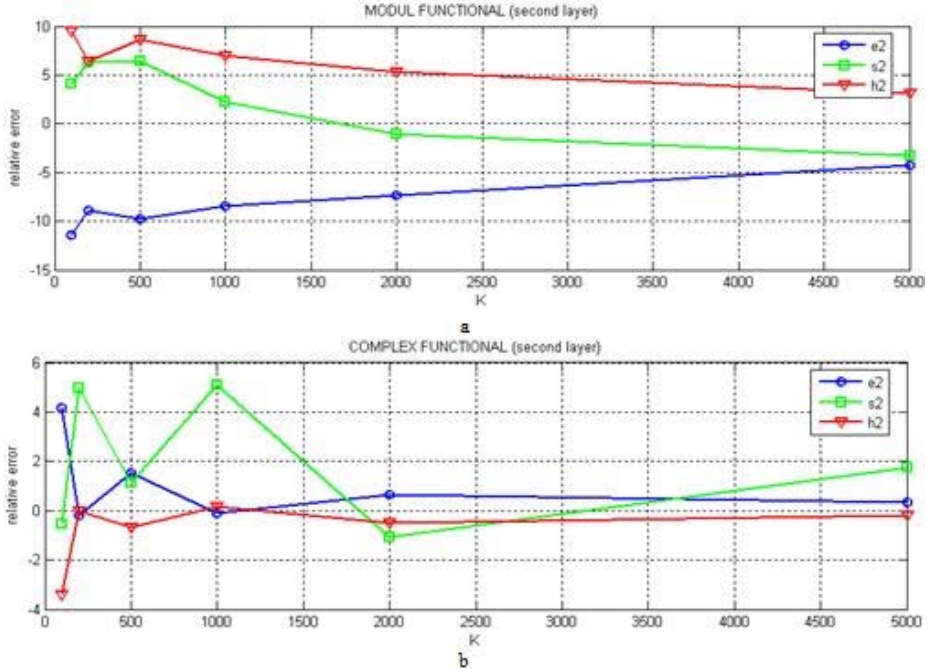

Figure 8. Influence of value K on accuracy reconstruction of second layer (base) parameters for using aim function Φ_1 (a) and aim function Φ_2 (b)

Influence of value K on lower semi-infinite space (subgrade) parameters reconstruction (Figure 9). Increase of value K leads to decrease of RMS errors for ε_3 and h_3 and therefore to decrease of relative errors of these parameters reconstruction.

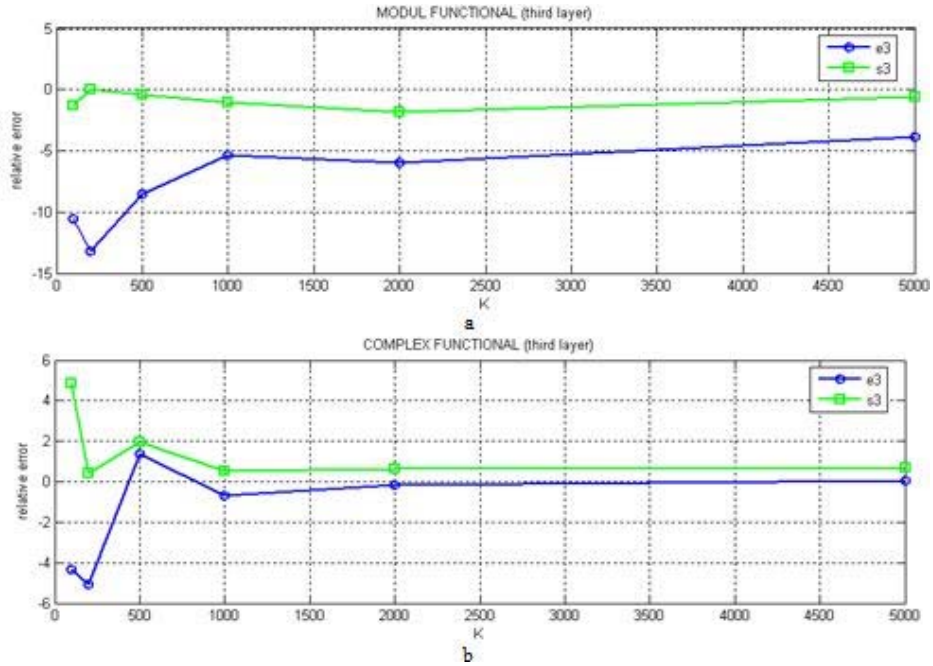

Figure 9. Influence of value K on accuracy reconstruction of lower semi-infinite space (sub grade) parameters for using aim function Φ_1 (a) and aim function Φ_2 (b)

When $K > 1000$ the relative errors hardly change. Using the aim function Φ_2 allows to obtain ε_3 and h_3 with relative error less than 1% already when $K = 1000$ (Figure 9,b).

3.2. Influence of frequency range on the error of parameter reconstruction of the modelled medium

Solving of a subsurface radar probing inverse problem in a frequency area can be performed with different number of spectral components, i.e. in frequency ranges of a different width as well as differently positioned on the frequency axe. The aim of choosing of the optimal frequency range is minimizing the relative error determination of medium electro-physical parameters: dielectric permittivity ε, electrical conductivity σ and the layer thickness h for all layers of roadway structure.

In this work solving of the inverse problem was carried out in the frequency range $[f_1 \ldots f_{\max}]$, where f_1 – is the frequency of the first spectral component, equal to 10 MHz, and value of $f_{\max}$ was changing in range from 50 MHz to 500 MHz .Influence of $f_{\max}$ on the solution of the inverse problem was researched with two values of K: K = 1000 and 2000. Both aim functions Φ_1 and Φ_2 were used in our experiments. Analysis of results shows that using aim function Φ_2 allowed to achieve lower relative error of parameter reconstruction compared to the results obtained using aim function Φ_1. Figure 10 illustrates influence of $f_{\max}$ on the relative error of pavement (first layer) and base (second layer) parameters reconstruction when aim function Φ_2 is used. From this figure one can see:

- relative error of parameter reconstruction h_1, ε_1' (Figure 10,a), h_2 and ε_2' (Figure 10,b) is less than 1% when $f_{\max} > 100$ MHz and is independent of K;
- relative error of parameter reconstruction σ_1 and σ_2 has a complex dependence on $f_{\max}$.

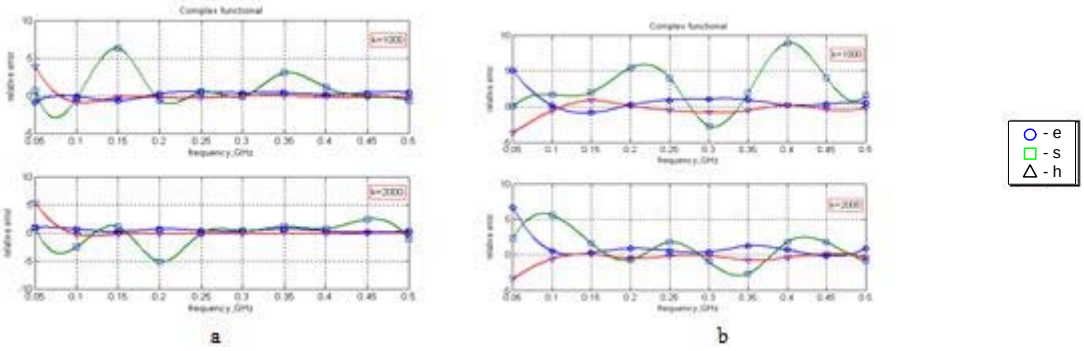

Figure 10. Influence of $f_{\max}$ on the relative error of the first layer parameter reconstruction (a) and the second layer parameter reconstruction (b) using Φ_2

The similar character of the dependencies shown in the Figure 15 can be explained by the fact that the electro-physical parameters of the first (pavement) and second (base) layers have an identical affect on Φ_2, where as an increase of $f_{\max}$ does not change the size of the areas around the global minimum, values of which are less of α (Figures 2,b and 3,b). When aim function Φ_2 is using then relative errors of σ_3 and ε_3' determination are approximately 1%. Note that when $K = 2000$ the values of the above variables can be obtained when used maximal frequency of reflected signal is in range $100\,MHz \le f_{\max} \le 450\,MHz$.

3.3. Influence of value K and of GA characteristics on the time for solving of inverse problem

As an estimate time for solving the inverse problem, we use the average population amount (iterations) of GA (Figure 11). When using the aim function of Φ_2, this quantity depends linearly on K. This means that the inverse problem always ends up as a result of the condition $\Phi_2 < \alpha$ (2.6). When using the aim function Φ_1 average population amount virtually unchanged for K > 2000. Consequently, for such values of K the solving of inverse problem stops more often if the number of iterations exceeded admitted number of population 500.

We have investigated the influence on the time for solving of inverse problem of the following GA characteristics: population size (number of individuals in the population) and bits of individuals (number of bit per parameter). Investigations conducted for the two aim functions Φ_1 and with fixed values of f_{max} = 300 MHz and α (K = 1000). Investigations show that these characteristics of genetic algorithm does not affect on the error of parameter reconstruction of the probed medium parameters. Terms of the end of inverse problem solving the (2.5 and 2.6) exclude the influence of these genetic algorithm characteristics. The population size varied from 20 to 1000 individuals.

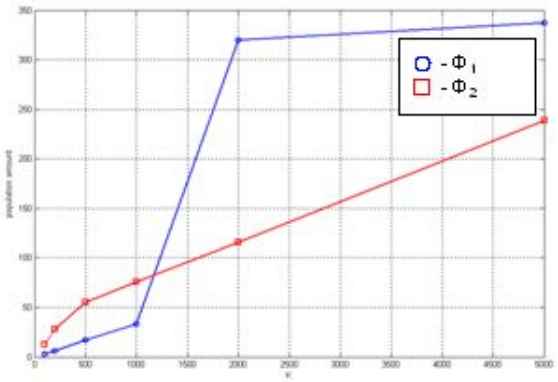

Figure 11. Influence of value K on population amount for using aim functions Φ_1 and Φ_2

Changing the number of individuals can change the time for solving of inverse problem. Dependence of the population amount (iterations), which were necessary for solving of the inverse problem, on the population size is shown on Figure 12.

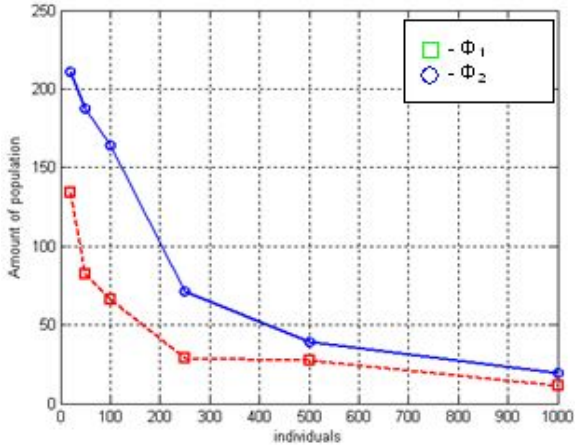

Figure 12. Influence of the population size on population amount for using aim functions Φ_1 and Φ_2

If the number of individual increases, it will increase the probability that in the next generation will be an individuals, whose aim functions are less than α, ie more probability to end the inverse problem in the current population. When aim function Φ_1 is using then amount of populations required less, although the reconstruction error of electrical parameters of the probed medium are noticeably lose (3.1., 3.2.). If the number of individuals of more than 250, the amount of population does not decrease significantly. This means that the time for solving the inverse problem will increase due to growth in population size. Consequently, the maximum size of an individual should not be more than 200 ... 500.

4. Hardware Implementation of Genetic Algorithm for Solving of the Inverse Problem of Subsurface Probing

4.1. Block diagram of the device for solving the inverse problem with using genetic algorithm

Hardware implementation of the device for solving the inverse problem of subsurface probing will create a portable automated (intelligent) system (device) for radar monitoring of the roadway. If we consider the algorithm shown on Figure 1, from the viewpoint of hardware implementation, we can distinguish two main objectives of hardware implementation:

- hardware implementation of genetic algorithm;
- hardware implementation of computing a aim function (fitness function).

Operators of the classic genetic algorithm are executed sequentially (Figure 13). When the hardware implementation of the genetic algorithm should consider the following features:

- for each individual or pair of individuals can arrange a separate process - parallel processing of all individuals in a population at each stage of the genetic algorithm;
- consistent application of all operators of the GA allows organizing the pipelining of all individuals.

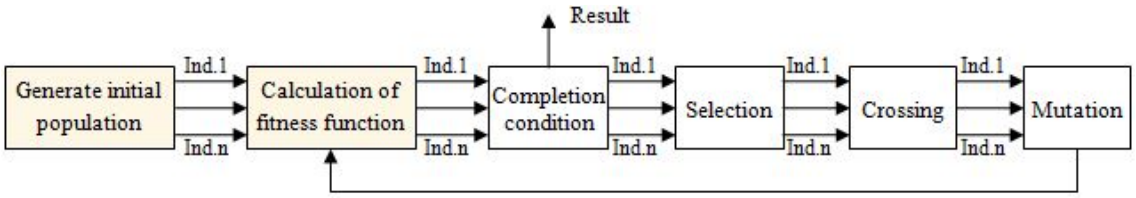

Figure 13. Flowchart of genetic algorithm

Each operator of genetic algorithm is a combination of elementary operators of Boolean algebra and applied to binary vectors. Therefore, micro controllers, digital signal processors or programmable logic arrays can be used for the hardware implementation of genetic algorithm; produced by analysis of the suitability of these devices for the hardware implementation of genetic algorithm. As programmable logic array has been selected programmable logic arrays such as FPGA. Criteria that assess the suitability of the above devices and estimations of suitability are presented in Table 1.

Table 1. Suitability of electronic devices for the hardware implementation of genetic algorithm

Criteria	Microcontroller	Digital Signal Processors	FPGA
Bit	Fixed	Fixed	Arbitrary
Clock frequency	Low	High	Medium
Effect of population size at run-time of genetic algorithm operators	Strong	Medium	Weak
Possibility of calculating the run-time of genetic algorithm operators	Good	Good	No
The possibility of implementing a quick calculation of the values of complex fitness functions	Bad	Medium	Good
The possibility of organizing parallel execution of genetic algorithm operators	No	Weak	Good
The complexity of making changes to the algorithm of the device for parallel execution of the genetic algorithm	-	Strong	No
The opportunity of pipelining for parallel execution of the genetic algorithm	No	No	Has
The complexity of the algorithm changes of the device	Strong	Medium	Weak

An analysis of the suitability assessment suggests that the FPGA is preferred for hardware implementation of genetic algorithm. Using the FPGA allows pipelining for parallel execution of the genetic algorithm and good opportunities for parallel execution of the genetic algorithm and rapid calculation of complex aim function values. The above features offer a maximum speed of the implemented device. Taking into account the architectural features of FPGA, a block diagram of the device for solving the inverse problem with using genetic algorithm was developed, which is shown on Figure 14.

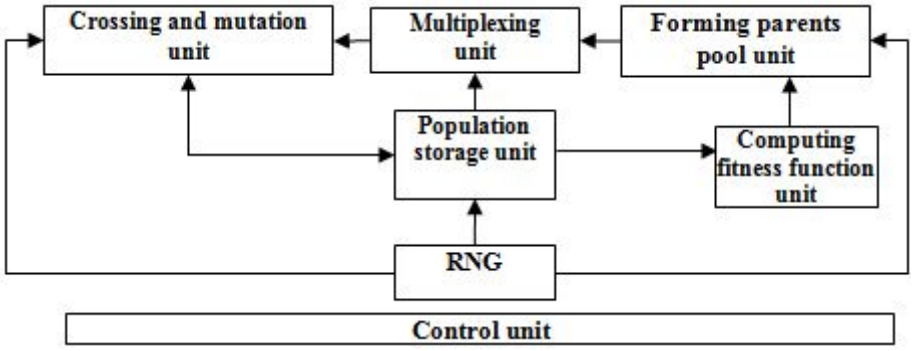

Figure 14. Block diagram of the device for solving the inverse problem with using genetic algorithm

Population storage device represents a block of memory cells. Each memory cell has its input and output ports, allowing for simultaneous treatment of all the memory cells. Each individual is stored in a single memory cell and has its own unique address.

Random number generator (RNG) generates random numbers with uniform distribution law. Random numbers are used to generate individual and addresses of individual, for a random selection of individual, to produce the parent pool, and to ensure the random nature of the operations of mutation and crossover.

Forming parents' pool device serves as a breeding. This device provides a device multiplexing the address of the chromosomes selected in the parent pool. Multiplexing device passes from the memory device of individuals in crossing and mutation device themselves in accordance with their addresses. Crossing and mutation device performs crossover and mutation at the same time, thus saving time and resources to the FPGA. The control unit has links with all the devices of the block diagram and provides the necessary sequence of operations of genetic algorithm and synchronization of all devices circuits.

Some options for hardware implementation in FPGA of some devices were investigated. The investigation purpose is to determine the fastest and least resource-intensive implementation of the genetic algorithm operators. Investigations were conducted by using the software package WebPack ISE, all characteristics were obtained for the family of crystal FPGA Spartan-6.

4.2. Hardware implementation of the forming parents pool device

In terms of hardware implementation is the most profitable tournament selection method. When using the method of selection based on the roulette you need to sum the values of fitness function of individuals. At one level of the logic can be executed only one summation. If the number of parallel processed chromosomes equal to 2^N, then N must be level logic to calculate the sum of fitness function of chromosomes. It takes a lot of FPGA resources and reduces the speed of device selection. Therefore, the choice of the selection method based on the roulette for hardware implementation of genetic algorithm is potentially disadvantageous.

Tournament selection method is implemented by two devices: comparison unit and the device selection of the individual. The inputs of the device came four values of the fitness function of individuals and their addresses. The output device is given the address of best individuals that participated in the tournament.

The choice of individuals for the tournament can be random or deterministic. In variant of the deterministic selection of individuals the population is divided into groups, including 4 individuals. For each group of tournament selection is carried out. As a result, 25% of individuals of parental pool (upper level) is formed Another 25% of individuals are selected by dividing the total population into four parts, which are extracted from the chromosome, standing in the same positions in each of the (average level). The remaining 50% of individuals are selected using the following algorithm: choose the first and second individuals s from the end and the beginning of the population, then the second and third individuals from the beginning and the end of the population, etc. When the deterministic choice of individuals during the formation of the parent pool and a flow of resources will be determined by the FPGA device of the tournament.

For case of a random selection address of individuals is formed by RNG. Figure 15 shows a schematic diagram of the device forming the parent pool for random selection of individuals.

The inputs of each data multiplexer fed fitness function values of all individuals simultaneously. The inputs to select the channel multiplexer receive randomly generated addresses. As a result, the

comparator (CMP) received two values of fitness function and the address of the individuals. The result of comparison is the address of the individual having the highest value of fitness function, which is issued on the external pins device.

For a random selection of chromosomes during the formation of the parent pool and consumption of resources will be determined by the FPGA multiplexers that provide a random selection of individuals.

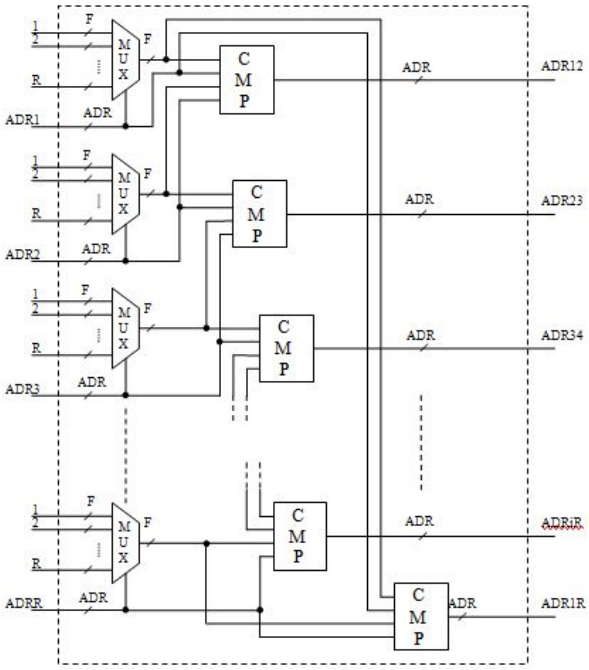

Figure 15. The device forming the parent pool for random selection of individuals

We have investigated the influence of population size:

- on the delay in forming a parent pool device for random selection of individuals (Figure 16, a) and the deterministic choice of chromosomes (Figure 16, b);
- on the use of LUT unit forming the parent pool for random selection of chromosomes (Figure 17,a) and the deterministic choice of chromosomes (Figure 17, b).

There are F - bit of aim function value, and R – the population size in these Figures .It is evident that a more rapid and effective method of choice is a deterministic choice of the individuals for parent pool. However, it is necessary to study the effect of this choice on the convergence of genetic algorithms in general, as the savings in time at this stage may lead to an increase in time to find an inverse problem solution.

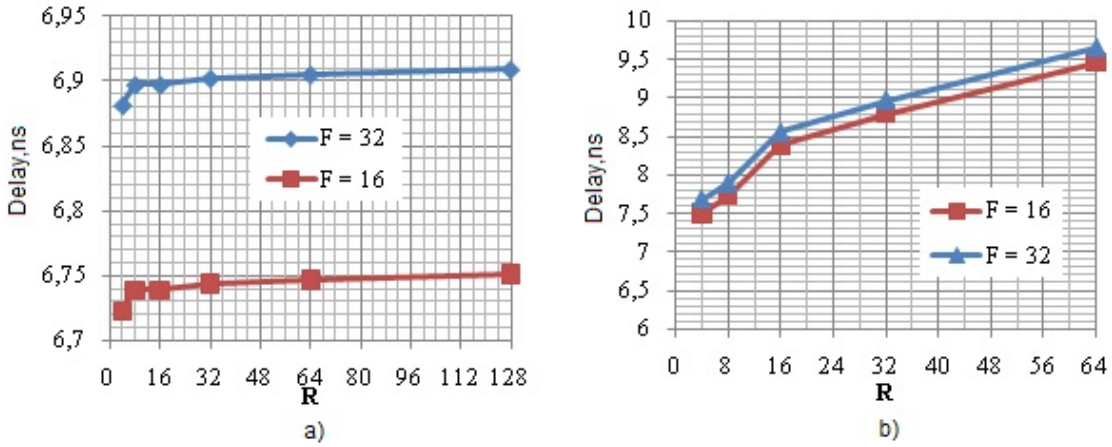

Figure 16. Influence of the population size on the delay in forming a parent pool

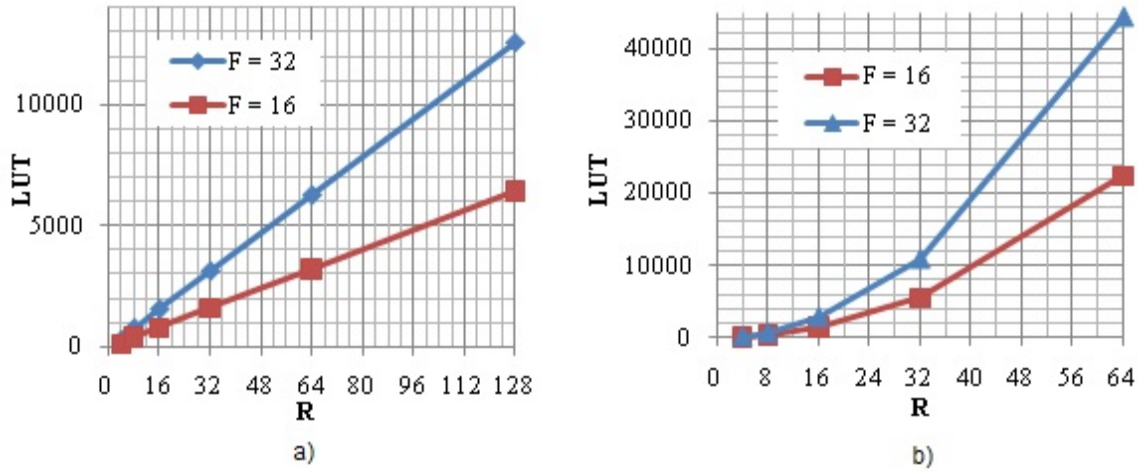

Figure 17. Influence of the population size on the using of LUT unit forming the parent pool

At a random choice the optimal number of parallel processed individuals is 32; for a fixed choice of individuals and at the same cost of resources 128 individuals can be treated. This population size reduces the number of iterations needed to find a solution.

4.3. Hardware implementation of the crossing and mutation device

The device must comply with crossing of individuals, selected at the stage of selection. The functional diagram of the device for crossing one pair of individuals is shown on Figure 18. The inputs of the device serve two parental individuals (P1 and P2) and the number of crossing point (T_C). Comparisons device compare the number of each bit with the number of crossing point, and depending on the result of comparing the multiplexer passes the output bit of one individual or another individual level, thus forming the two individuals are descendants (CH1 and CH2). L – is bit of individuals.

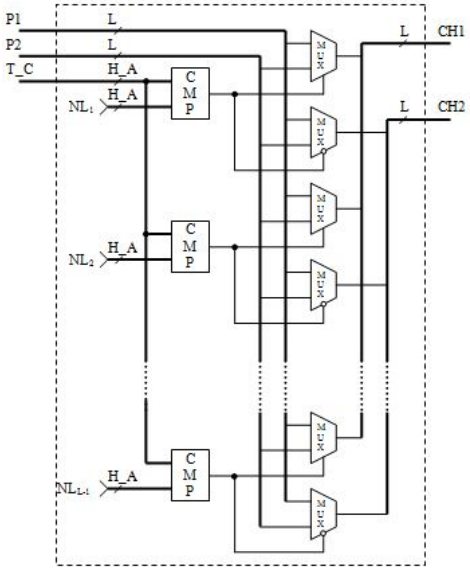

Figure 18. Functional diagram of the crossing device

Figure 19 shows the using of FPGA resources and time delay on the bit of the individuals, respectively.

For a crossing device requires a small amount of FPGA resources. The device has a high speed, it can be used with great individual bit (for example, when a large number of parameters of the aim function) and a large number of parallel processed individuals. The device of mutation is offered combined with a crossing device.

RNG has been implemented on the basis of parallel bit Fibonacci generators. This allowed us to receive one individual in a single cycle of the RNG at a low cost of logical resources. In forming the entire population in one cycle the number of required resources increases in R.

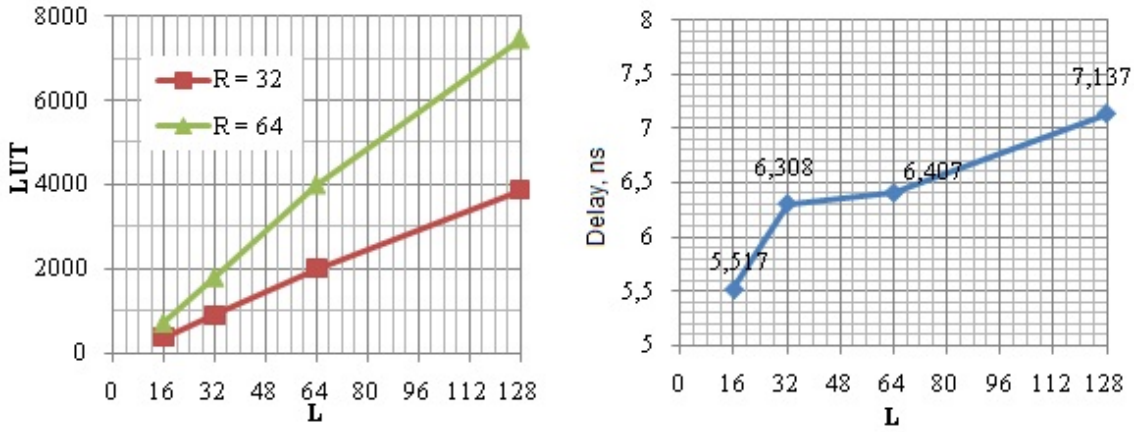

Figure 19. Influence of bits of chromosomes on the using of LUT device crossing (a) and the time of the delay in the crossing device (b) with use multiplexers

5. Conclusions

The main results are as follows:

- using complex spectral density $\dot{S}(\omega)$ as an informational characteristic increases sensitivity of an aim functions to changes in parameters of the probed medium;
- using an aim function Φ_2 with a complex spectral density of reflected signal allows for regeneration of ε' and h of the layers with error less than 1%, which is not possible to achieve using an aim function Φ_1 with a module of spectral density;
- the implementation of selection with a random selection of individuals requires a substantial expenditure of FPGA resources due to the introduction of additional multiplexing devices;
- avoiding the use of random number in the choice of individuals, crossing points etc. to reduce the consumption of FPGA resources, and free resources to spend on increasing the number of parallel processed individuals in order to reduce the search time for solving the inverse problem of subsurface probing.

References

1. Rexford, M. Morey. *Ground Penetrating Radar for Evaluating Subsurface Conditions for Transportation Facilities (Synthesis of Highway Practice).* Washington D.C.: National Academy Press, 1998. 37 p.
2. *Ground penetrating radar: theory and applications / Editor Harry M. Jol*. Elsevier Science, 2009. 524 p.
3. Krainyukov, A., Kutev, V. Model-based results of inverse problem solution for radar monitoring of roadway coverage. In: *Proceedings of the International Conference „Modelling of Business, Industrial and Transport Systems", 7th-10th May 2008, Riga, Latvia.* Riga: Transport and Telecommunication Institute, 2008, pp. 169-176.
4. Krainyukov, A., Kutev, V., Opolchenov, D. Reconstruction of the roadway coverage parameters from radar subsurface probing data. In: *Proceedings of the 8th International Conference "Reliability and Statistics in Transportation and Communication (RelStat'08), 15th-18th October 2008, Riga, Latvia"*. Riga: Transport and Telecommunication Institute, 2008, pp. 146-154.
5. Krainyukov, A. and D. Opolchenov. Using genetic algorithm for solution of inverse structural problem for radar subsurface probing, *Computer Modelling & New Technologies,* Vol. 14, No 1, 2010, pp.56-63. ISSN 1407-5806.

Transport and Telecommunication, 2010, Volume 11, No 4, 29–35
Transport and Telecommunication Institute, Lomonosova 1, Riga, LV-1019, Latvia

SOME FEATURES OF THE HOP MODEL OF EARTH-IONOSPHERE WAVEGUIDE

Yury A. Krasnitsky

Transport and Telecommunication Institute
Lomonosova str. 1, Riga, LV-1019, Latvia
Ph.: +371 67100608. Fax: +371 67100660. E-mail: krasn@tsi.lv

The problem of electromagnetic pulse radiator location from single station observation is considered, based on the hop model of pulse propagation in spherical waveguide 'Earth-ionosphere'. Pulse characteristics both ground wave and hop (sky) waves of that waveguide are modelled as functions of the distance from radiation source. The waveguide parameters, namely, the distance from the radiator and the effective reflecting heights of the ionosphere, can be evaluated through the delays of the waves reflected by the ionosphere with respect to the ground wave. The errors in values of delays give rise to the errors in the waveguide parameters. These connections are investigated. It is demonstrated how the waveguide parameter errors depend on the distances and heights of reflections. A method to reinterpret the hop model features by using some equivalent antenna array conception is proposed.

Keywords: electromagnetic radiation, ionosphere, waveguide, hop model, distance, effective heights, delays, lightning discharge, atmospherics

1. Introduction

Ionospheric layers and the Earth's surface which create a spherical waveguide with both semiconducting walls should have a significant influence on features of electromagnetic (EM) fields propagating in it. The rigorous method to find the EM field structure in this waveguide is based on a wave equation. The solution of it is an infinite series which divergence is too slow for distances lesser than 700-1000 km from radiation source. However those are the distances representing the region of interest for many technical applications, for instance, finding of lightning discharges positions by analysis of their own EM pulses named atmospherics only.

At relatively low frequencies (ELF, VLF and LF bands) the higher layers of ground and the lower ionospheric layer (D in daylight or E in night time) are good conductors. It is known that EM fields cannot penetrate deeply into those media. Consequently, geometric dimensions, namely the distance between the radiating and receiving points and the effective heights of the waveguide 'Earth-ionosphere', become the main factors, which determine the characteristics of propagation.

If the distance is not larger than 1500–1700 km, a hop model of propagation could be considered. It is supposed that the received signal consists of a ground wave and some waves reflected from the D or E ionospheric layer (Fig. 1). This model permits some methods for evaluating waveguide dimensions from a receiving signal only.

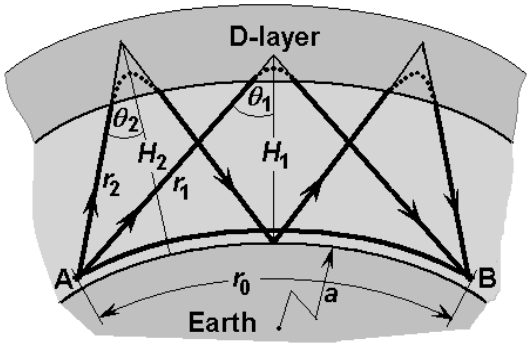

Figure 1. The hop model of ionospheric waveguide (in daytime)

EM radiation initiated from point A propagates to point B. The receiver in B registers the process of interaction of the ground wave $E_g(t)$ which has to pass the distance r_0 along the surface of the Earth,

and a few ionospheric waves. Only two waves from them are shown on Figure 1. The single-hop wave $E_{i1}(t)$ and the two-hop wave $E_{i2}(t)$ pass the ways signed as r_1 and r_2 being reflected from the effective heights H_1 and H_2 with angles θ_1 and θ_2 respectively.

The receiving signal in point B can be written as

$$u(t) = E_g(t) + \sum_{n=1}^{N} E_{in}(t) = I(0,t) * [h_c(0,t) * h_g(t) + \sum_{n=1}^{N} h_c(\theta_n, t) * h_{in}(t)], \quad (1)$$

where sign $*$ is symbol of convolution, $I(0, t)$ is the temporal form of the current pulse at antenna input points; $h_c(\theta, t)$ is the pulse function of antenna radiation in the direction set by angle θ, $h_g(t)$ and $h_{in}(t)$ are pulse functions of traces for ground wave and n-th ionospheric wave respectively.

Evidently, the reflected waves $E_1(t)$ and $E_2(t)$ are delayed in relation to the ground wave by the times indicated as τ_1 and τ_2 respectively.

2. Modelling the Waveguide Pulse Functions

The procedures for calculating of pulse functions $h_g(t)$ and $h_{in}(t)$ in Eq. (1) are briefly exposed below. Detailed description is in preparation to be published. Spectra all of these functions are evaluated in frequency domain in the band [500 - 0.25×10^6] Hz for different distances with subsequent return and restoration to the temporal forms by inverse fast Fourier transformation (IFFT).

a) Modelling of the ground wave

Representation proposed by V.A. Fok [1, 2] includes the infinite series with members which contain coefficients described by Airy functions. These series diverge slowly for short distances, and too many members (up to 40) may be necessary to keep in even if simplification for good conducting ground commonly employed in low frequencies bands is used in order to force calculations.

The graphs of the ground wave pulse functions $h_g(t)$ for different distances up to 600 km are represented on Figure 2 a. As one can look forward, the ground wave pulse function suffers distortions (becomes blurred) as the distance from EM radiation source is increased.

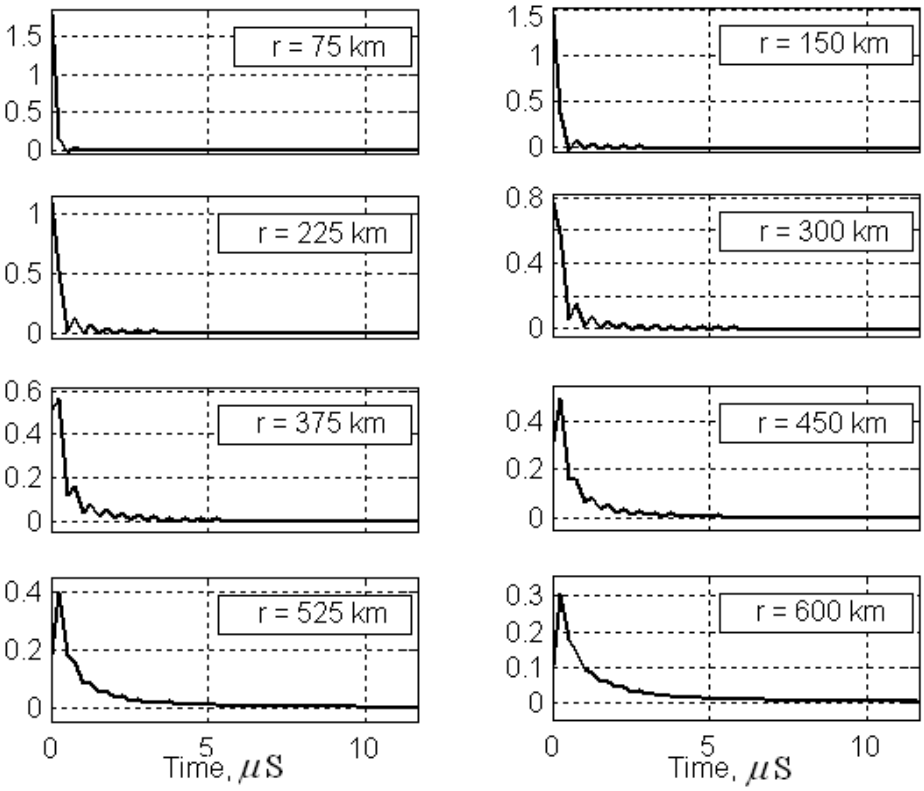

Figure 2 a. Ground wave pulse function

b) Modelling of the hop waves

Below the simplified procedure for calculation of first hop pulse function $h_{i1}(t)$ and in the event of vertical polarisation is considered only. If an inner spherical surface of ionospheric layer is approximated locally as a plane then reflected waves may be evaluated by Fresnel coefficients (see, e.g., [3]) with due regard for complex dielectric permeability of reflected ionospheric layer. The first hop function $h_{i1}(t)$ is IFFT of the frequency spectrum of named Fresnel coefficients.

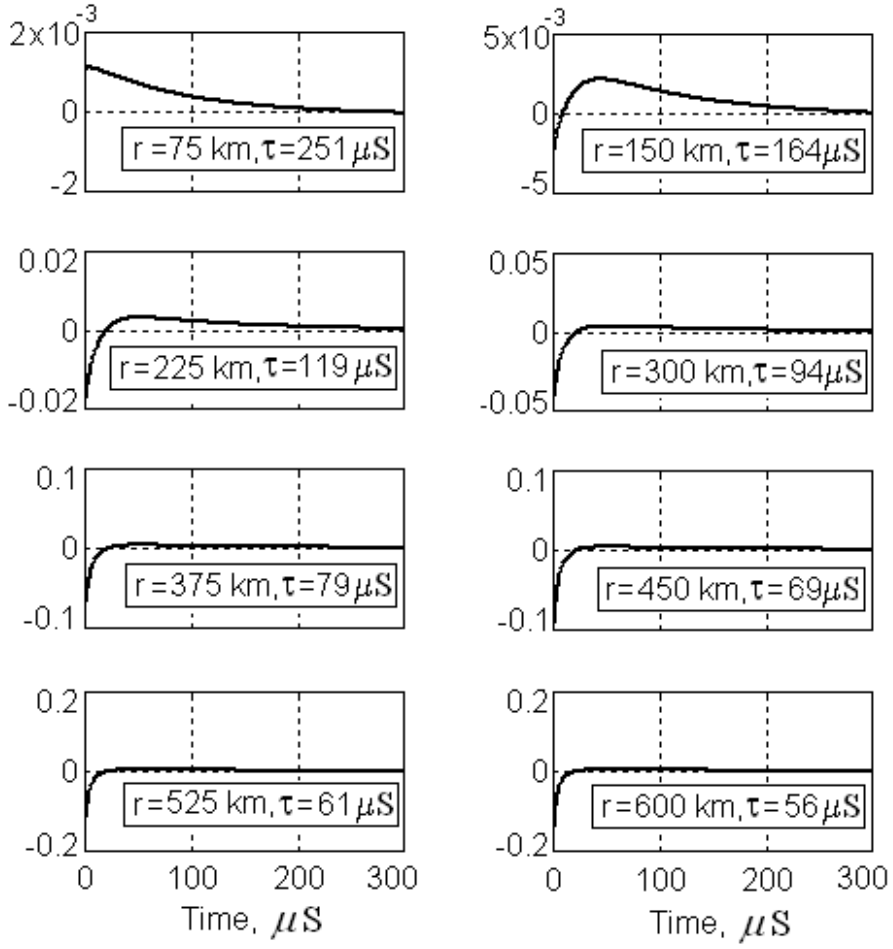

Figure 2 b. First hop sky wave pulse function

The graphs of $h_{i1}(t)$ represented on Figure 2 b for different distances are non-trivial. One can see that the pulse has to change the own sign as the distance is among 150-300 km from EM radiation source. Most likely, it has to be explained by pseudo-Brewster effect having a place in the event of electromagnetic waves with vertical polarisation.

3. Evaluation of Delays of Ionospheric Waves

The waveguide inherent features should appear as delays, or arrival times of those reflected waves. From the geometrical properties of the spherical waveguide with good conducting walls, one can obtain the system of equations

$$T_n = (1 - 2Z_n \cos R_n + Z_n^2)^{1/2} - R_n, \quad n = 1, 2, \ldots, \tag{2}$$

where $T_n = c\tau_n / 2na$, $R_n = r_0 / 2na$, $Z_n = 1 + H_n / a$ are normalized delays, distances and effective reflection heights respectively; $c = 2{,}998 \cdot 10^8$ *m/sec* is light velocity in a vacuum, $a = 6378$ *km* is the radius of the

Earth. Previously we have proposed to estimate these delays from the received signal with a pseudocepstral method using Huang – Hilbert decomposition [4].

As the two-hop model is considered, the system (2) consists of two equations, but three unknown quantities are in it, namely, the distance r_0 and the ionospheric waves' effective heights H_1 and H_2. Therefore, this system is undetermined, since the number of equations is less in 1 than the number of unknown quantities. The algorithms have been examined in [5] to expand the system based on some common physical considerations; Fermat's theorem, in particular.

Errors in the solving of the undetermined system have decisive influences on precision in the evaluation of waveguide parameters. The errors in estimation of ionospheric waveguide length and effective heights are considered below.

If digital processing of receiving signals is used these errors depend strongly on the sampling rate.

4. Inaccuracy in the Estimation of Ionospheric Waveguide Length

It is important to find specific relations for inaccuracy in the estimation of waveguide length r_0 with effective heights H_n and delays τ_n in equation (2). Differentiating the Eq. (2) by τ_n as an implicit function which relates the distances in spherical waveguide with the delay, one can obtain the relative inaccuracy of the waveguide length estimation

$$\delta r_0 = \frac{\Delta r_0}{r_0} = -\frac{c\Delta\tau_n}{2naR_n}\left(1 - \frac{Z_n \sin R_n}{T_n + R_n}\right)^{-1}, \tag{3}$$

where value $\Delta\tau_n$ is the absolute error of the estimation of the delay τ_n. It is obvious that the potential accuracy in the τ_n estimation by means of digital processing procedures has to correspond to the considered signal sampling rate.

The graphs of Eq. (3) for different reflection heights are represented on Figure 3. One can establish that the relative inaccuracy δr_0 depends on the evaluated distance r_0 non-monotonously. There are minima in middle distances (100–700 km) with positions depending on reflecting heights.

If ionospheric conditions are unperturbed (i.e. lower ionosphere edge H_0 is higher than perhaps 50 km) then the value $\delta r_0 \le 0.05$, as the sampling interval is no more than 1 microsecond. The errors increase noticeably as the height of reflecting layer is reduced. Thus, they would be larger in the daylight when the D-layer plays a main part in reflection process than in the night time when the D-layer disappears and the E-layer becomes the essentials. It would be expected in the last case that the value δr_0 does not exceed 0.02.

The area painted over on Figure 3 corresponds to the ordinary locations of reflecting D and E layers in the ionosphere.

Extremely great errors of distance estimation should be observed when ionospheric perturbations are influenced by strong ionisation factors, and reflecting layers can rise to smaller heights than in unperturbed conditions. The hypothetic case for $H_0 = 20$ km is also illustrated on Figure 3. It is found in this situation that the errors for middle distances have to increase very sharply up to more than four times in contrast to errors for ordinary conditions.

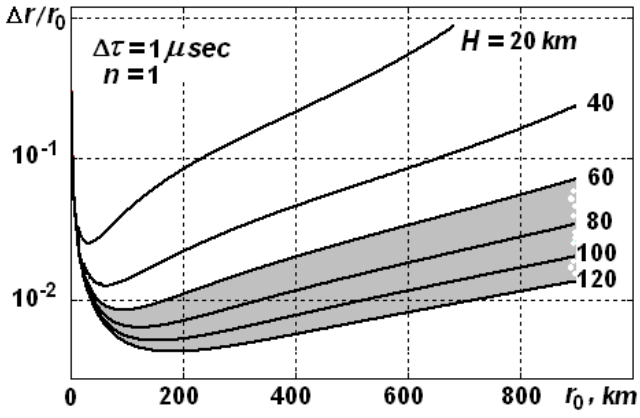

Figure 3. Relative inaccuracy of waveguide length estimation

As the value δr_0 depends on the evaluated distance r_0 non-monotonously, it can find the minimum position of r_0 for every reflection height. Examining Eq. (3) for extreme points, one can obtain the transcendental equation for the distance r_{0min}

$$[(Z_n \cos(r_{0min}/2na)-1](r_{0min}+c\tau_n)r_{0min}+[2naZ_n \sin(r_{0min}/2na)-r_{0min}-\tau_n]c\tau_n=0. \quad (4)$$

The required value r_{0min} is determined by the positive root in it. As the argument of trigonometric functions is small, then expression (4) can be approximated after corresponding simplifications by the quadratic equation in the form

$$r_{0min}^2+2c\tau_n r_{0min}-(c\tau_n)^2 a/H_n \approx 0. \quad (5)$$

The positive root of it is

$$r_{0min}=c\tau_n[(1+a/H_n)^{1/2}-1] \approx c\tau_n (a/H_n)^{1/2} \approx 0., \quad (6)$$

where it is taken into account that $a/H_n >> 1$.

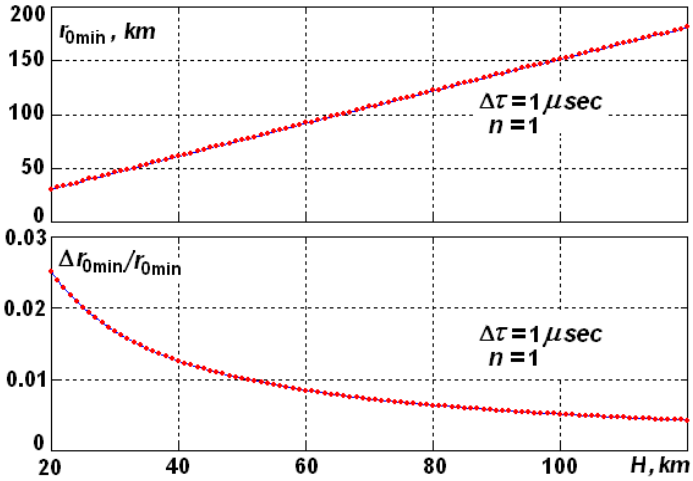

Figure 4. Solutions of Eq. (4)

Positions of the minima of Eq. (4) are displayed on Figure 4 in relation to the reflection height H_1. It follows from it that the approximation of the function $r_{0min}(H)$ with a straight line is rather good. In that time, errors of distance estimation at minima points are very small.

It is seen from Figure 2 that the errors of distance estimation become especially great if r_0 is very small (r_0<10 km) or if r_0 is near maximum distances (r_0~1800 km) still satisfied the hop model. In order to reduce these errors the usual method can be used, namely, to scale down the sampling interval in received signal digital processing. However, a necessary condition for this is the extension of the receiver frequency band. Complex upgrading of the receiver set may be necessary because of this. An alternative is simulated frequency band dilation using digital processing methods which leads to an evaluation of delays with a higher resolution than the sampling interval.

It is necessary to note that one can use Eq. (3) as an additional condition to redefine the undetermined system (2). Setting the maximum tolerable limit δr_{0tol} for distance estimation error, Eq. (3) may be apply as the inequality in a form $\delta r_0 < \delta r_{0tol}$ which restricts additionally the decision space of (2) by limiting r_0 and H_0 coupling.

5. Inaccuracy in Estimation of Ionospheric Waveguide Reflection Height

By analogy with (3) the error in the estimation of waveguide reflection height may be expressed via waveguide length r_0 and reflected wave delay τ_n. Supposing $H_n = H_n(\tau_n)$ and differentiating Eq. (2) by τ_n as an implicit function which relates the reflection height with the delay, one can obtain the relative inaccuracy of the estimation for H_n

$$\delta H_{\rm n} = \frac{\Delta H_{\rm n}}{H_{\rm n}} = \frac{c\Delta\tau_{\rm n}}{2nH_{\rm n}} \frac{T_{\rm n} + R_{\rm n}}{Z_{\rm n} - \cos R_{\rm n}}. \tag{7}$$

If r_0 is increased, the error (7) enlarges monotonically as it is seen on Figure 5. The painted over area corresponds with the ordinary heights of reflecting D and E layers in ionosphere.

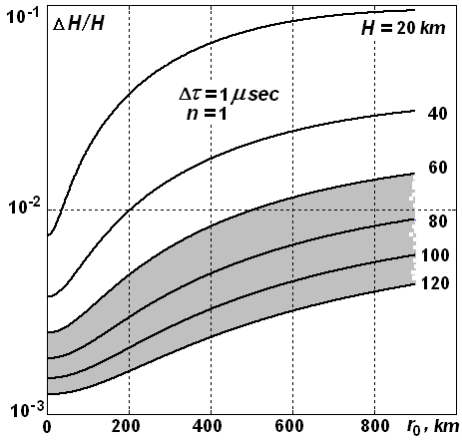

Figure 5. Relative inaccuracy of waveguide reflection height estimation

For the small $r_0 \to 0$ it may be discovered that $\tau_{\rm n}$ tends to $2nH_{\rm n}/c$. Thus, the error (7) achieves the minimum value

$$\delta H_{{\rm n}min} = \delta H_{\rm n}\Big|_{r_0 \to 0} = \frac{c\Delta\tau_{\rm n}}{2nH_{\rm n}}. \tag{8}$$

If sampling interval $\Delta\tau$ is no more than 2 microseconds and conditions in the ionosphere are unperturbed, error values (8) have not to exceed $0.5 \cdot 10^{-2}$. This is better by up to approximately one order than the errors (3) of waveguide length estimation.

6. Array Antenna Model of EM Waves Excitation in the Ionospheric Waveguide

The explanation for the fairly high accuracy of waveguide parameters estimation in hop model frames may be proposed as follows. Let us suppose that every wave which is a part of the sum in (1) is excited by a separate source S_0, S_1, S_2, as it is on Figure 5 for two-hop model. These waves pass from the mentioned sources to receiving point B. The ways r_0, r_1, r_2 are different but they are the same as in the initial hop model (see Fig. 1). The sources form a discrete antenna array S_0, S_1 and S_2 represented on Figure 6.

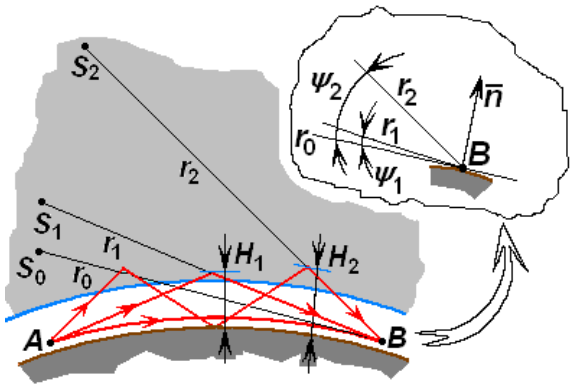

Figure 6. The equivalent antenna array included in the hop model

If the origin of the spherical coordinates system is selected at the point *B* then the positions of the sources have to be described by the equations:

$$R_{\mathrm{n}} = (Z_{\mathrm{n}}^2 - 2Z_{\mathrm{n}}\cos(r_0/2na) + 1)^{1/2}, \tag{9}$$

$$\psi_{\mathrm{n}} = \arccos\frac{\boldsymbol{Z}_{\mathrm{n}}\sin(\boldsymbol{r}_0/2\boldsymbol{na})}{\boldsymbol{R}_{\mathrm{n}}}, \qquad \boldsymbol{n} = 1, 2 \tag{10}$$

The distance r_0 is read off along the tangent line direction to the Earth's surface at the point *B*. The spacing d_{10} and d_{21} among radiators S_1, S_0, and S_2, S_1 are correspondingly

$$\boldsymbol{d}_{10} = (\boldsymbol{r}_0^2 + \boldsymbol{r}_1^2 - 2\boldsymbol{r}_0\boldsymbol{r}_1\cos\psi_1)^{1/2}, \tag{11}$$

$$\boldsymbol{d}_{21} = [\boldsymbol{r}_1^2 + \boldsymbol{r}_2^2 - 2\boldsymbol{r}_1\boldsymbol{r}_2\cos(\psi_2 - \psi_1)]^{1/2}. \tag{12}$$

In general, these spacings are not small in terms of wavelengths even if radiation frequencies are relatively low (ELF, VLF or LF bands). Hence, the antenna array has to possess obviously pronounced directivity. Perhaps, that is the feature which allows us to explain the high potential accuracy in waveguide parameters estimation using the hop model.

This situation is typical for lightning discharge location when an EM pulses of lightning (atmospherics) are received at a single point only.

7. Conclusions

In this research the hop model of the propagation of an electromagnetic pulse from a source allocated in the Earth-ionosphere spherical waveguide is considered. The procedures for calculating of pulse functions of ground wave and hopped sky waves are briefly exposed. The results are represented for distances up to 600 km. The pseudocepstral method is recommended for evaluating the delays of reflected ionospheric waves. Specific dependencies are established for waveguide parameters estimation accuracy in the hop model propagation frames. If ionospheric conditions are not perturbed, this accuracy is acceptable for many operational applications. A modification of the hop model is offered by introducing of a discrete antenna array based on conservation of the lengths for all the rays as in the initial hop model.

References

1. Fok, V.A. *Problems of diffraction and propagations of electromagnetic waves*. Moscow: Soviet Radio, 1970. 517 p.(In Russian)
2. Kalinin, A.I., Cherenkova, E.L. *Propagation of radiowaves and radio traces design*. Moscow: Svyaz, 1971. 439 p. (In Russian)
3. Orfanidis, S.J. Electromagnetic waves and antennas. (2002 – on-line version) – http:\\www.ece.rutgers.edu/~orfanidi/ewa
4. Krasnitsky, Y.A. Pseudocepstral analysis of electromagnetic transients using empirical mode decomposition. In: *Proc. of the9th Int. Conf. "Reliability and Statistics in Transport and Communication" (RelStat'09), Riga, Latvia*, 2009, pp. 329-334.
5. Krasnitsky, Y.A. Lighting stroke passive location by atmospherics analysis in the hop model frames. In: *Proc. of the 2nd Int. Symp. "Space and Glob. Security of Human" (SGS2010), Riga, 5-9 July 2010.*

Transport and Telecommunication, 2010, Volume 11, No 4, 36–45
Transport and Telecommunication Institute, Lomonosova 1, Riga, LV-1019, Latvia

COVERAGE ESTIMATION IN SINERGIC NETWORKED INTELLIGENT TRANSPORTATION SYSTEMS WITH NON-ISOTROPIC NODES

***Victor Krebss*[1], *Boris Tsilker*[2]**

[1]*CPS, Ltd*
Skanstes str. 13, Riga, LV-1013, Latvia
Ph.: +371 29243923. E-mail: victor@cps.lv

[2]*Transport and Telecommunication Institute*
Lomonosova str.1, Riga, LV-1019, Latvia
Ph.: +371 67100604. Fax: +371 67100560. E-mail: tsilker@tsi.lv

Safety of road travel is of the most considerable tasks solvable by intelligent transportation systems (ITS). It can be solved by mutual interaction of nodes equipped by sensors forming a sensor network. The wireless sensor networks can be integrated into ITS as vehicles through vehicle-to-vehicle or infrastructure-to-vehicle communication models to monitor the road condition, construction sites or obstacles for driving safety and to announce such road. Wireless sensor networks also pose a number of challenging optimisation problems. Coverage problem was and remains a fundamental issue in construction of wireless networks.

Most of known investigations, concerned with optimal (in sense of ensuring of necessary coverage level at every point in service area) deployment of networks' nodes, i.e., with optimal network topology, study the problem on the assumption that wireless network service area is free from obstacles, impeding normal propagation of information signals [1-3]. As a result, suggested network topologies become far from optimal at presence of obstacles within serviced area. More realistic solution presumes taking into account of obstacles within the serviced area.

Possible approaches for efficient placement of wireless network nodes on condition that service area contains obstacles are discussed at present work. Problem is examined from two points of view: as a probabilistic task, as well as a task of computational geometry. A probabilistic model is more realistic because the sensor design and environmental conditions are all stochastic in nature. Interference and noise in the environment can be modelled by stochastic processes. The investigation has resulted in some algorithms and considerations for near to optimal deployment of nodes within network service zone with obstacles.

Keywords: Intelligent Transportation System, anisotropic sensor, sensor network, coverage, service area

1. Introduction

Among the wide range of transportation problems, more or less successfully solvable by means of intellectual transportation systems (ITS), the road safety problem undoubtedly is the most significant. Such kind ITS, due to the real time processing of information, incoming both from onboard and road infrastructure sensors, give a chance to ensure on-time response on vehicle movement within the traffic stream.

Each sensor in its sensing range, gives a certain information type, whether on approaching obstacles or dynamically changing transport stream characteristics, such as velocity, acceleration, turns, oncoming vehicles, etc. Creation of ITS presupposes organization of transport flow participant interaction. Consequently, such ITS, are organized as ad hoc sensor networks, based both on infrastructure sensors and on-board ones.

One of the important tasks in ad hoc sensor network development is insurance of coverage over transport flow area should be controlled. In the most studied area of coverage problems (e.g. [1–5]), the sensing ability of sensors is abstracted as isotropic (a circular region or disk), and an event or target is detected in a binary sense, depending on whether it is inside such sensing disk or not. To the contrary, in real life situations most of sensors, being used in the ITS, such as cameras, directional microphones, radars, etc. have anisotropic coverage area, represented by directional sector and determined both by its location and orientation.

Coverage estimation and optimal placement of anisotropic sensors, forming sensor network, still remains insufficiently studied. In this paper several approaches that can be applied to such type of tasks are overviewed and evaluated. A few typical traffic scenarios are discussed as well as corresponding approaches for anisotropic coverage evaluation and optimal sensor placement.

2. Sensory Devices

The intersection collision avoidance (ICA) is one of the significant issues in developments of intelligent traffic system. At many intersections, some buildings or trees may obscure the crossing traffic near the road or other vehicles. Moreover, the vehicle sensors cannot often detect the threat conditions alone. Development of intersection collision countermeasures systems is a crucial and urgent challenge.

For preventing of potentially dangerous transport situations it is essential to know relative position and velocity, direction and acceleration of transport traffic participants .Such kind information can be obtained either explicitly or implicitly, depending on type of information sensors employed.

In ICA systems, the positioning of the vehicles in lanes should be very accurate within some required tolerances before the vehicles cross the intersection. For instance, a vehicle will move 20m in 1 second if its speed is 72 km/hr. ICA system architecture has to provide a mechanism to acquire reliable positioning of the approaching vehicles at an intersection. In general, the positioning accuracy tolerance is less than 1 m for a moving vehicle approaching the intersection with 100 km/hr.

Taking into consideration specifics of given task, following sensor types could be applicable for ITS: microwave radars, ultrasonic and infrared range sensors. Sensing range of these sensors can reach up to 250 meters distance. Sensing zone, as a rule, represents a sector of a disk. For instance, FMCW radar systems have an aperture angle within 60^o in horizontal plain and 5^o in vertical plane.

In Figure 1, the subscript i denotes the specified properties in Lane i of an intersection, e.g., D_i is the horizontal distance of a vehicle from the radar sensor at the intersection, $D_{max,i}$ and $D_{min,i}$ denote the maximal and minimal distances measured by the radar sensor, respectively, $D_{F,i}$, and $D_{R,i}$, respectively denote the front and rear buffer distances of the measured vehicle, H_i is the height of the sensor, R_i is the range between the sensor and the vehicle, V_i is the speed of the vehicle, $\Delta\theta_i$ is the bore size angle of the radar transmitter, and the inclination angle of radar antenna is equal to $\theta_i + \frac{\Delta\theta_i}{2}$. H_i, θ_i, and $\Delta\theta_i$ are assigned when the radar system is installed. $D_{F,i}$ and $D_{R,i}$, depend on the traffic conditions of different lanes and can be assigned. $D_{F,i}$ and $D_{R,i}$, are suggested to be longer if the speed limit of the lane is higher. They can overcome the positioning errors and can comply with the safety requirements. In addition, R_i and V_i can be measured by this radar system [9].

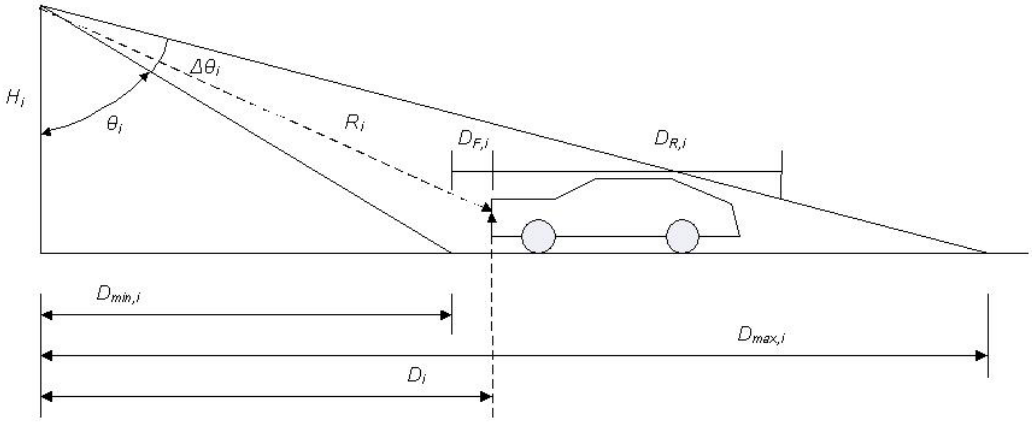

Figure 1. The configuration of the radar system in Lane *i* of an intersection

Figure 1 shows a typical configuration of the radar system in Lane i at intersections for the ICA system. An overhead mounted microwave radar system transmits energy to an object and receives the reflected energy from a measured object. The reflected signal from a vehicle can be used to detect the positions, speeds, presences, lane occupancy, and passages of vehicles in the lane. There are two types of microwave radar sensors used in roadside applications. One is the continuous wave Doppler radar utilized to measure the speed of vehicles. The other is the frequency modulated continuous wave (FMCW) radar utilized to detect the positions of vehicles usually. The measured range, R_i, can be

$$R_i = \frac{c\Delta f_i}{4 f_{m,i} \Delta F_i}, \tag{1}$$

where c is the light speed, Δf_i is the instantaneous difference in frequency of the transmitter at the times the signal transmitted and received, $f_{m,i}$, is radio frequency (RF) modulation frequency, and ΔF_i is the bandwidth of the modulated frequency. The range resolution, ΔR_i, resolved by an FMCW radar is

$$\Delta R_i = \frac{c}{2\Delta F_i}. \tag{2}$$

In case the radar operates in 10.5GHz band with the bandwidth 45MHz, the range resolution is 3.3m at best.

Comprehensive facilities open up since vehicles more and more widely are being provided with the global positioning system receivers, giving the coordinates of the vehicle, equipped with such a receiver. In any case, Prevention of accidents is reached by sharing of the information from the both vehicle onboard and transportation infrastructure sensors. It is obvious that all objects involved should be equipped with communications facilities.

Two types of communications are possible, namely, Vehicle-to-Vehicle (V2V) and Vehicle-to-Infrastructure (V2I) communications. In the V2V, vehicles are equipped with sensors in order to exchange information that is crucial to avoid severe situations like traffic jam avoidance. In V2I, information flow from vehicles to sensors installed on roadway infrastructure. This communication is necessary in propagating awareness about traffic conditions, especially on highways, to support safer commuting.

3. Traffic Scenarios

There are several typical traffic scenarios [6], which may lead to potential accidents and then it is shown how the potential accidents can be avoided, if the vehicles involved in these situations are equipped with sensors and have communicating capabilities to exchange data with other vehicles in the inter-vehicle network.

Rural area with single lane traffic

Considering the typical traffic situation depicted on Figure 2, three vehicles A, B and C are shown on the road. Initially, assume that the vehicles are not equipped with any sensors and are not part of any sensor network. Vehicle A and vehicle C cannot see each other. If vehicle A tries to overtake vehicles B, it may collide with the approaching vehicle C. These types of accidents can be avoided with the help of sensors and intelligent sensor networks. Now, consider that vehicles A, B and C are equipped with front-collision avoidance sensors using millimetre-wave radar or scanning laser. They also must have communication capability, so that they can exchange sensors' data among themselves. Vehicles B and C can sense each other and so can vehicles A and B. So vehicle A knows that there is a vehicle approaching i.e. vehicle C and it will not overtake.

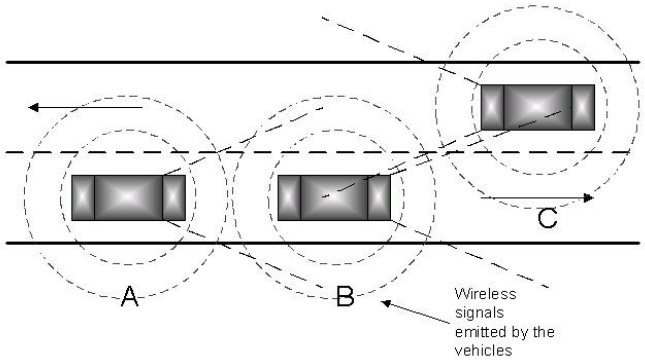

Figure 2. Traffic on a bridge or in a rural area

Freeway: Entry and Exit ramps

Ramps, being the entries and exits of freeway systems, usually are places where many high velocity accidents take place because of the merging traffic and variation of the vehicle speed. Consider the case shown on Figure 3. It shows an entry ramp onto a freeway. Vehicle A and vehicle C cannot see

each other and this may lead to a collision since vehicle A wants to enter the lane. But if the vehicles can exchange data among them, then this can be avoided. As soon as vehicle A nears the ramp it becomes a part of the ad hoc network and joins vehicle B and C. So now vehicle C knows that there is a vehicle entering from the ramp and it can adjust its speed to let vehicle A merge in between itself and vehicle B.

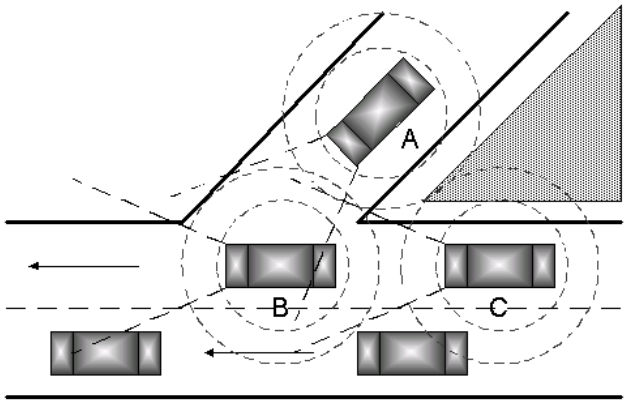

Figure 3. Typical situation at an entry ramp

Street Corners

The traffic patterns at street corners are unpredictable and can often lead to dangerous situations. On Figure 4, vehicle A wants to overtake vehicle B. Vehicle A cannot see vehicle C. If vehicle A changes the lane to overtake vehicle B it may collide with the approaching vehicle C. This could be avoided if the vehicles can exchange data. If vehicle B is equipped with vision sensors, it can sense vehicle C and send a signal to vehicle A that vehicle C is approaching. So vehicle A will not overtake and the collision will be avoided. The data flow from vehicle C to vehicle A has to pass through vehicle B.

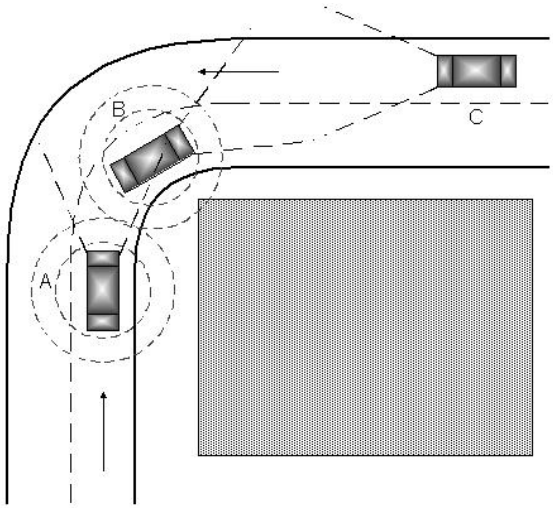

Figure 4. Corners like these host many accidents due to driver misjudgement around the blind turn

Intersections

Even though the common ITS infrastructure based safety system may exist at certain intersections, still, a networked approach for communication among vehicles can increase the level of safety. On Figure 5, a traffic scenario at a road intersection is shown. Assume that the signal for the horizontal lanes has been turned green and consequently the signal for the vertical lanes is red. Vehicle B wants to make a right turn while vehicle A wants to proceed straight from left to right. Neither of the vehicles can see each other due

to vehicle C. If the vehicles are able to communicate with each other, then vehicles A, B, D, E and F could form a sensor network and could communicate with each other. A and B can use their sensed data and data from other vehicles to avoid a collision even though vehicle C is blocking the direct line-of-sight view between them. Each vehicle would know the position and the velocity of the other vehicle using area coverage techniques and would take appropriate measures to avoid the accident and cross the intersection safely. The major challenges in such cases are that, there being many vehicles in its communication range, vehicle B should be able to obtain only those data which are useful while neglecting data from other vehicles. On Figure 4, vehicle G has already turned right, so its information is not useful for vehicle B and hence should be neglected.

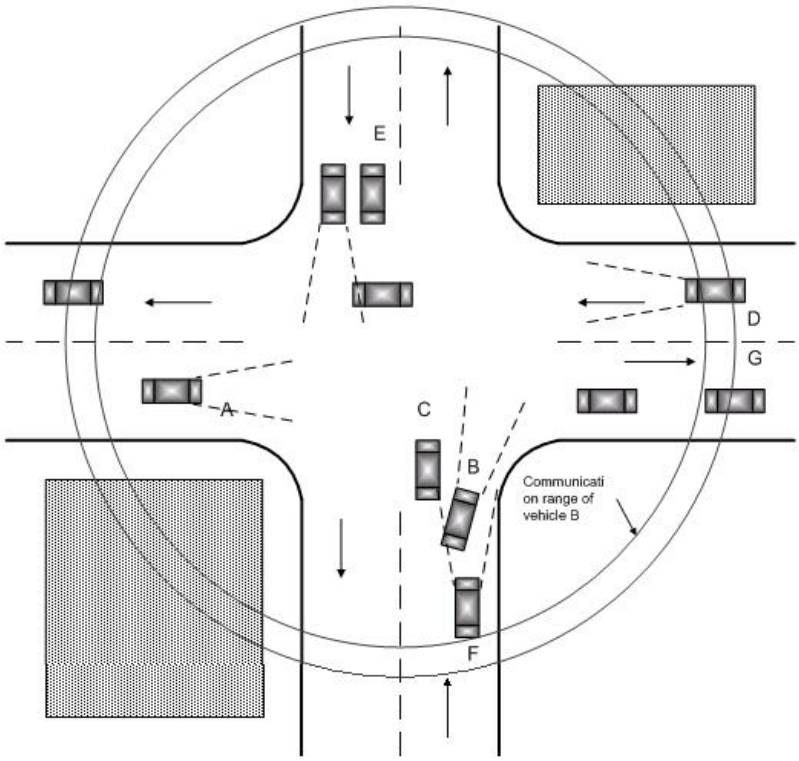

Figure 5. Vehicles at an intersection

4. Coverage in Sensor Networks

The millimetre-wave radar can be used for detecting the distance of obstacles or other vehicles. It can detect targets even during stormy conditions and simultaneously measure both the target's distance and its relative velocity. Common, isotropic sensors detection model can be described as (3),

$$p(d) = \frac{K}{d^k}, \tag{3}$$

where K – is the energy emitted, κ – is the decay coefficient and d – is the distance between the sensor and the object. The sensing power of such sensors can be expressed as a normally distributed function as shown in equation 4. The sensing model follows a Gaussian distribution with mean μ and variance σ.

$$p(d \mid \mu, \sigma^2) = \frac{1}{\sqrt{2\pi\sigma^2}} e^{\frac{-(d-\mu)^2}{2\sigma^2}}. \tag{4}$$

When the sensing ranges of vehicles overlap, the sensing strength in the overall area around the vehicles also increases. This in turn increases the probability of detection of any other sensors or obstacles or other vehicles without sensors which may enter that area. Hence, this leads to the overall increase of sensing ability of the sensors in that area (5).

$$p = 1 - (1 - p_1)(1 - p_2)(1 - p_3), \tag{5}$$

where p is the total probability of detection and p_1, p_2 and p_3 are the probabilities of detection of individual sensors.

In the above detection fusion scheme, the distance between two sensors/vehicles is very important. In case when V2I communication scheme is possible, additional road infrastructure based sensors can be used to increase resulting detection probability.

However, most of the sensors such as cameras, directional microphones, radars etc are anisotropic. And its coverage area can be described rather as a sector than a circular region (Fig. 6). This makes network coverage evaluation task much more complicate. Several possible approaches to coverage evaluation for an anisotropic sensor net coverage overviewed in the next section.

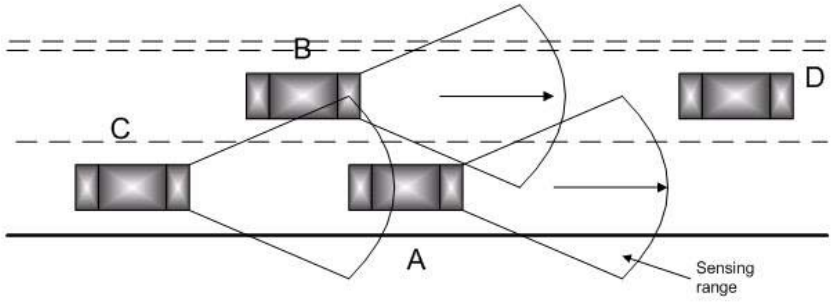

Figure 6. Vehicles with MMW radar on the road

5. Approaches to Coverage Evaluation

Geometric Approach

The following parameters completely characterize the sensing sector of an anisotropic sensor node i. (x_i, y_i): the Cartesian coordinates that denote the location of the sensor in a two-dimensional plane. θ: the field of view (FOV), describing the maximum angle of sensing achieved by directional sensor. R_s: maximum sensing range of the sensor, beyond which a target will not be detected in a binary detection sense. $\overrightarrow{d_{i,j}}$: a unit vector which cuts the sensing sector into half. This parameter defines the orientation of the directional sensor.

It is assumed that a directional sensor can only take a finite set of orientation set of orientations. For example, a directional sensor with $\frac{\pi}{4}$ of FOV can pick eight orientations with mutually disjoint sensing sectors which can be combined to generate the full circular view of an isotropic sensor. With each choice of orientation, a certain subset of targets is covered by the directional sensor.

The relationship of a directional sensor, its orientation and a target can be determined by a Target in Sector (TIS) test [7]. The TIS test can be described as follows. Consider a target k located at $\vec{t}_k$ and a directional sensor i located at $\vec{l}_i$. In order to determine whether the target k can be sensed by the directional sensor i with the j-th orientation, we follow the following steps:

Calculate the distance vector $\overrightarrow{v_{i,k}}$, pointing from the directional sensor i to the target k $\overrightarrow{v_{i,k}} = \vec{t}_k - \vec{l}_i$. Check whether the resulting distance vector is within the FOV of the directional sensor i by performing the inner product operation:

$$\vec{d}_{i,j}^{T} \cdot \vec{v}_{ik} \geq \left\| \vec{v}_{ik} \right\|_2 \cos\left(\frac{\theta}{2}\right). \tag{6}$$

Then verify whether or not target *k* is within the sensing range of the directional sensor *i* or not by checking

$$\left\| \vec{v}_{ik} \right\|_2 \leq R_s, \tag{7}$$

with equality when the target *k* is on the arc of the sensing sector of the directional sensor *i*.

If both (6) and (7) hold, the result of the TIS test is true (i.e. node *i* covers the target *k* if it sets its orientation to *j*) otherwise, it is false.

Let Φ_{ij} denote the set of targets that are covered by sensor *i* when its orientation is *j*. Then we can determine all the sets $\Phi_{ij} \forall i, j,$ by running the TIS test for every *i* ,*j*.

Voronoi Tessellation Based Approach

The approach is based on Voronoi tessellation. The consideration of a general anisotropic sensor model results in an anisotropic Voronoi tessellation which is difficult to analyse. Therefore the optimal control law for the coverage problem is derived assuming a fixed, equal sensor orientation and a specific class of anisotropic sensors with elliptic sensing performance level sets is assumed instead of circles as for the isotropic case. The idea is to transform the anisotropic problem to the isotropic one. By the transformation properties the control law obtained for the isotropic problem also solves the problem for the considered anisotropic case (Fig. 7).

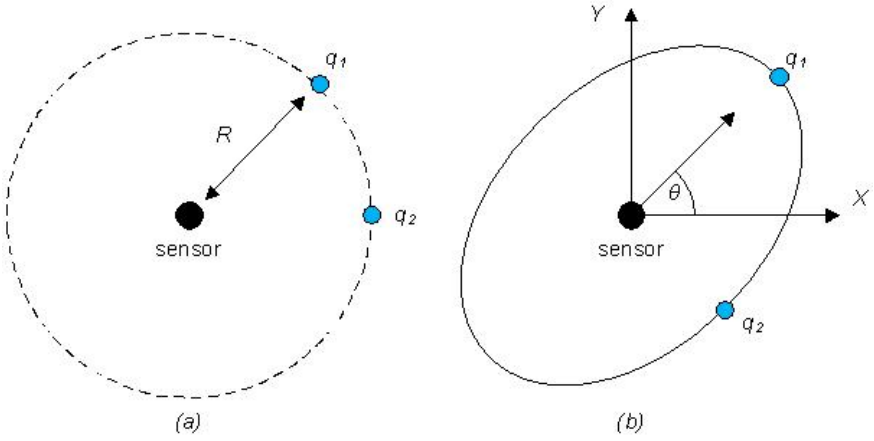

Figure 7. (a) Isotropic sensor model, (b) Anisotropic sensor model

Euclidean distance measure the Voronoi region [8] V_i associated with its generator p_i is defined as:

$$V_i^* = \left\{ q \in Q \mid \left\| q - p_i \right\|_{L_i} \leq \left\| q - p_j \right\|_{L_i}, \forall j \neq i \right\}. \tag{8}$$

Where the sensing performance defined as $f\left(\left\| q - p_i \right\|\right)$ that degrades with the distance between a point $q \in Q$ and the *i*-th sensor position p_i. The points where probability is equal are represented by a circle of radius *R*, and the centre is the sensor location. Point's q_1 and q_2 with the same distance to the sensor will result to the same sensing probability. The sensing performance of the anisotropic sensor model is given by the non-Euclidean distance measure defined as $\left\| q - p_i \right\|_{L_i}^2 = \left(q - p_i\right)^T L_i \left(q - p_i\right),$ where the matrix L_i is positive definite and can be decomposed as $L_i = F_i^T F_i$, with

$$F_i = \left[\begin{pmatrix} \frac{c}{a} & 0 \\ 0 & \frac{c}{b} \end{pmatrix} \begin{pmatrix} \cos\theta_i & \sin\theta_i \\ -\sin\theta_i & \cos\theta_i \end{pmatrix} \right], \tag{9}$$

where θ_i is the orientation of the *i*-th sensor, and $a,b,c > 0$ are the parameters.

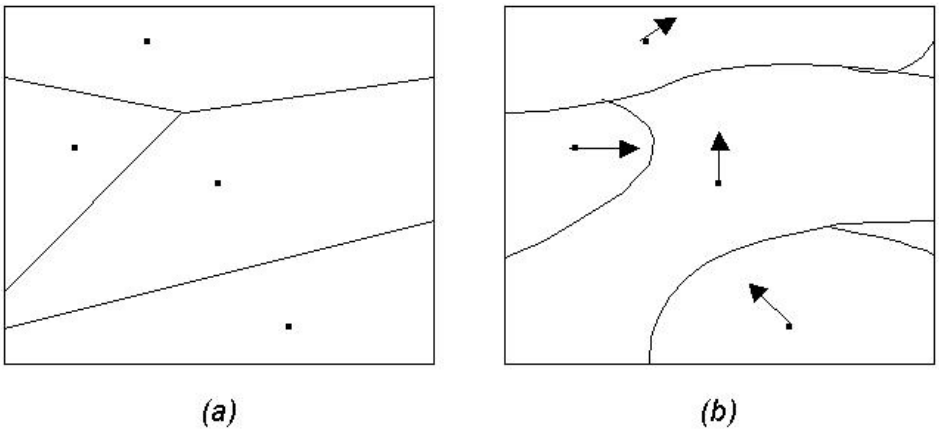

Figure 8. (a) Isotropic Voronoi partition, (b) anisotropic Voronoi partition

This anisotropic Voronoi partition is not only determined by the sensors position but also the sensor orientation θ_i as observable from matrix L_i. As a result the anisotropic Voronoi tessellation is no longer composed of convex polytopes, but of curved possibly non-convex regions (Fig. 8). Major difference to isotropic Voronoi tessellations is that anisotropic tessellations may contain regions without a generator, i.e. Voronoi cell of an anisotropic Voronoi diagram is not necessarily connected.

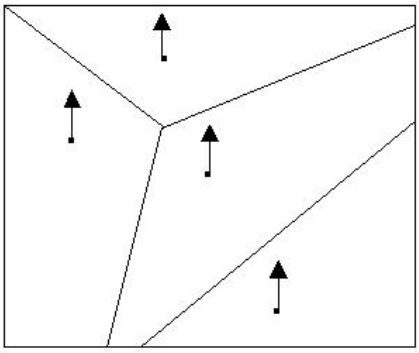

Figure 9. Anisotropic Voronoi partition with equal orientation

To avoid this problem, another assumption should be considered. The orientations of all agents are equal and fixed over time, i.e. $\theta_i(t) = \theta_j(t), \forall_i \neq j$ and $t \geq 0$. One example of the anisotropic Voronoi diagram with fixed and equal orientation is shown in Fig. 9. Worth to mention, that such assumption significantly reduces described method relevance.

Probabilistic Approach

A more realistic model of anisotropic sensor is considered. Instead of using the Voronoi approach where each sensor is assumed to have its own sensing region and the joint detection probability approach applied [8].

This model depends on the distance and orientation from the sensor to the target in the region of interest. Let $S = (s_1, ..., s_n)$ be the location of the n identical sensors located in the region Q. Each sensor has a limited sensory domain Q_i with the maximum sensing range R and the maximum sensing direction Θ (Fig. 10). The sensing ability of each sensor declines along the radial distance and the radial angle from the sensor to the point to be sensed.

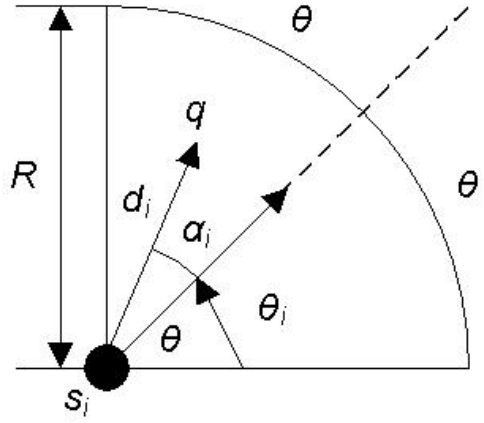

Figure 10. Limited-range anisotropic sensor model

The sensing performance of sensor i depends on the distance d_i and the orientation a_i from sensor i to the target q. Mathematically, the sensory domain of each sensor is given by

$$Q_i = \{q \in Q : d_i \le R \wedge |\alpha_i| \le \Theta\}, \tag{10}$$

where:

$$\begin{aligned} &d_i = \|q - s_i\|, \\ &\alpha_i = \cos^{-1}\left(\frac{(q - s_i)(\cos\theta_i, \sin\theta i)}{\|q - s_i\|}\right), \\ &\Theta \in \left(0, \frac{\pi}{2}\right]. \end{aligned} \tag{11}$$

Moreover the following assumption on the sensing performance of the above sensor model is made.

$$p_i(q) = 0, \frac{\partial p_i(q)}{\partial d_i(q)} = 0, \ \frac{\partial p_i(q)}{\partial \alpha_i(q)} = 0 \text{ if } q \notin Q_i . \tag{12}$$

The assumption tells that the sensor i can only sense the point inside its region of sensing Q_i. Hence example of the sensor model will be:

$$p_i(q) = \begin{cases} \dfrac{(d_i - R)^2 (\alpha_i - \Theta)^2}{R^2 \Theta^2} & \text{if } q \in Q_i \\ 0 & \text{otherwise} \end{cases}. \tag{13}$$

This approach is effective to tackle some problems faced in the Voronoi based approach for the anisotropic sensor model i.e. the anisotropic Voronoi tessellations, which is difficult to analyse.

6. Conclusions

Present study presents a promising outlook on application of sensor networks in intellectual transportation systems. The parameter analyses of the ICA system based on radar sensor, basic scenarios of the situations, which safety can be essentially improved by using sensor controls located on vehicles, and integrated with a road infrastructure are considered.

The problems arising at designing of similar networks, in particular, a problem of an estimation of a coverage zone, are analysed. The most known methods of an estimation of network coverage are overviewed and advantages and lacks of the specified methods are conceptually considered.

As it is possible to see from the review, the geometrical method of estimation has the serious lacks limiting its application. First of all, to estimate coverage of object that is subject to detection its coordinates should be known in advance. Also it is impossible to calculate probability of object detection as the method states only a binary estimation – in a zone/not in a zone.

The method based on the Voronoi diagram though is one of the most effective, for networks with isotropic sensor controls, assumes not quite realistic assumptions for anisotropic sensor controls. The elliptic form of a covering isn't characteristic for the sensor controls applied in areas considered in work as well as probability of identical orientations of all sensor controls is insignificant. In a case of assumption of identical orientation of sensor controls discarding, such diagram can't be used, in case of need, for sensor controls placement optimisation by Lloyd's algorithm since it will have regions without corresponding generators. This circumstance reduces its value.

Probabilistic approach appears to be the most perspective from presented approaches since it gives the chance to consider not only probability of a covering for each separate sensor control, but also total probability in case of overlapping of zones. The method can be scaled for *n* measured space, and in need of optimisation of sensor controls placement can be used in McQueen's algorithm since this algorithm doesn't demand construction of the Voronoi diagram, and calculated probability of detection of object can be used as the metrics.

Suitability, algorithms and efficiency of the given method for a sensor networks covering estimation in considered ITS typical scenarios further can become a subject of the subsequent researches.

References

1. Slijepcevic, S., Potkonjak, M. Power efficient organization of wireless sensor networks. In: *IEEE International Conference on Communications (ICC), vol. 2, Helsinki, Finland, June 2001*. Helsinki, 2001, pp. 472-476.
2. Tian, D., Georganas, N. D. A coverage-preserving node scheduling scheme for large wireless sensor networks. In: *Proceedings of the ACM International Workshop on Wireless Sensor Networks and Applications (WSNA), Atlanta, GA, United States, September 2002*. Atlanta, 2002, pp. 32-41.
3. Wang, X., Xing, G., Zhang, Y., Lu, C., Pless, R., Gill, C. Integrated coverage and connectivity configuration in wireless sensor networks. In: *Proceedings of the First International Conference on Embedded Networked Sensor Systems (SenSys), Los Angeles, CA, United States, November 2003*. Los Angeles, 2003, pp. 28-39.
4. Zhang, H., Hou, J. C. Maintaining sensing coverage and connectivity in large sensor networks, *The Wireless Ad Hoc and Sensor Networks*, (an International Journal), 2005.
5. Cardei, M., Du, D.-Z. Improving wireless sensor network lifetime through power aware organization, *ACM Wireless Networks*, Vol. 11, 2005, pp. 333-340.
6. Hemjit, Sawant; Jindong, Tan; Qingyan, Yang. A Sensor Network Approach for Intelligent Transportation Systems. In: *Electrical and Computer Engineering.* Houghton, Michigan, USA: Michigan Technological University.
7. Jing Ai and Alhussein A. Abouzeid. *Coverage by Directional Sensors in Randomly Deployed Wireless Sensor Networks*. Troy, NY 12180, USA: Electrical, Computer and Systems Engineering Department, Rensselaer Polytechnic Institute.
8. Jieh-Shian Young, and Chan Wei Hsu. The Parameters Analysis for the Intersection Collision Avoidance Systems Based on Radar Sensors World Academy of Science, *Engineering and Technology,* Vol. 53, 2009.

Transport and Telecommunication, 2010, Volume 11, No 4, 46–58
Transport and Telecommunication Institute, Lomonosova 1, Riga, LV-1019, Latvia

PATTERN-ORIENTED DECISIONS FOR LOGISTICS AND TRANSPORT SOFTWARE

Sergey Orlov, Andrei Vishnyakov

Transport and Telecommunication Institute
Lomonosova str.1, Riga, LV-1019, Latvia
E-mail: sorlov@tsi.lv, andrei.vishnyakov@gmail.com

Software architecture design and estimation play the key role for logistics and transport software development process. One of the design approaches is to reuse the architectural patterns, which express a fundamental structural organization of software systems and its behaviour. The usage of the proven and tested solutions allows us to increase the software quality and reduce potential risks.

In this paper, the most suitable architectural patterns are chosen for the typical logistics and transport software. For the evaluation of architectural patterns the metrics such as Functional Points, Coupling and Cohesion are used. Based on these metrics the criterion of efficiency has been obtained, which helps us to evaluate and select the optimal architectural patterns for specified logistics or transport software.

Keywords: software architecture, architectural patterns, logistics and transport software, coupling, cohesion, FP-metrics

1. Introduction

Software architecture design and estimation play the key role for logistics and transport software development process. The mistakes which are introduced at this development stage can lead to the project failure. Unfortunately, at the moment there are no any effective methods for the software architecture quality estimation. Thus the software engineer relies on his own experience or the experience and architecture quality evaluation of other experts during the architecture design stage.

Another approach is to take a look from the structural organization point of view, so it's obviously that the major part of architectures use some set of the common architectural patterns. The architectural patterns express a fundamental structural organization of software systems and software behaviour. They influences to its base characteristics as well. Such usage of the proven and tested approaches allows increasing the software quality and reducing a budget and potential risks.

2. Software Architecture, Architecture Patterns

The software architecture is the structure of the system, which comprises software components, the externally visible properties of those components, and the relationships among them [1]. The software architecture is a complex design artefact.

An architectural pattern, expresses a fundamental structural organization schema for software systems. It provides a set of predefined subsystems, specifies their responsibilities, and includes rules and guidelines for organizing the relationships between them [2].

It's a complicated task to make a validation at early design stage and it's much easier to rely on tried and tested approaches for solving certain classes of problems. So the architectural patterns improve partitioning and promote design reuse by providing solutions to frequently recurring problems. They allow reducing a risk by reusing successful designs with known engineering attributes.

Different architectural patterns are focused on some areas and that is why they might be categorized in several groups. There are several approaches of architectural patterns classification. In the Table 1 is presented generalized classification based on [2, 3].

Table 1. Architectural patterns classification

Category	Architectural patterns
Communication	• Service Oriented Architecture (SOA) • Message Bus • Broker
Deployment	• Client-server • Multitier (N-Tier)
Domain	• Domain Driven Design
Structural	• Component-Based • Object-oriented • Layered architecture • Pipes and Filters pattern
Interactive	• Model-View-Controller pattern • Presentation-Abstraction-Control pattern
Adaptive	• Reflection pattern • Micro kernel pattern

Usually the software isn't limited to a single architectural pattern. It is often a combination of architectural patterns that make up a complete system. For instance, there might be SOA based architecture where some services are designed using layered or N-tier architecture approach.

2.1. Architecture patterns for logistics and transport software

There are a number of logistics related software available at the moment, in [4] is listed the following Logistic System types:

1. Enterprise Resource Planning (ERP);
2. Supply Chain Management (SCM);
3. Warehouse Management System (WMS);
4. Customer Relationship Management System (CRM);
5. Material Requirements Planning (MRP) / Manufacturing Resource Planning (MRP II).

The general transport software type is Intelligent Transportation Systems (ITS), which is often used synonymously to the term Transport Information and Control Systems (TICS). Such kind of software may contain several services, which are listed in Table 2. This table gives a composite taxonomy of Transport Information and Control Systems services, as standardized by the International Organisation for Standardization [5].

Table 2. Taxonomy of Transport Information and Control System services

Category	Service
Traffic and travel information	• Pre-trip information • On-trip driver information • On-trip public transport information • Personal information services • Route guidance and navigation
Traffic management	• Transportation planning support • Traffic control • Incident management • Demand management • Policing/enforcing traffic regulations • Infrastructure maintenance management
Vehicle-related	• Vision enhancement • Automated vehicle operation • Longitudinal collision avoidance • Lateral collision avoidance • Safety readiness • Pre-crash restraint deployment

Category	Service
Commercial vehicles	• Commercial vehicle pre-clearance • Commercial vehicle administrative processes • Automated roadside safety inspection • Commercial vehicle on-board safety monitoring • Commercial vehicle fleet management
Public transport	• Public transport management • Shared transport management
Emergency management	• Emergency notification and personal security • Emergency vehicle management • Hazardous materials and incident notification
Electronic payment	• Electronic financial transactions
Safety	• Public travel security • Safety enhancement for vulnerable road users • Intelligent junctions

There are many existing transport software systems available with the different functionality listed above and includes such systems like Car Navigation, Traffic Signal Control Systems, Safety/Speed Cameras Systems, Electronic Toll Collection Systems, etc.

The major amount of the logistics software is Information Systems, which may contain some specific mathematical modules for optimisation, planning, scheduling, etc. The main components of SCM are optimisation models, which contains databases.

The transport software doesn't have such well noticeable characteristics like logistics software, i.e. it has more variations. For instance, it may contain modules for controlling in real time, modelling modules, optimisation modules, GPS navigation modules, communication (VoIP, Video conference) modules, recognition (plate number recognition, RFID) modules, etc. Some type of transport software may contain databases as well, but it isn't a core component for such type of software.

According to the listed characteristics, one of the most suitable architectural pattern for the logistics software is N-their architecture. For the transport software (or more precisely for ITS), the architectural patters like Distributed Architecture and SOA can be used. N-tier architecture might be used for the transport software as well.

3. Architecture Patterns Quality Estimation

For the selected architectural patterns quantitative metrics must be obtained to being able make a decision regarding its influence on software architecture.

During the architecture design stage the architectural patterns are treated as a "black box", therefore the complexity metrics should be based on indirect measures instead of directs ones. Functional point (FP) metric is an example of such complexity metrics. It measures the amount of functionality in a system [6]. On the next design stage (on the detailed design stage) a deeper analysis could be made with the usage of such metrics like OOP and others.

In addition to the complexity metrics, outer (Coupling) and inner (Cohesion) relations in architectural patterns can be measured. Coupling is a metrics which express the degree of data interconnection between modules. Low coupling is an indication of a well-designed system. Cohesion is a measure of how strongly the functionality inside a module is related. High cohesion of a module is a desirable trait [6].

Let's consider the mentioned metrics usage for the following architectural patterns:

- Service Oriented Architecture;
- Multitier architecture;
- Model-View-Controller.

3.1. Service oriented architecture

Service Oriented Architecture (SOA) offers a modular approach to software development. A service with a standardized interface is used as a module in this architectural pattern. This architectural pattern is based on the principles of multiple reuse of system elements, elimination of a similar functionality, unification and centralization of the standard operational processes, providing a single integration platform for the system. System services can be distributed to different hosts and be

independent and loosely coupled [3]. This architecture pattern is used by many major software companies and it's well proven. There is available the successor of this architectural pattern – Service Component Architecture. In the future it may completely replace SOA. In Table 3 the profile of this pattern is represented.

Table 3. Service Oriented Architecture pattern's profile

Name	**Service Oriented Architecture**
Definition	The policies, practices, frameworks that enable application functionality to be provided and consumed as sets of services published at a granularity relevant to the service consumer. Services can be invoked, published and discovered, and are abstracted away from the implementation using a single, standards-based form of interface [3].
Examples	Common examples of SOA applications include applications with multistep processes such as reservation systems and online stores, applications which combine information from multiple sources, applications with expose industry specific data or services.
When to use	• For cloud-based applications; • For applications like Software plus Services (S+S), Software as a Service (SaaS); • When it's necessary to build an applications that compose a variety of services into a single UI; • For integrations different Enterprise Software; • For reusing existing suitable services.
Benefits	• Services has standard interface and can be easily reused; • Services are autonomous and loose coupled; • Minimized the duplication of the functionality, since services provides specific functionality; • As long as services expose description, other applications can locate them and automatically determine the interface; • Can be easily deployed on different platforms.
Disadvantages	• Too complex especially for small applications; • Low interoperability performance; • SOA services are still too constrained by applications they represent.

Functional Points

The concept of the SOA does not apply any restrictions on services internal implementation, so the services can be treated as "black boxes" which implement certain functionality. Therefore, to evaluate the complexity of the services, Functional Points metric should be used. So, Functional Points should be measured for each service. Based on these measures the total number of Functional Points for the architecture can be calculated. The values of Functional Points might be used for obtaining performance and quality metrics. LOC values might be also obtained based on Functional Points.

Coupling

Since every single service in this architecture should be loosely coupled, it is essential to measure the interconnection between architecture services. Services with a low coupling have a low impact on changes in other services and could be easily reused.

Cohesion

As long as every single service in this architecture should implement a unique functionality, it is essential to measure cohesion for each service. High cohesion should indicate the right functionality splitting between the services. A service with high cohesion has focused functionality; it's easy maintainable and comprehensible.

Evaluation example of Traffic Congestion System

Let's suggest that the system engineer has developed the following structural representation of system architecture based on SOA (see Figure 1).

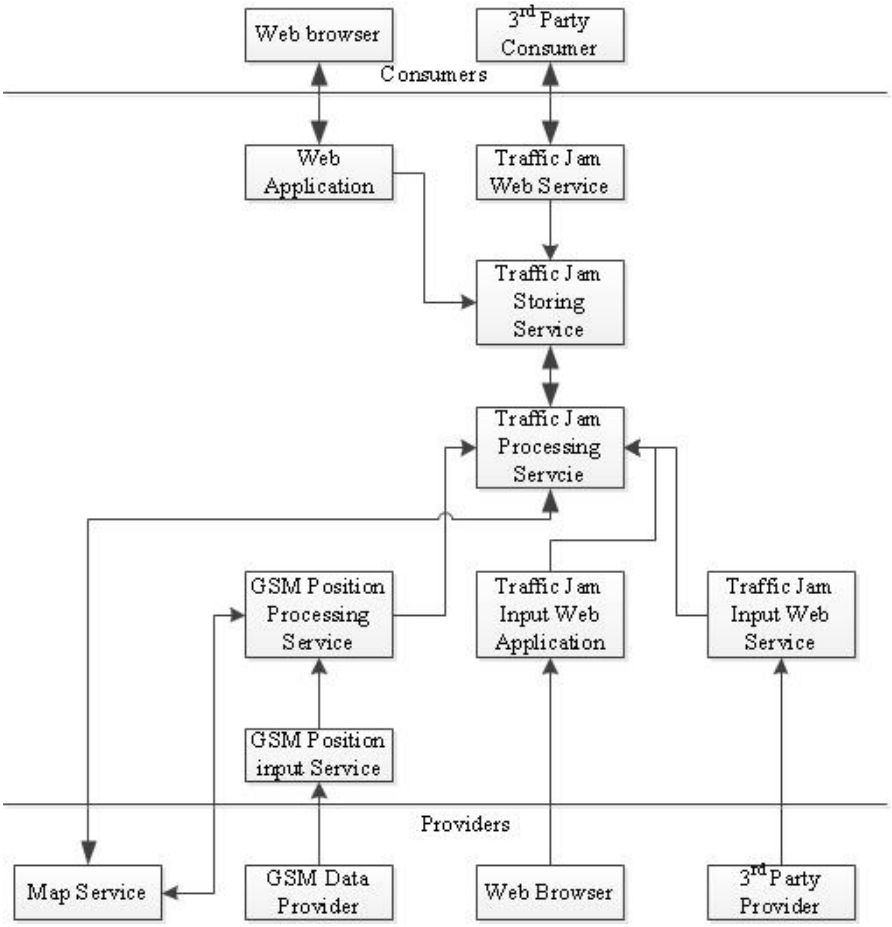

Figure 1. Structural representation of the system architecture

This system uses third-party services to obtain some information which is used for traffic jam determination (from three different providers) and map data. On the other hand, the system provides the information regarding traffic congestion to several consumers. They access that information with the help of Web applications and Web services. In addition to the interface services, which provide and consume the information, there are another three services. Two of them analyze the received events and determine an existence or absence of traffic congestion on specific roads. The remaining service has the database for storing current information regarding roads and it provides this information to other services.

Values of the metrics for "Traffic Jam Storing Service"

Let's calculate the values of the metrics for "Traffic Jam Storing Service". This service contains an internal database and provides an interface for adding/removing traffic jams as well as retrieving a list of traffic congestion for a given map area.

For Functional Point calculation it's necessary to determine the total number of characteristics. This service has two external inputs (add and remove road congestion) with a low degree of difficulty, also there is an external request (for retrieving a list of traffic congestion) with an average complexity and one internal logical file (table in Database) with a low degree of complexity.

$$\textbf{\textit{FP}} = \text{Unadjusted Function point Count} \times (0.65 + 0.01 \times \sum_{i=1}^{14} F_i) = 17 \times (0.65 + 0.01 \times 31) = 16.32.$$

Coupling level = 1 (Data coupling), i.e. this service has the lowest value of coupling. This is explained by the fact that this service does not depend on the other services.

Cohesion level = 9 (Sequential cohesion), i.e. this service has almost the highest value of cohesion. This result is based on the fact that this service provides three operations (add, delete, get a list of traffic congestion), and the results of previous operations is used as an input data for the current operation.

Values of the metrics for the system

In the Table 4 are represented the values of the metrics for the each service and for the system.

Table 4. The values of the metrics for the services

Service	FP	Coupling	Cohesion
Web Application	24.18	3	9
Traffic Jam Web Service	7.12	3	9
Traffic Jam Storing Service	16.32	1	9
Traffic Jam Processing Service	54.08	3	7
GSM Position Processing Service	44.72	3	7
GSM Position Input Service	6.96	3	9
Traffic Jam Input Web Application	19.58	3	9
Traffic Jam Input Web Service	7.92	3	9
	Total: 180.88	***Average:*** 2.75	***Average:*** 8.5

The total value of the Functional Points equals to 180.88. The low value of the average coupling for the services shows a week dependencies between them, so they might be easily reused and replaced. The high value of the average cohesion points to a correct splitting of functionality between the services.

3.2. Multitier architecture

Multitier architecture or N-tier architecture is a client-server architecture where each part of the system is logically divided into separate tiers [3]. Such separation gives to a developer an ability to create a flexible architecture with reusable tiers. So if the developer wants to change something in the system there is no need to implement everything from scratch, it might be enough to add or replace a specific tier. The most commonly used model is with three tiers (Three-tier model), including the presentation tier, application (or business) tier and data tier. In Table 5 is represented the profile of this pattern.

Table 5. Multitier architecture pattern's profile

Name	Multitier architecture
Definition	Multitier architecture (N-tier) is client/server architectural deployment style that describes the separation of functionality into segments where each segment being a tier that can be located on a physically separate computer. It evolved through the component-oriented approach, generally using platform specific methods for communication instead of a message-based approach [3].
Examples	Common example is a typical rich client connected application, where on client PC is implemented the presentation tier. The other tiers are deployed on servers. Another example includes typical financial Web application where security is important.
When to use	• When client-server type of application is required; • When application must be distributed between several computers; • When business logic should be shared between several applications; • When existing tiers could be reused.
Benefits	• Good scalability, reusability and maintainability; • Changes or updates can be made without affecting the whole application; • Application can be extended or updated by adding or changing only one tier.
Disadvantages	• Application is more complex therefore it requires some extra effort at design and development stages; • Interoperability performance between tiers might be slow.

Functional Points

Each layer of the architecture implements some functionality and it can be treated as a "black box", so Functional Points should be used for evaluation the complexity of each tier. Based on these measures the total number of Functional Points for the N-tier architecture can be obtained.

Coupling

In this architecture the values of coupling for each tier is constant. Each tier is connected only with the nearest tiers, due to the structure of the architectural pattern.

Cohesion

As long as each tier of the architecture implements a specific functionality, it is essential to measure cohesion for each tier. High cohesion indicates the right splitting of the functionality between the tiers as well as the optimal number of tiers in the architecture.

Evaluation example of Traffic Congestion System

According to the requirements, a system engineer has developed the following structural representation of the architecture based on Three-tier architectural pattern (see Figure 2). Note that the object domain remained the same that was used in the example with SOA, but in this sample the different architectural pattern was used.

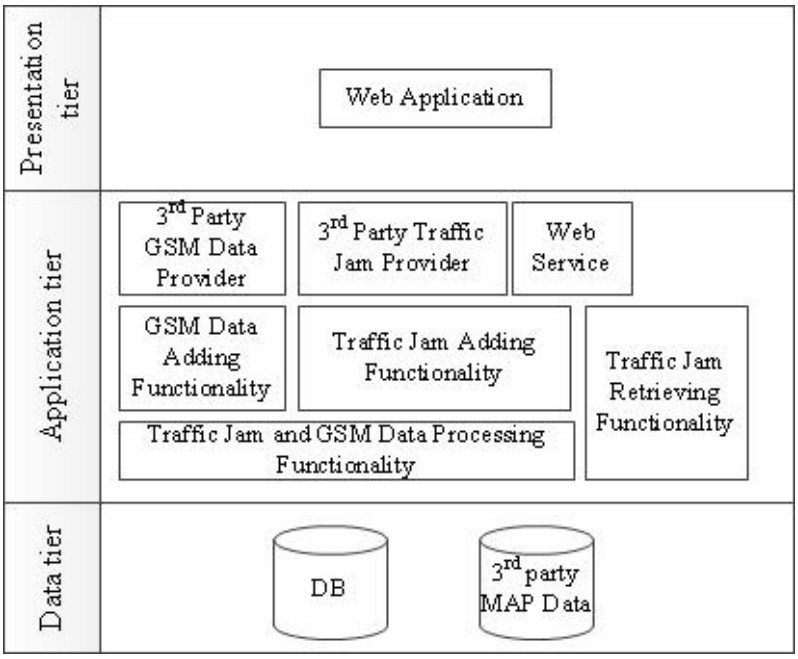

Figure 2. Structural representation of the system architecture

The Application tier contains the functionality for receiving and processing information regarding roads and traffic congestion status. The Data tier has the database which stores traffic congestion related information, also this tier contains map data which is provided by third-party supplier. Just as in the example with SOA, the system provides access to traffic congestion information with the help of Web applications and Web services. Web application is located in Presentation tier and serves for obtaining and adding information regarding some roads.

Values of the metrics for Application tier

Let's calculate the metrics values for the Application tier. This tier contains the functionality for road status processing. Also it uses the underlying tier for storing data and provided processed data to the overlying tier. So this tier has:

- three external inputs with average complexity, which are necessary to obtain information regarding roads state;
- five external inputs with high complexity, which are used for the database and map data accessing;
- four external outputs with average complexity, which are used by the overlying tier and external systems for obtaining information regarding traffic congestions;

- two external outputs with a high degree of complexity, which are used for adding information into the database;
- one external interface file with a high degree of complexity, which is used by the overlying tier for obtaining a list of traffic congestions.

According to the data listed above, let's calculate the values of the metrics.

$$\textbf{\textit{FP}} = \text{Unadjusted Function point Count} \times (0.65 + 0.01 \times \sum_{i=1}^{14} F_i) = 86 \times (0.65 + 0.01 \times 41) = 91.16.$$

Coupling level = 4 (Control coupling). Such value can be explained by the fact that this tier directly controls the underlying tier.

Cohesion level = 5 (Procedural cohesion). This result is based on the fact that this tier has the functionality which depends on execution sequence.

Values of the metrics for the system

In the Table 6 are represented the values of the metrics for the each tier and for the system.

Table 6. The values of the metrics for the tiers

Tier	FP	Coupling	Cohesion
Presentation tier	52.02	4	7
Application tier	91.16	4	5
Data tier	66.95	1	7
	Total: 210.13	***Average:*** 3	***Average:*** 6.33

The total value of Functional Points equals to 210.13, which is slightly above than the total value of the architecture based on SOA. The low value of coupling for tiers shows weak dependencies between them, which is explained by the architecture structural model, where each tier is related only with underlying and overlying tiers. Using this architectural pattern the developer can not affect on this characteristic too much, so coupling evaluation doesn't bring too many benefits. Not a very high value of cohesion within the application tier can be explained by architectural pattern nature, i.e. this pattern allows inclusion of unrelated functionality in this layer. To improve this value the additional layers might be added or more detailed design of components could be made.

3.3. Model-view-controller

This architectural pattern splits the system to three separate components: model, view and controller [2]. The responsibilities of "Model" include data storing and interface to it. "View" is responsible for showing information to the user. "Controller" manages the components by receiving user actions and notifying the model regarding the updates. Such structure guarantees the reliability and extensibility of the system. In Table 7 the profile of this pattern is represented.

Table 7. Model-View-Controller pattern's profile

Name	Model-View-Controller
Definition	MVC is tree layer pattern (model, view and controller) for isolating business logic from user interface. The model is an object that represents some information about the domain. The view represents the display of the model in the UI. The controller takes user input, manipulates the model, and causes the view to update appropriately [7].
Examples	• A lot of Web-based systems use MVC pattern for UI part implementation; • Java Swing's library architecture is based on MVC design.
When to use	• When it's required to have multiple options for data processing and presentation; • When the requirements regarding interoperability and data presentations are unknown.
Benefits	Allows changing the data regardless of their views. Data changes made in one view is displayed in all other views.
Disadvantages	Code redundancy for a simple data model and for a simple interaction model.

This pattern is mainly used for the User Interface part of the system. If, for example, we compare this pattern with Three-tier architecture, the functionality provided by this pattern covers only the functionality of Presentation tier.

Functional Points

Each component of the architecture implements some functionality and can be treated as a "black box".

Coupling

In this architecture the value of coupling for each component is constant.

Cohesion

As long as each component implements specific functionality, it's essential to measure cohesion for each component of the system.

Evaluation example when MVC pattern is used

Let's consider the use of MVC pattern for the Presentation tier (for N-tier architecture from the previous chapter), i.e. let's make more detailed design for the User Interface from the Presentation tier. The functionality of Web application from Presentation tier includes the ability to view existing traffic congestion and ability to enter information regarding status for specific road.

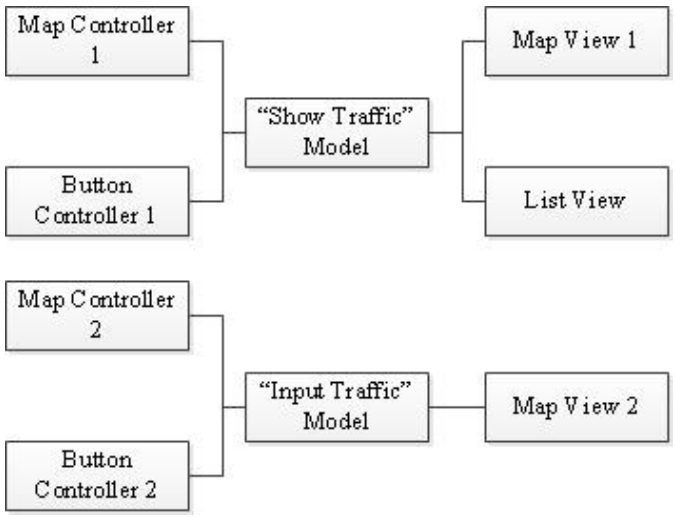

Figure 3. Structural representation of the architecture UI model when MVC pattern is used

The UI model of the system (see Figure 3) contains 2 Model components; each of them provides the interface to the data. Each Model component is connected with several Controller and View components. Controller and View components are responsible for receiving user interaction and showing the requested information.

Values of the metrics for "Show Traffic" Model

Let's calculate the values of the metrics for "Show Traffic" Model component. This component provides the interface to the data and notifies controllers and views when there are some updates. Also it has an access to storage for retrieving the required information.

For Functional Point calculation it's necessary to determine the total number of characteristics. This service has one internal logic file (some data structure for passing data from storage to components) with average degree of complexity.

$$\textbf{\textit{FP}} = \text{Unadjusted Function point Count} \times (0.65 + 0.01 \times \sum_{i=1}^{14} F_i) = 10 \times (0.65 + 0.01 \times 40) = 10.5.$$

Coupling level = 3 (Stamp coupling). This is explained by the fact that this component shares a composite data structure with other components.

Cohesion level = 5 (Procedural cohesion). This result is based on the fact that component has the functionality, which depends on execution sequence.

Values of the metrics for the components of the system

In the Table 8 the values of the metrics for the components of the system are represented.

Table 8. The values of the metrics for the MVC components

Service	FP	Coupling	Cohesion
Map Controller 1	3.84	4	7
Map View 1	15.81	3	9
"Show Traffic" Model	10.5	3	5
Button Controller 1	2.7	4	10
List View	5	3	10
Map Controller 2	5.76	4	7
Map View 2	13.02	3	9
"Input Traffic" Model	7.35	3	5
Button Controller 2	2.7	4	10
	Total: 66.68	***Average:*** 3.4	***Average:*** 8

The total value of Functional Points for UI implementation using MVC pattern equals to 66.88, which is slightly higher than value for the Presentation tier, obtained with using N-tier pattern. It's higher since this system structure is more detailed. Also in this example there are some additional functionality added, which is not required for N-tier architecture. The low value of coupling for components shows weak dependencies between them and can be explained by the pattern nature. The developer cannot affect on this characteristic too much. High cohesion points to the proper choosing and functionality splitting between the components.

3.4. Criterion of efficiency for choosing architectural patterns

At the architecture design stage the designer may choose from a certain number of available architectural patterns. There are several groups of patterns, which are separated by the object domain. Some architectural patterns from one group can be used as part of other patterns. For example, Presentation tier from N-tier architecture can be implemented using MVC Pattern. Another example, some services in SOA might be implemented using N-tier architecture.

It's necessary to have a tool that indicates the optimal architectural pattern in the specified group or even in different groups, where such is possible. For such purposes the criterion of efficiency can be used, which allows to select the optimal solution from proposed alternatives.

The efficiency indicators should be selected for criterion of efficiency construction as well as ratio between them, which determines the type of criterion of efficiency [8].

The elements of any architecture can be treated as "black boxes", so its functional and structural complexity (the complexity of internal relations) can be evaluated using such metrics as FP and Cohesion. Therefore the topology of "black boxes" connections in the architecture can be measured with such metric as Coupling (the complexity of external relations). It is obvious that the rate of Coupling should be minimized and the high value of Cohesion is desirable. Since the value of FP is proportional to the functional complexity, the greater value is more desirable.

According to the preceding, the generalized architecture metric has the following representation:

$$P = \frac{a_1 \times FP + a_2 \times Cohesion}{a_3 \times Coupling}.$$

Hence the criterion of architecture efficiency is formulated as follows:

$$P = \frac{a_1 \times FP + a_2 \times Cohesion}{a_3 \times Coupling} \to \max,$$

where a_1, a_2, a_3 – weight coefficients of efficiency indicators.

As long as the dimension of these indicators is heterogeneous, i.e. the values of Coupling and Cohesion can vary from 1 to 10 and the value of FP is not limited, the choice of efficiency indicator's weight coefficients might require additional investigation.

The weight coefficient of efficiency indicator can be selected by expert review and the value for a_1 should be determining carefully, since wrongly selected value may suppress the values of Coupling and Cohesion.

Evaluation of SOA and N-tier architectural patterns with the help of coefficient of efficiency

In Table 9 the metric's values for the two architectural patterns are listed. These values were obtained for the same object domain, which allowed us to use coefficient of efficiency for their evaluation.

Table 9. The values of the metrics

Architectural patterns	FP (total)	Cohesion (average)	Coupling (average)
SOA	180	8.5	2.75
N-tier	210	6.33	3

As long as efficiency indicators have different scale it is necessary to standardize them. To do so let's reduce it to single dimension using the following equation [8]:

$$\overline{A_i} = \frac{A_i}{A_{\max_i}}.$$

Thus the standardization of the efficiency indicators for SOA pattern is defined as:

$$\overline{FP}_{SOA} = \frac{180}{210} = 0.857,$$

$$\overline{Cohesion}_{SOA} = \frac{8.5}{10} = 0.85,$$

$$\overline{Coupling}_{SOA} = \frac{2.75}{10} = 0.275.$$

In Table 10 the standardized values of the efficiency indicators are listed.

Table 10. The standardized values of the metrics

Architectural patterns	Standardized FP	Standardized Cohesion	Standardized Coupling
SOA	0.857	0.85	0.275
N-tier	1	0.633	0.3

It is obvious that these efficiency indicators have different degrees of importance; therefore it's necessary to take into account their priority. The priority of efficiency indicators can be taken into account with the help of weight coefficient vector (a_1, a_2, …, a_n).

The optimal combination of the weight coefficient vector differs depending on architecture. In our case it's necessary to determine the weight coefficient vector for comparison of specific architectural patterns. For determination of these weight coefficients the expert evaluation has been used. So the weight coefficients of efficiency indicators for the Functional Points, Coupling and Cohesion are defined as:

$a_1 = 0.6$, $a_2 = 0.8$, $a_3 = 1$.

In other words, Coupling has the greatest weighting coefficient of efficiency indicator and Functional Points the least.

Hence the generalized metrics for architectural patterns are defined as follows:

$$\boldsymbol{P}_{\mathbf{SOA}} = \frac{\alpha_1 \cdot \overline{FP_{SOA}} + \alpha_2 \cdot \overline{Cohesion_{SOA}}}{\alpha_3 \cdot \overline{Coupling_{SOA}}} = \frac{0.6 \cdot 0.857 + 1 \cdot 0.85}{0.8 \cdot 0.275} = 4.34.$$

$$\boldsymbol{P}_{\mathbf{N\text{-}tier}} = \frac{\alpha_1 \cdot \overline{FP_{N-tier}} + \alpha_2 \cdot \overline{Cohesion_{N-tier}}}{\alpha_3 \cdot \overline{Coupling_{N-tier}}} = \frac{0.6 \cdot 1 + 1 \cdot 0.633}{0.8 \cdot 0.3} = 3.69.$$

As long as it is necessary to maximize the value of the coefficient of efficiency, the use of SOA architectural pattern is more preferable.

Evaluation of MVC pattern and Presentation tier from N-tier architecture with the help of coefficient of efficiency

In Table 11 the obtained metric's values for MVC pattern and Presentation tier for N-tier pattern are listed.

Table 11. The values of the metrics

Architectural pattern	FP (total)	Cohesion (average)	Coupling (average)
Presentation tier from N-tier	52	7	4
MVC	67	8	3.4

Since the efficiency indicators have different scale it is necessary to standardize them. The standardization of the efficiency indicators for N-tier pattern is defined as:

$$\overline{FP}_{N-tier} = \frac{52}{67} = 0.78,$$

$$\overline{Cohesion}_{N-tier} = \frac{7}{10} = 0.7,$$

$$\overline{Coupling}_{N-tier} = \frac{4}{10} = 0.4.$$

In Table 12 the standardized values of the efficiency indicators for the two architectural patterns are listed.

Table 12. The standardized values of the metrics

Architectural pattern	Standardized FP	Standardized Cohesion	Standardized Coupling
Presentation tier from N-tier	0.78	0.7	0.4
MVC	1	0.8	0.34

Let's define the weight coefficient vector for the specified patterns with the help of an expert evaluation. The weight coefficients of efficiency indicators for the Functional Points, Coupling and Cohesion are defined as:
$a_1 = 0.6$, $a_2 = 0.8$, $a_3 = 1$.

So, Coupling has the greatest weighting coefficient of efficiency indicator and Functional Points the least.
Hence the generalized metrics for architectural patterns are defined as follows:

$$\boldsymbol{P}_{\mathbf{Presentation\ tier}} = \frac{\alpha_1 \cdot \overline{FP_{P-tier}} + \alpha_2 \cdot \overline{Cohesion_{P-tier}}}{\alpha_3 \cdot \overline{Coupling_{P-tier}}} = \frac{0.6 \cdot 0.78 + 1 \cdot 0.7}{0.8 \cdot 0.4} = 2.57.$$

$$\boldsymbol{P}_{\mathbf{MVC}} = \frac{\alpha_1 \cdot \overline{FP_{MVC}} + \alpha_2 \cdot \overline{Cohesion_{MVC}}}{\alpha_3 \cdot \overline{Coupling_{MVC}}} = \frac{0.6 \cdot 1 + 1 \cdot 0.8}{0.8 \cdot 0.34} = 3.64.$$

The values of the generalized metric indicate that the use of MVC pattern for Presentation tier increases the efficiency of the system.

4. Conclusions

Analysis of the typical logistics and transport software allowed us to identify the most representative architectural features and characteristics. Based on that analysis the most useful architectural patterns were selected for such software types.

For the selected architectural patterns the quantitative metrics are selected, which allows make a decision regarding its influence on software architecture. During the architecture design stage the architectural patterns are treated as a "black box", so their complexity metrics are based on indirect measures instead of direct ones. In addition to the complexity metrics, inner (cohesion) and outer (coupling) relations of architectural patterns can be measured.

This paper contains the metrics calculation for the variety of architectural patterns. Based on these calculations the conclusions are made regarding the architectural patterns optimal choices for the proposed object domain.

The criterion of efficiency is proposed, which is based on such metrics as FP, Coupling and Cohesion. It allows making a conclusion regarding the usage of some architectural patterns for the logistics and transport software.

References

1. Bass, L., Clements, P., Kazman, R. *Software Architecture in Practice, Second Edition*. Addison Wesley, 2003. 560 p.
2. Buschmann, F., Meunier, R., Rohnert, H., Sommerlad, P., Stal, M. *Pattern-Oriented Software Architecture Volume 1: A System of Patterns*. Wiley, 1996. 476 p.
3. Microsoft Patterns & Practices Team. *Microsoft Application Architecture Guide, 2nd Edition (Patterns & Practices)*. Microsoft Press, 2009. 560 p.
4. Sergeev, V.I., Grigoriev, M.N., Uvarov, S.A. *Logistics. Information systems and technology*. Alpha-Press, 2008. 608 p. (In Russian)
5. International Organisation for Standardization. *Transport Information and Control Systems - Reference Model Architecture(s) for the TICS sector - Part 1: Fundamental TICS services*. ISO/TC204/WG1/N310R, 1997.
6. Orlov, S.A. *Software Engineering: A Textbook for Universities, 3rd ed*. SPb.: Piter, 2004. 527 p. (In Russian)
7. Fowler, M. *Patterns of Enterprise Application Architecture.* Addison Wesley, 2002. 560 p.
8. Orlov. S.A., Tsilker, B.J. *Organization of computers and systems: textbook for high schools, 2nd ed.* SPb.: Piter, 2010. 688 p. (In Russian)

Transport and Telecommunication, 2010, Volume 11, No 4, 59–65
Transport and Telecommunication Institute, Lomonosova 1, Riga, LV-1019, Latvia

RELIABILITY OF AIRCRAFT AND AIRLINE

Yu. Paramonov, M. Hauka

Aviation Institute, Riga Technical University
Lomonosova 1, Riga LV 1019, Latvia
Tel.: +371 67255394; fax: +371 67089990
E-mail yuri.paramonov@gmail.com, Maris.Hauka@ gmail.com

The reliability of aircraft (AC) and airline (AL) operation can be ensured by the implementation of a specific inspection program, which can be planned using full-scale fatigue test data and the theory of Markov Chains (MC) and a Semi-Markov process (SMP) with rewards. The process of the operation of aircraft is considered as absorbing MC with $(n+4)$ states. The states $E_1, E_2, ..., E_{n+1}$ correspond to AC operation in time intervals $[t_0, t_1), [t_1, t_2), ..., [t_n, t_{SL})$, where n is an inspection number, t_{SL} is specified life (SL), i.e. AC retirement time. States E_{n+2}, E_{n+3}, and E_{n+4} are absorbing states: AC is withdrawn from service when the SL is reached or fatigue failure (FF) or fatigue crack detection (CD) takes place. In the corresponding matrix for the operation processes of AL the states E_{n+2}, E_{n+3} and E_{n+4} are not absorbing, but correspond to the return of the MC to state E_1 (AL operation returns to first interval). The problem of inspection planning is the choice of the sequence $\{t_1, t_2, ..., t_n, t_{SL}\}$ (in case of equal inspection intervals and fixed t_{SL}, the choice of n) corresponding to the maximum of airline gain taking into account the limitations imposed by the intensity of AL fatigue failure (or AC failure probability).

This paper considers the case when the parameters of the fatigue crack growth exponential model are known. Numerical examples are given.

Keywords: inspection program, Markov chains, reliability

1. Introduction

This paper is devoted to the problem of the reliability of airlines and this is a development of previous publications [1-6] where the problem of the reliability of fatigue-prone aircraft has been considered. The reliability of aircraft (AC) and airline (AL) operations can be ensured by the implementation of a specific inspection program, which can be planned using full-scale fatigue test data and the theory of Markov Chains (MC) and a Semi-Markov process (SMP). The process of the operation of AC is considered as absorbing MC with $(n+4)$ states. The states $E_1, E_2, ..., E_{n+1}$ correspond to AC operation in time intervals $[t_0, t_1), [t_1, t_2), ..., [t_n, t_{SL})$, where n is an inspection number, t_{SL} is specified life (SL), i. e. AC retirement time. States E_{n+2}, E_{n+3}, and E_{n+4} are absorbing states: AC is withdrawn from service when the SL is being reached or fatigue failure (FF) or fatigue crack detection (CD) takes place. In the corresponding matrix for the operation process of AL the states E_{n+2}, E_{n+3} and E_{n+4} are not absorbing, but correspond to the return of the MC to state E_1 (AL operation returns to first interval). In the matrix of transition probabilities of AC, P_{AC}, there are three units in the three last lines in the diagonal (bias), but for corresponding lines in the matrix for AL, P_{AL}, the units are in the first column, corresponding to state E_1. Using P_{AC} we can get the probability of FF of AC and cumulative distribution function, mean and variance of AC life, and the same characteristics under the condition of absorption in a specific absorbing state. Using P_{AL} we can get the stationary probabilities of AL operation $\{\pi_1, ..., \pi_{n+1}, \pi_{n+2}, ..., \pi_{n+4}\}$. Here π_{n+3} defines the part of MC steps when FF takes place and the MC appears in state E_{n+3}. The ratio of this value to the mean life of a new aircraft defines the intensity of FF, λ_F, i.e. the number of FF in one time unit. It can be calculated also using the theory of Semi-Markov Process (SMP) with rewards [7, 8]. Using this theory we can calculate also the gain of the process. The problem of inspection planning is the choice of the sequence $\{t_1, t_2, ..., t_n, t_{SL}\}$ (in the case of equal inspection intervals and fixed t_{SL}, choice of n) corresponding to the maximum gain, taking into account the limitations imposed by the intensity of AL fatigue failure of AL or AC fatigue failure. A numerical example is given.

2. Formal Setting of the Problem

For the formal setting of the problem we should define the matrix of transition probabilities of MC and the matrix of rewards for SMP. However, first the fatigue crack growth model should be defined.

2.1. Fatigue crack growth model

We suppose the following exponential approximation of fatigue crack growth function when the size of a fatigue crack is defined by the equation:

$$a(t) = a(0)\exp(Qt)\,. \tag{1}$$

$T_{\rm d}$ represents the time when a crack reaches detectable size, a_d is when the probability of its discovery is equal to a unit if inspection is made (before this size this probability is equal to zero). $T_{\rm c}$ is the time when the crack reaches its critical size, $a_{\rm c}$, and FF takes place. The value of $a_{\rm c}$ corresponds to the minimum residual strength of an aircraft component allowed by special design regulations. We have

$$T_d = (\ln a_d - \ln a_0)/Q = C_d/Q\,, \tag{2}$$

$$T_c = (\ln a_c - \ln a_0)/Q = C_c/Q\,, \tag{3}$$

where a_0 is $a(0)$. Despite its simplicity, the formula (1) in interval $[T_d\,,\,T_c\,)$ shows clear results.

The values $C_{\rm c,}$ and $C_{\rm d,}$ can be derived each from another.

$$C_d = C_c - \delta\,, \tag{4}$$

$$C_c = C_d + \delta\,, \tag{5}$$

$$\delta = \ln a_c - \ln a_d = \ln\frac{a_c}{a_d}\,. \tag{6}$$

If δ and a_0 are constants then actually considering the model of fatigue crack growth, the distribution of random variables (r.v.) T_d, T_c is defined by distribution of only two r.v.: $C_{\rm c}$ and Q. Let us denote

$$X = \ln Q\,,\ Y = \ln C_c = \ln\left(\ln\left(a_c/a_d\right)\right). \tag{7}$$

From the analysis of the fatigue test data it can be assumed, that r.v. $\ln T_c$, is distributed normally. It comes from the additive property of the normal distribution that $\ln T_c$ could be normally distributed if both $\ln C_c$ and $\ln Q$ are normally distributed or if one of these value is constant. Here we consider the simplest case. We suppose that random variable X has normal distributions with unknown mean value θ_0 and known θ_1 but Y is constant.

2.2. Failure of AC probability calculation using the theory of absorbing Markov chains

Let the probability of crack detection during the inspection number i at time moment t_i be denoted as v_i; the probability of failure in service time interval (t_{i-1},t_i) as q_i; and the probability of absence of the above-mentioned events as u_i. These three events form a complete set $u_i + v_i + q_i = 1$. In our model we also assume that there is an inspection at t_{SL}. This inspection at the end of (n+1)-th interval does not change the reliability, but it should be done in order to know the state of aircraft (to know if there is any FC or if there are no fatigue cracks). *Effective number of inspections* is equal to n but in following, for short, we say that n is *number of inspections*. The transition probability matrix of this process, P_{AC}, can be composed as presented on Figure 1.

	E_1	E_2	E_3	…	E_{n-1}	E_n	E_{n+1}	E_{n+2} (SL)	E_{n+3} (FF)	E_{n+4} (CD)
E_1	0	u_1	0	…	0	0	0	0	q_1	v_1
E_2	0	0	u_2	…	0	0	0	0	q_2	v_2
E_3	0	0	0	…	0	0	0	0	q_3	v_3
…	…	…	…	…	…	…	…	…	…	…
E_{n-1}	0	0	0	…	0	u_{n-1}	0	0	q_{n-1}	v_{n-1}
E_n	0	0	0	…	0	0	u_n	0	q_n	v_n
E_{n+1}	0	0	0	…	0	0	0	u_{n+1}	q_{n+1}	v_{n+1}
E_{n+2} (SL)	0	0	0	…	0	0	0	1	0	0
E_{n+3} (FF)	0	0	0	…	0	0	0	0	1	0
E_{n+4} (CD)	0	0	0	…	0	0	0	0	0	1

Figure 1. The transition probability matrix for absorbing MC

An example of a corresponding state transition diagram for the case of three inspections is shown on Figure 2. We suppose that if, in interval (T_d , T_c), some inspection is made, then fatigue failure will be eliminated.

$$u_i = P(T_d > t_i \mid T_d > t_{i-1}) = P(Q < C_d / t_i) / P(Q < C_d / t_{i-1}); \tag{8}$$

$$q_i = P(t_{i-1} < T_d < T_c < t_i \mid t_{i-1} < Td) = \begin{cases} 0, & if \quad t_{i-1}C_c / C_d > t_i, \\ P(C_c / t_i < Q < C_d / t_{i-1}) / P(Q < C_d / t_{i-1}), & if \quad t_{i-1}C_c / C_d > t_i, \end{cases} \tag{9}$$

$$v_i = 1 - u_i - q_i \,. \tag{10}$$

Unfortunately, in general the corresponding integrals are not expressed by elementary functions, but if it is assumed that C_c and C_d are some constants, then

$$u_i = a_i / a_{i-1} \,, \tag{11}$$

$$q_i = \max(0, (a_{i-1} - b_i) / (1 - a_{i-1})) \,, \tag{12}$$

$$a_i = \Phi\left(\ln(C_d / t_i) - \theta_0\right) / \theta_1) \,, \tag{13}$$

$$b_i = \Phi\left(\ln(C_c / t_i) - \theta_0\right) / \theta_1) \,, \tag{14}$$

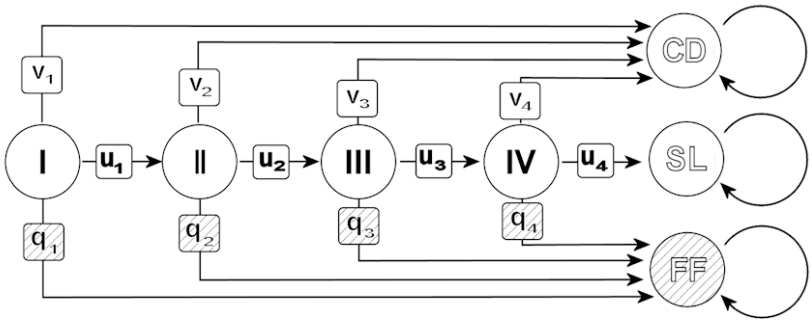

Figure 2. State transition diagram for a three-inspection program

$\Phi(.)$ is a distribution function of a standard normal variable.

The structure of considered matrices can be described as follows on Figure 3.

Q	R
0	I

Figure 3. Sub-matrices of transition probabilities matrix

Here I is a matrix of identity corresponding to absorbing states, 0 is a matrix of zeros. Then the matrix of probabilities of absorbing in different absorbing states for different initial transient states is defined by formula (18)

$$B = (I - Q)^{-1} R \,. \tag{15}$$

The first row of the matrix B defines the probabilities of absorption in states SL, FF, CD if the initial state is E_1. Particularly, $B(1,2)$ defines the failure probability of a new aircraft which begins operation during the first interval. The following rows of the matrix B define the same probabilities for different initial states (for aircraft which begin operation in different time intervals). Therefore, if, for example, aircraft begins operation in the first interval, the failure probability of aircraft in the fleet is defined in formula (19)

$$p_f = aBb \,, \tag{16}$$

where vector row $a = (1,0,...,0)$ means that all aircraft begin operation in the first interval (state E_1), vector column $b = (0,1,0)$ '.

2.3. Calculation of the cost of airline operation using theory of stationary semi-Markov chains with rewards

In order to analyse the cost of permanent operations of AL or aircraft fleets, it is necessary to modify the transition probability matrix.

The process is not absorbed or stopped in states SL, FF or CD. If these states are reached, the process restarts from the in initial state E_1. This means that an entirely new aircraft is acquired. The modified transition probability matrix, P_{AL}, is shown on Figure 4. **An e**xample of the state transition diagram is shown on Figure 5.

	E_1	**E_2**	**E_3**	**…**	**E_{n-1}**	**E_n**	**E_{n+1}**	**E_{n+2} (SL)**	**E_{n+3} (FF)**	**E_{n+4} (CD)**
E_1	0	u_1	0	…	0	0	0	0	q_1	v_1
E_2	0	0	u_2	…	0	0	0	0	q_2	v_2
E_3	0	0	0	…	0	0	0	0	q_3	v_3
…	…	…	…	…	…	…	…	…	…	…
E_{n-1}	0	0	0	…	0	u_{n-1}	0	0	q_{n-1}	v_{n-1}
E_n	0	0	0	…	0	0	u_n	0	q_n	v_n
E_{n+1}	0	0	0	…	0	0	0	u_{n+1}	q_{n+1}	v_{n+1}
E_{n+2} (SL)	1	0	0	…	0	0	0	0	0	0
E_{n+3} (FF)	1	0	0	…	0	0	0	0	0	0
E_{n+4} (CD)	1	0	0	…	0	0	0	0	0	0

Figure 4. The transition probability matrix for stationary AL operation process

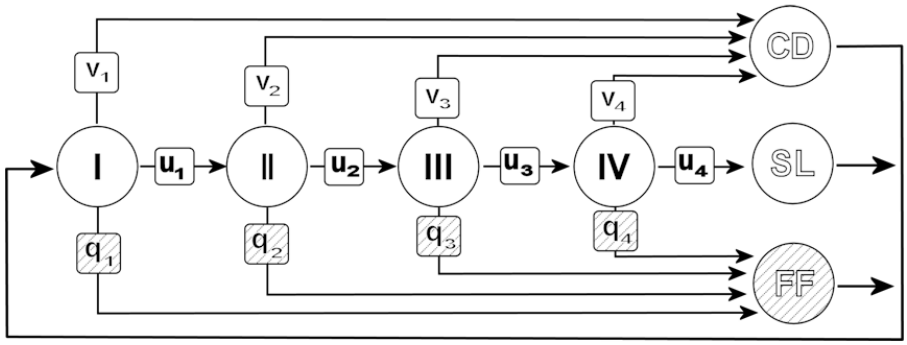

Figure 5. State transition diagram for stationary AL operation process with three inspections

Next we will consider economic analysis. The theory of Semi-Markov process with rewards is usually used to find the solution to similar problems [8]. A reward structure is described by the reward matrix R , the component of which, r_{ii}, describes the reward, connected with the transition from state i to state j ; here $i,j=1,2,...,n+4$. Let us define the reward, related to successful transitions from one operation interval to the following one by value $a(n)$; the reward related to transitions to state CD (or E_{n+4}) from any state $E_1,...,E_{n+1}$ – by value b, to state FF (or E_{n+3}) – by value c; and from states SL, FF, CD to state E_1 (acquisition of new AC) – by value d.

Let us define the gain:

$$g(n)=\sum_{i=1}^{n+4}\pi_i g_i(n), \tag{17}$$

where $\pi=(\pi_1,...,\pi_{n+4})$ is the vector of stationary probabilities, which is defined by the equation system

$$\pi P=\pi,\quad \sum_{i=1}^{n+4}\pi_i=1; \tag{18}$$

$$g_i(n)=\begin{cases} a(n)\cdot u_i+b\cdot q_i+c\cdot v_i, & i=1,...n+1,\\ d, & i=n+2,...,n+4\end{cases}; \tag{19}$$

u_i, q_i, v_i , $i=1,...,n+1$, are probabilities of successful transitions from one to the following interval, to E_{n+3} and E_{n+4} states;

$a(n)=a_0(n)+d_i t_{SL}$, $a_0(n)=a_1 t_{SL}/(n+1)$ – is the reward, related to successful transitions from one operation interval to the following one, and the cost of one inspection (negative value), d_i, which is supposed to be proportional to t_{SL} if it is supposed that all intervals are equal, a_1 defines the reward of operation in one time unit (one hour or one flight). This dimension should coincide with dimensions of t_{SL}); $b=b_1 a_0$, $c=c_1 a_0$ are the rewards related to transitions from any state $E_1,...,E_{n+1}$ to state E_{n+3} (FF takes place) and E_{n+4} (CD takes place) which are supposed to be proportional to a_0 ; $d=d_1 t_{SL}$ is the negative reward, the value of which is the cost of new aircraft after SL, FF or CD and transition to E_1 takes place (it is supposed to be proportional to t_{SL}).

If $a(n)=b=c=1$, $d=0$ and time transition to state E_1 are equal to zero. Then $\pi_{tj}=\pi_j g_j/g$ defines the part of time which SMP spends in state $E_j, j=1,...,n+1$; $L_j=g/\pi_j$ defines the mean return time for state E_j ; specifically, L_1 is the mean time of renewal of AL operation in the first interval, L_{n+3} is the mean time between FF; $\lambda_F=1/L_{n+3}$ is the intensity of fatigue failure. It should be remembered that the same value can be obtained using the theory of absorbing MC. This value is equal also to the ratio of aircraft failure probability to the mean life of new aircraft.

The problem is to maximise gain g under limitations of intensity of fatigue failure λ_F .

3. Choice of Inspection Number. Numerical Example

To simplify the numerical example we suppose that all intervals of operation are equal. On Figures 6 and 7 we see numerical examples of calculations of gain, g, and of intensity of fatigue failure, λ_F, as functions of n.

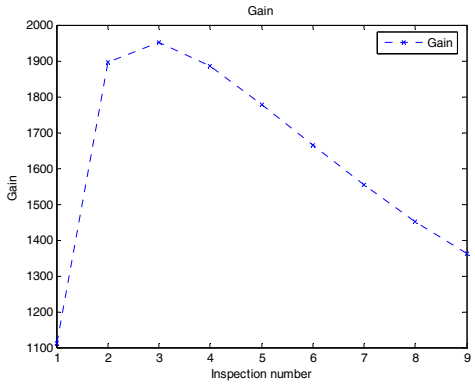

Figure 6. Gain as function of inspection number

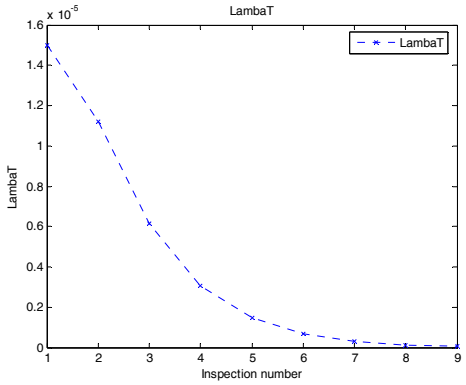

Figure 7. AL intensity of AC fatigue failure as function of inspection number

First we should choose the number of n, corresponding to the maximum of gain g: $n_g = \arg\max g(n)$. Then we should choose the minimum value of n under condition; that of intensity of fatigue failure λ_F, which is a function of n, $\lambda_F(n)$, will be equal or less than some design allowed value of intensity of fatigue failure, λ_F^*: $n_\lambda = \min\left\{n : \lambda_F(n) \le \lambda_F^*, \text{ for all } n \ge n_\lambda\right\}$.

And finally we should choose $n = \max(n_g, n_\lambda)$.

Consider the numerical example of calculation of gain, g, and intensity of fatigue failure, λ_F, for n=2 and following initial data: t_{SL}=40 000, θ_0= -8.5885, θ_1=0,34600, a_c= 102, a_d=20 (these values have been used already, for example, in [1]); $a_1 = 1$, $b_1 = 0.05$, $c_1 = -0.05$, $d_1 = -0.3$, $d_i = -0.0001$.

Using equation (10-14) we have (using the MATLAB notation for the matrix)

P_{AC} = [0 9.3958e-001 0 0 6.3833e-003 5.4037e-002
0 0 3.4655e-001 0 2.6900e-001 3.8445e-001
0 0 0 1.6030e-001 2.4240e-001 5.9730e-001
0 0 0 1.0000e+000 0 0
0 0 0 0 1.0000e+000 0
0 0 0 0 0 1.0000e+000]

In matrix P_{AL} the first three lines are the same, but in the last three lines the units are in the first column. Using P_{AL} and equations (18) we have a stationary distribution

π = [3.06e-001, 2.88e-001, 9.97e-002, 1.60e-002, 1.04e-001, 1.87e-001].

Let us define the matrix P_{uqv} with u_i, q_i, v_i in every line for $i = 1,...,n+1$. In the example

P_{uqv} =[9.3958e-001 6.3833e-003 5.4037e-002
3.4655e-001 2.6900e-001 3.8445e-001
1.6030e-001 2.4240e-001 5.9730e-001].

Then $g = \pi[P_{uqv}[a;b;c];d;d;d]$. In considered case $g = 1\,896$.

If the time unit is interval then the vector of return times for every state

$L = [g_t / \pi_1,...,g_t / \pi_6]$=[2.27, 2.41, 6.96, 4.34, 6.70, 3.72].

Here $g_t = \pi[1;1;1;0;0;0]$ is the mean gain if income is time and the time unit is interval. It is useful to note that $g_t = g$ if $a = b = c = 1$, $d = 0$. In considered case $g_t = 0.694$.

The return time of failure (state FF) is equal to corresponding (n+3)-th component of vector $L : L_F = L(n+3)$ =6.7. The time length of one interval $t_1 = t_{SL} / (n+1)$ =13 333.

The intensity of failure in t-time unit (flight or flight hour) $\lambda_F = (1 / L_F) / t_1$ = 0.0000112.

It is useful to note that the same values can be obtained using the theory of absorbing MC. We calculate the matrix of absorption

B =[5.2196e-002 3.3806e-001 6.0975e-001
5.5552e-002 3.5300e-001 5.9145e-001
1.6030e-001 2.4240e-001 5.9730e-001].

Then we take from it the probability of absorption of new aircraft in state FF, p_f =0.338, calculate the mean time to absorption of new aircraft, $T_1 = \tau_1 t_1$ (where τ_1=2.27 is the mean time to absorption if the time unit is interval-which coincides with $L(1)$!) and calculate the ratio p_f / T_1 =0.0000112.

On Figures 6 and 7 we see similar calculations for n=1, …, 9. And we see that the maximum of g we have for n =3. We can choose this number of inspections if allowed failure intensity is higher or equal to (approximately) 0.000006, because λ_F is equal just to this value at this number of inspections.

4. Conclusions

This paper presents (based on MC and SMP with rewards theory) a method to solve the problem of inspection planning corresponding to maximum airline gain while respecting limitations due to the intensity of fatigue failure. In this paper the case is considered when parameters of fatigue crack growth exponential models are known. If a parameter is unknown, the minimax approach (see [1]) should be used. Numerical examples are given.

References

1. Paramonov, Yu., Kuznetsov, A. Reliability of Fatigue-Prone Airframe, *International Review of Aerospace Engineering (IRAEASE)*, Vol. 2, No 3, 2009, pp. 145-153.
2. Paramonov, Yu., Kuznetsov, A. Using of p-set function for airframe inspection program development, *Communication of Dependability and Quality Management*, Vol. 9, No 1, 2006, pp. 51-55.
3. Paramonov, Yu.M. Aircraft fatigue problem solution by use of modern mathematical statistics methods, *Aviation*, No 6, 2002, pp. 83-96. (Vilnius: Technika)
4. Paramonov, Yu.M. P-set function application for specified life nomination and inspection program development. In: *Proceedings of International Conference "Probabilistic Analysis of Rare Events: Theory and Problems of Safety. Insurance and Ruin", Jurmala, Latvia. June 28 - July 3, 1999.* Riga: RAU, 1999, pp. 202- 208.
5. Paramonov, Yu.M., Paramonova, A.Yu. Inspection program development by the use of approval test results, *International Journal of Reliability, Quality and Safety Engineering,* Vol. 7, No 4, 2000, pp. 301-308.
6. Paramonov, Yu., Kuznetsov, A. Inspection program development for fatigue crack growth model with two random parameters. *Aviation*, Vol.12, No 2, 2008, pp. 33-40.
7. Gertsbakh, I. Reliability Theory. With Application to Preventive Maintenance. Berlin Heidelberg. New York: Springer-Verlag, 2000. 220 p.
8. Howard, R.A. *Dynamics Programming and Markov Processes*. New York, London: John Wiley & Sons, Inc., 1960. 136 p.

Transport and Telecommunication, 2010, Volume 11, No 4, 66–74
Transport and Telecommunication Institute, Lomonosova 1, Riga, LV-1019, Latvia

COMPUTING EFFICIENCY METRICS FOR SYNERGIC INTELLIGENT TRANSPORTATION SYSTEMS

B. Tsilker[1], S. Orlov[2]

Transport and Telecommunication Institute
Faculty of Computer Science and Electronics
Lomonosova str. 1, Riga, LV-1019, Latvia
E-mail: tsilker@tsi.lv[1], sorlov@tsi.lv[2]

Considerable progress in computing and telecommunications opened new approaches for solving of transportation problems, affected in the concept of intelligent transportation systems (ITS). Technically such systems represent a set of interacting computational nodes with various sensors, and can be considered as distributed computer systems. Distributed nature of the ITS implies parallelization of solvable transportation tasks in conjunction with their distributed realization.

Under efficiency of parallelized calculations we presuppose several aspects. Three of them are picked out in the work: calculation speed, efficiency of system scaling, and efficiency of parallel computations as compared to sequential ones. Typical metrics for numerical characterization of parallelized computations form three groups: index of parallelism and speedup (*PI* and *S*), efficiency and utilization (*E* and *U*), redundancy and compression (*R* and *C*).

The main peculiarity of synergic intelligent transportation systems shows up in bulk of intercommunications, substantially affecting the indexes of the system. Present work focuses on influence of these communication overheads on overall efficiency of the synergic ITS.

Keywords: intelligent transportation system, parallelization, distributed systems, efficiency, performance metrics

1. Introduction

Information technologies (IT) have transformed many industries. In respect to transportation systems such transformations started in the past decade and are now in the early stages. IT enables elements within the transportation system — vehicles, roads, traffic lights, message signs, etc. — to become intelligent by embedding them with microchips and sensors and empowering them to communicate with each other through wireless technologies. Transportation systems realizing this approach are known as intelligent transportation systems (ITS). According to definition of the Intelligent Transportation Systems Society ITS are those utilizing synergistic technologies and systems engineering concepts to develop and improve transportation systems of all kinds.

Through the use of advanced computing, control, and communication technologies, ITS promises to greatly improve the efficiency and safety of the existing surface transportation system and reduce the transportation-related energy consumption and negative environmental impact. ITS encompass a broad range of wireless and wire line communications-based information and electronics technologies. Depending on nature of the solvable transportation tasks, ITS is made up of 16 types of technology-based systems (Fig. 1).

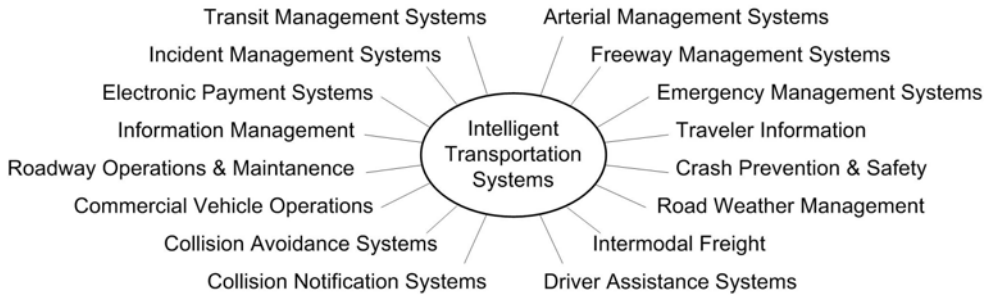

Figure 1. Classification of ITS applications

In less detail all ITS types are divided into intelligent infrastructure systems and intelligent vehicle systems.

2. Specificity of Parallel and Distributed Computing

The variety of transportation tasks stipulates a spectrum of ITS construction methods, and, of course, differing requirements to ITS hardware and software architecture. However in any case each system as much as possible must be economically and technically effective. It's clear, that for the estimation of technical-and-economic efficiency it is necessary to define the most suitable criteria and system of indexes, numerically characterizing the degree of ITS compliance with these criteria.

From the presented classification of transportation tasks (Fig. 1) follows that the majority of ITS applications on their synergic nature presume distributed solution, where outcome is reached due to cooperative processing of information, incoming from numerous sources, for example, from different sensors. Information processing, as a rule, is also decentralized. By other words, such ITS represent distributed computer systems. Only limited range of ITS is realizable by centralized computer systems, but even here, by reason of high performance requirements, parallel computer systems are usually used. Thus, at examining of ITS estimation, we must talk about parallel and distributed computer systems.

The problem of efficiency estimation for parallel systems is well studied [1-3]. By now exists universally recognized harmonious system of indexes, fully applicable to ITS of this type. On the other hand, universal evaluation metrics for distributed systems at the present time are unknown. Typical attempts usually come to separate estimation of distributed systems' components and getting some integral index based on these particular appraisals. Besides of complexity of such approach realization, it imperfectly takes into account influence of particular components interaction on the total system efficiency.

We offer another approach to efficiency estimation of ITS having distributed nature, based on considering of distributed calculations as a special case of parallel calculations. At distributed calculations each task is actually segmented, i.e. is partitioned on concurrent subtasks. The main property of distributed computing is in extra costs, arising due to interaction of system constituents. Because of ideological closeness of parallel and distributed calculations it is suggested to take the advantage of parallel system efficiency indexes by mapping them on the distributed systems.

3. Overheads in Parallel and Distributed Computations

Overheads in parallel and distributed computations fall in three groups:

- intercommunications (typically the most significant overhead in distributed computations);
- idling (processor may become idle because of load imbalance, synchronization, and presence of serial computation);
- excess computations (difference in computation fulfilled by the parallel program and the best sequential program is the excess computation overhead incurred by the parallel program).

Parallel overhead is encapsulated into a single expression referred to as the overhead function. Overhead function (or total overhead), T_0, of a parallel system is defined as the total time collectively spent by all n processing elements over and above time $T(1)$, required by the fastest known serial algorithm for solving the same problem on a single processing element:

$$T_0 = n \times T(n) - T(1) .$$

4. Communication Overhead in Distributed Computing

For determining communication time between elements of distributed computations t_{comm} three parameters usually are used:

- Start-up time (t_s): The time required to handle a message at the sending processor including the time to prepare the message, the time to execute the routing algorithm, and the time to establish an interface between the local processor and router.
- Per-hop time (t_h): The time, also known as node latency, for message header to travel between two directly connected processors.
- Per-word transfer time (t_w): The time for a word traverse a link. If the channel bandwidth is r words per second, then per-word transfer time is $t_w = \frac{1}{r}$.

Thus, $t_{comm} = t_s + t_h + t_w$.

Consider two routing modes: store-and-forward routing (Fig. 2,*a*) and cut-through routing (Fig. 2,*b*).

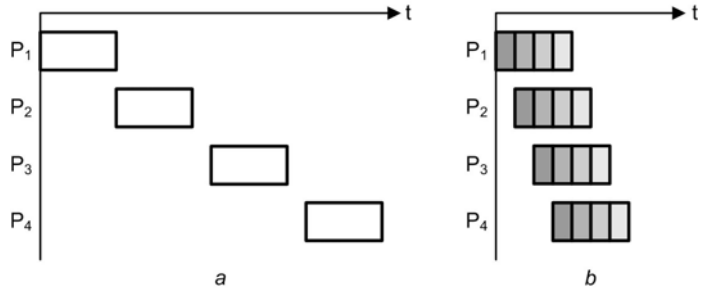

Figure 2. Routing modes: *a* – store-and-forward; *b* – cut-through

At store-and-forward routing a message is traversing a path with multiple links: each intermediate processor on the path forwards the message to the next processor after it has received and stored the entire message. In that case the communication overhead can be described by expression

$$t_{comm} = t_s + (mt_w + t_h)l ,$$

where m — message size in words, l — path length in channel number.

Usually $t_h << mt_w$, therefore the expression is simplified to

$$t_{comm} = t_s + mt_w l .$$

At cut-through routing a message is forwarded at intermediate node without waiting for entire message to arrive with no buffering in memory (busy link causes worm to stall; deadlock may ensure). Here the communication overheads are represented by expression

$$t_{comm} = t_s + mt_w + lt_h .$$

Again, considering t_h, to be small compared to mt_w, the communication overhead is

$$t_{comm} = t_s + mt_w .$$

5. Parallel Computing Metrics

To study the performance of systems or to compare different systems for a given purpose, we must first select some criteria. These criteria are often called metrics in performance evaluation. Different situations need different sets of metrics. Thus, selecting metrics are highly problem oriented. Different metrics may result in totally different values. Hence, selecting proper metrics to fairly evaluate the performance of a system is difficult. Another problem with selecting metrics is that in a real system different metrics may be relevant for different jobs. Good metrics are to be reliable, repeatable, consistent and independent. Additional, but not necessary requirements for good metrics are linearity and easiness of use.

Parallel computing metrics are a system of indexes, making possible quantitative estimation of advantages, got at parallel task solution on n processors, as compared to the serial solution of the same task on single processor. On the other hand, they make it possible to judge about the legality of processor amount growth for solving of given task. Under *parallel computing* will understand the sequence of steps, where each step consists of i operations, implemented simultaneously by a set of i processors, working in parallel. The basis for definition of the mentioned metrics form followings characteristics:

- n — number of processors, used for organization of parallel calculations;
- $O(n)$ — amount of calculations, expressed through the number of operations, executable by n processors during the task solution;
- $T(n)$ — total time of calculations (task solution) with the use of n processors.

We will arrange, that time changes discretely, and a processor executes any operation in time slice. The followings correlations are hereupon valid for time and volume of calculations: $T(1) = O(1)$, $T(n) \leq O(n)$. The last correlation formulates assertion: *time of calculations can be shortened due to distributing of calculation volume on a few processors*.

The number of processors used by a program at a particular point in time defines the *degree of parallelism P*(*t*). The plot of parameter *P* against time is called the *parallelism profile* for the program. Changes in the *P*(*t*) depend on many factors (algorithm, available resources, compiler optimisations, etc.). A typical parallelism profile for a *divide-and-conquer* algorithm is shown on Figure 3.

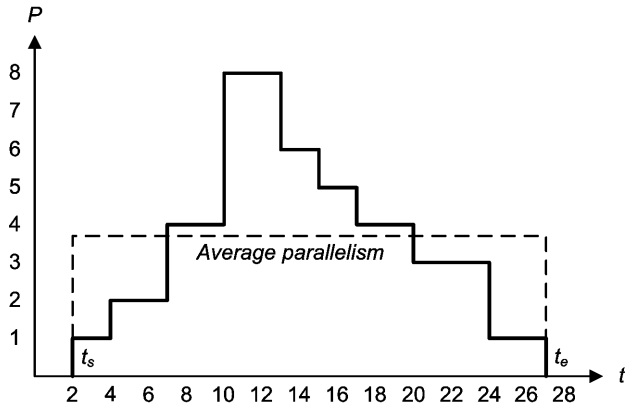

Figure 3. Parallelism profile for typical divide-and-conquer algorithm

Suppose that system consists of *n* of homogeneous processors. Let's express the computing capacity of a single processor *Δ.* as an amount of operations in a time unit, not taking into account overheads, related to memory access and data transmission. If for observed period of time (certain amount of time slices) are loaded *i* processors, then *P* = *i*. Thus, a program run from the start time t_s to the moment of completion t_e needs a total of *O*(*n*) operations. *O*(*n*) is proportional to area under to the curve of parallelism profile:

$$O(n) = \Delta \sum_{i=1}^{n} it_i,$$

where t_i is a time interval (common amount of time slices), during which *P* = *i*, and $\sum_{i=1}^{n} t_i = t_e - t_s$ is common time of calculations.

Average parallelism A is defined as

$$A = \frac{\sum_{i=1}^{n} it_i}{\sum_{i=1}^{n} t_i}.$$

The parallelism profile on the Figure 3 in course of observation time (t_s, t_e) grows from 1 to peak value *n* = 8, then go down to 0. Average parallelism *A* = (1 × 5 + 2 × 3 + 3 × 4 + 4 × 6 + 5 × 2 + 6 × 2 + 8 × 3) / (5 + 3 + 4 + 6 + 2 + 2 + 0 + 3) = 93/25 = 3,72.

In essence it is possible to single out four groups of metrics.

The first group characterizes speed of calculations. This group is presented by a pair of metrics – *parallel index* and *speedup*.

Parallel Index characterizes average speed of parallel calculations through the amount of the executed operations:

$$PI(n) = \frac{O(n)}{T(n)}.$$

Speedup due to program concurrent execution serves as the index of effective speed of calculations. It expresses how much the performance improves when compared to the sequential execution (relative benefit). Speedup is calculated as the ratio of runtime for solving a problem on a

single processor (using the best sequential algorithm) to the time taken for the same problem by a parallel system of *n* processors (at using the best parallel algorithm).

$$S(n) = \frac{T(1)}{T(n)}.$$

Remark in relation to the algorithms of task solution algorithms underline the fact that different algorithms can in the best case appear for serial and parallel realization, and at the estimation of the speedup it is necessary to come exactly from the best algorithms. If the fastest sequential algorithm is not known, the fastest practical approach usually is used.

The second group is formed by *efficiency* and *utilization* metrics, making possible to judge about the efficiency of bringing to the task solution of additional processors.

Efficiency characterizes the reasonability of processor number increasing through the fraction of speedup, attained due to parallel calculations, which falls on one processor:

$$E(n) = \frac{S(n)}{n} = \frac{T(1)}{nT(n)}.$$

Efficiency measures the fraction of time the processor is usefully employed. It indicates the actual degree of speedup achieved in a system as compared with the maximum possible speedup.

Utilization takes into account contribution of every processor at a parallel computing, expressed as amount of operations, executed by a processor in time unit. It indicates the degree to which the system resources were kept busy during execution of the program.

$$U(n) = \frac{O(n)}{nT(n)}.$$

The third group of metrics, — *redundancy* and *compression*, — characterizes efficiency of parallel computing by comparison of volume of calculations, executed at the parallel and serial task solution.

Redundancy is a ratio of parallel calculations volume and equivalent successive calculations volume:

$$R(n) = \frac{O(n)}{O(1)}.$$

It shows the extent of the workload increase for going from serial to parallel execution. Importance of this metrics is in that it will proceed not from the relative speedup and efficiency indexes, got from calculation time, but from the absolute indexes, being based on the volume of the executed computational work. The R (n) figure indicates to what extent the software parallelism is carried over to the hardware implementation without having extra operations performed.

Note that utilization can be expressed through the redundancy and efficiency metrics:

$$U(n) = \frac{O(n)}{nT(n)} = R(n)E(n).$$

Correlation $T(1) = O(1)$ is taken into account here.

Compression is calculated as a reciprocal value of redundancy:

$$C(n) = \frac{O(1)}{O(n)}.$$

Finally, the fourth group is formed by the only metrics – *quality*, joining three considered groups of metrics.

Quality is defined as:

$$Q(n) = \frac{T^3(1)}{nT^2(n)O(n)} = S(n)E(n)C(n).$$

This measure is directly related to speedup and efficiency, and inversely related to redundancy R. As far as this metrics ties up speedup, efficiency and compression metrics, it is more objective index of performance improvement due to parallel calculations, and can be considered as an common measure (integral index) defining the whole system performance.

For an example will define the numerical values of metrics in respect to the task, used for parallelism profile concept illustration (Fig. 1). Supposing that the best algorithm for a successive and parallel calculation match, have: $n = 8$; $T(1) = O(1) = O(8) = 93$; $T(8) = 25$. Then:

$$PI(8) = \frac{O(8)}{T(8)} = \frac{93}{25} = 3,72; \qquad S(8) = \frac{T(1)}{T(8)} = \frac{93}{25} = 3,72;$$

$$E(8) = \frac{T(1)}{8T(8)} = \frac{93}{8 \times 25} = 0,465; \quad U(8) = \frac{O(8)}{8T(8)} = \frac{93}{8 \times 25} = 0,465;$$

$$R(8) = \frac{O(8)}{O(1)} = \frac{93}{93} = 1; \qquad C(8) = \frac{O(1)}{O(8)} = \frac{93}{93} = 1;$$

$$Q(8) == S(8)E(8)C(8) = 3,72 \times 0,465 \times 1 = 1,73.$$

At completion note that for the considered metrics the following correlations are true:

$$1 \le S(n) \le PI(n) \le n; \quad 1 \le R(n) \le \frac{1}{E(n)} \le n; \quad \frac{1}{n} \le E(n) \le C(n) \le 1;$$

$$\frac{1}{n} \le E(n) \le U(n) \le 1; \quad Q(n) \le S(n) \le PI(n) \le n.$$

6. Speedup Models

There are several laws that have been observed in parallel computing. Three well-known speedup models – fixed-size, fixed-time, and memory-bounded – define the upper limit of speedup achievable by a parallel system. All laws assume that workload in parallel computing comprises of two parts, a sequential part, and a perfectly parallel part. Let f be the percentage of the sequential portion.

In the fixed-size model, known as Amdahl's law [4], it is assumed that the problem size, or workload, is fixed (Fig. 4), and the respective expression for speedup is

$$S(n) = \frac{T(1)}{T(n)} = \frac{1}{f + \frac{1-f)}{n}}.$$

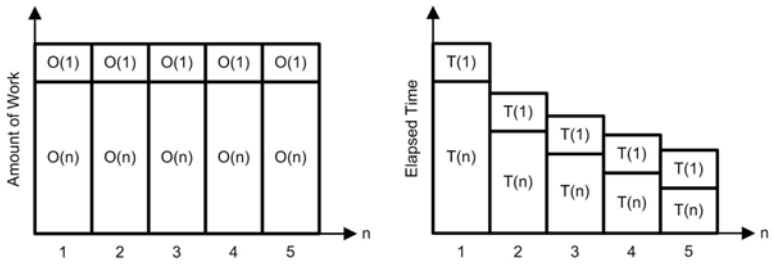

Figure 4. Illustration for Amdahl's law statement

John Gustafson [5] proposed a fixed law using time concept to scale the speed up model and remove the fixed load restriction. This law states that problem size scales with the number of processors and idea is to keep all processors busy by increasing the problem size. When the system size is increased and more computing power obtained, we may increase the problem size and perform more operations,

thus obtaining more accurate solution, yet keeping the turnaround time unchanged (Fig.5). This observation is in a basis of Gustafson's law:

$$S(n) = \frac{O(n)}{O(1)} = f + (1-f)n$$

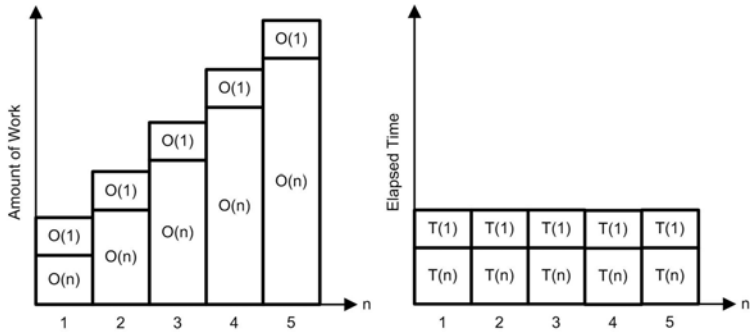

Figure 5. Illustration for Gustafson's law statement

Sun and Ni [6] notice that in parallel systems the scaled problem size is limited by memory space. Under the assumption (Fig.6) they developed the memory-bounded speedup law:

$$S(n) = \frac{O(n) / T(n)}{O(1) / T(1)} = \frac{f + (1-f)G(n)}{f + (1-f)\dfrac{G(n)}{n}},$$

where $G(n)$ is the increase of parallel workload as the memory capacity increases n times.

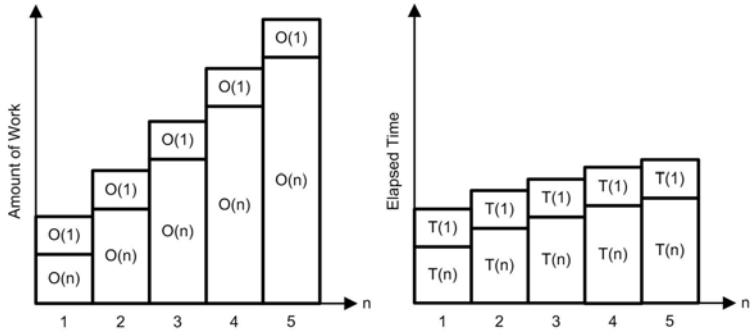

Figure 6. Illustration for Sun's and Ni's law statement

At $G(n)=1$ Sun' and Ni's speedup transforms into fixed-sized form (Amdahl), but at $G(n)=n$ – into fixed-time version (Gustafson). $G(n) > n$ represents parallel computing with overheads.

7. Metrics for Distributed Computing

For obtaining of similar system of metrics for distributed computing we propose mapping of main parallel computing metrics on the case of distributed computing by taking into account communications overheads. Such mapping results in following "distributed" metrics.

In particular, the speedup metrics goes over:

$$S_d(n) = \frac{T(1)}{T(n) + \sum_{i=1}^{n} t_{comm}(i)},$$

where $t_{comm}(i)$ is communications overhead of *i*-th processor, $\sum_{i=1}^{n} t_{comm}(i)$ is total communication overhead of all *n* processors of the distributed system.

Accordingly the efficiency and utilization metrics are written down in a form of:

$$E_d(n) = \frac{T(1)}{n \times T(n) + \sum_{i=1}^{n} t_{comm}(i)},$$

$$U_d(n) = \frac{O(n)}{n \times T(n) + \sum_{i=1}^{n} t_{comm}(i)}.$$

Formula of integral index *of quality* is modified as follows:

$$Q_d(n) = \frac{T^3(1)}{(T(n) + \sum_{i=1}^{n} t_{comm}(i)) \times (n \times T(n) + \sum_{i=1}^{n} t_{comm}(i)) \times O(n)}.$$

Expressions for the rest metrics remain unchanged.

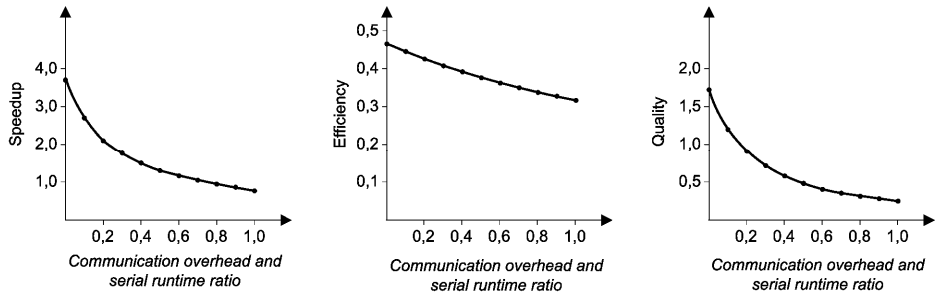

Figure 7. Efficiency indexes of a distributed system, realizing the divide-and-conquer algorithm

Figure 7 illustrates influence of communication overhead on the efficiency indexes of a computer system at distributed solution of the before considered divide and concur algorithm. Value on a vertical axis corresponds to absence of communication overhead, i.e. to the parallel system.

8. Speedup Models for Distributed Computing

Speedup laws for parallel computing also can be mapped on the distributed computation case by taking into account communication overheads typical for last ones.

Fixed-size speedup low (Amdahl) with overheads transforms in the following expression ($\sum_{i=1}^{n} t_{comm}(i)$ is denoted as T_{comm}).

$$S_d(n) = \frac{T(1)}{T(n)} = \frac{1}{f + \frac{1-f}{n} + \frac{T_{comm}}{T(1)}}.$$

Fixed-time Speedup (Gustafson) with overheads will be

$$S_d(n) = \frac{O(n)}{O(1)} = f + (1 - f - \frac{T_{comm}}{T(1)})n.$$

As follows from the expressions the upper speedup bound is not only limited by the sequential bottleneck but also by the average overheads.

9. Conclusions

The issue of the day in intelligent transportation systems development still is a task of effective selection and design of the used software and hardware tools. Within the framework of decision of this task, authors had analysed characteristics of given problem domain, singularities of structural organization and functioning for this family of computer systems, had explored their specificity, had offered a set of metrics for the estimation of efficiency of parallel and distributed modes of operation. These metrics permit estimation of integral efficiency of intelligent transportation systems, and take into account basic features of both parallel and distributed computing.

References

1. Voevodin, V.V., Voevodin, Vl. B. *Parallel computing*. SPb.: BHV-Petersburg, 2002. 608 p. (In Russian)
2. Orlov, S.A., Tsilker, B.J. *Computer organization and systems. 2nd ed.* SPb.: Peter, 2010. 688 p. (In Russian)
3. Zomaya, Albert Y.H. *Parallel and Distributed Computing Handbook: McGraw-Hill Series on Computing Engineering.* New York, 1996.
4. Amdahl, G. M. Validity of the single processor approach to achieving large scale computing capabilities. In: *Proc. AFIPS Conference*, Reston, VA. April 1967. Vol. 30, pp. 483-485.
5. Gustafson,, J. L. Re-evaluating Amdahl's law, *Communications of the ACM*, Vol. 31, No 5, May 1988, pp. 532-533.
6. Sun, X. -H. and Ni, L. M. Scalable problems and memory-bounded speedup, *Journal of Parallel and Distributed Computing*, Vol. 19, 1993, pp. 27-37.

Transport and Telecommunication, 2010, Volume 11, No 4
Transport and Telecommunication Institute, Lomonosov 1, Riga, LV-1019, Latvia

Authors' index

Igor V. Kabashkin (born in Riga, August 6, 1954)

- Vice-rector for Research and Development Affairs of Transport and Telecommunication Institute, Professor, Director of Telematics and Logistics Institute
- Ph.D in Aviation (1981, Moscow Institute of Civil Aviation Engineering), Dr.sc.habil. in Aviation (1992, Riga Aviation University), Member of the International Telecommunication Academy, Member of IEEE, Corresponding Member of Latvian Academy of Sciences (1998)
- **Publications:** 390 scientific papers and 67 patents
- **Fields of research:** information technology applications, operations research, electronics and telecommunication, analysis and modelling of complex systems, transport telematics and logistics

Eugene A. Kopitov (born in Lignica, Poland, December 5, 1947)

- Rector of Transport and Telecommunication Institute, professor, Dr.habil.sc.ing, Member of International Telecommunication Academy
- Director of Programs "Master of Natural Sciences in Computer Science" and "Master of Engineering Sciences in Management of Information Systems" (Transport and Telecommunication Institute)
- **University study**: Riga Civil Aviation Engineering Institute (1966–1971); Candidate of Technical Science Degree (1984), Kiev Civil Aviation Engineering Institute); Dr.sc.ing. (1992) and Dr.habil.sc.ing. (1997), Riga Aviation University
- **Publications:** 240 publications, 1 certificate of inventions
- **Fields of research:** computer science and information technology applications, mathematical and computer modelling, system analysis, modern database technologies

Alexander N. Pavlov (born in Leningrad, May 14, 1957)

- Senior researcher, Laboratory for Information Technologies in Systems Analysis and Modelling, St. Petersburg Institute for Informatics and Automation of the Russian Academy of Sciences (SPIIRAS)
- **Education:** Leningrad State University, Department of Mathematics and Mechanics (1979)
- Ph.D. Eng (1990), Associate Professor (2004)
- **Publications:** more than 100 scientific papers and 6 teaching books
- **Fields of research:** systems analysis and operations research, analysis and modelling of complex systems, development of research fundamentals for the control theory by structural dynamics of complex organizational-technical systems

Valery A. Kutev (born in Leningrad, January 20,1945)

- Professor of Transport and Telecommunication Institute, a Head of Electronics Department
- Director of Academic Programme "Bachelor of Engineering Sciences in Electronics" and Professional Programme "Electronics" (Transport and Telecommunication Institute)
- **University study**: Riga Civil Aviation Engineering Institute (1963–1968); Candidate of Technical science degree in Radiolocation and Radio navigation (1973)**,** Riga Civil Aviation Engineering Institute; Dr.sc.ing.(1992) and Dr.habil.sc.ing. (1993), Riga Aviation University
- **Publications**: 126 publications, 8 certificates of inventions
- **Scientific activities**: electronics, digital technology, radar subsurface probing, radar data processing

Vyacheslav A. Zelentsov (born in Gorky, August 4, 1955)

- Leading researcher, Laboratory for Information Technologies in Systems Analysis and Modelling, Head of Research Consulting Center for Space Information Technologies and Systems at St. Petersburg Institute of Informatics and Automation of the RAS (SPIIRAS), Professor and Director of Research and Education Centre "AeroSpaceInfo" in St Petersburg State University of Aerospace Instrumentation
- **Education:** A.F. Mozaisky Academy in Leningrad (1977)
- **Scientific and university degrees:** Ph.D. Eng, Dr. sc. ing. and Professor in 1984, 1994 and 1998 respectively.
- **Scientific activities:** Member of IEC, Member of Doctoral Degrees Granting Committee in The Bonch-Bruevich Saint-Petersburg State University of Telecommunications.
- **Publications:** more than 180 scientific paper, more than 50 research and engineering projects, 5 teaching books
- **Fields of research:** basic and applied research in integrated modelling, multi-criteria optimisation under uncertainties, reliability theory, and mathematical models and methods of decision-making support in complex technical-organizational systems with the use of aerospace information.

Alexander V. Krainyukov (born in Frunze, October 31, 1956)

- Lecturer of Transport and Telecommunication Institute
- **University study**: Riga Civil Aviation Engineering Institute (1974-1980); Master degree in engineering (1995), Riga Aviation University
- **Publications**: 40 publications, 1 certificate of inventions
- **Scientific activities**: electronics, programming, radar subsurface probing, radar modelling

Daniil A. Opolchenov (born in Ventspils, March 24, 1984)

- Mg.sc.ing., assistant at Transport and Telecommunication Institute
- **University study**: Bachelor of engineering sciences in electronics (2007); Master of engineering sciences in electronics and electrical engineering science (2010).
- **Publications**: 3 publications
- **Scientific activities**: electronics, hardware programming, computer modelling

Jury A. Krasnitski (born in Penza, April 11, 1938)

- Professor, Dr.habil.sc.ing., Professor of Telecommunication Department of Transport and Telecommunication Institute
- **Education:** Leningrad Precise Mechanics and Optics Institute (radio engineer diploma, 1961)
- **Scientific degrees:** Candidate of Technical Science Degree (Riga Civil Aviation Engineering Institute, 1969), Dr.phys.-math.sci. (Leningrad Main Geophysical Observatory, 1989), Dr.habil. sc.ing. (Riga Aviation University, 1992)
- **Publications:** about 150 scientific papers, 5 patents, 9 books and tutorials
- **Fields of research:** radio physics, electrodynamics and antennas, non-stationary processes, computer modelling, digital signal processing

Boris Y. Tsilker (born in Riga, November 19, 1948)

- Associate Professor, Dr.sc.ing., Ass. Professor of Telecommunication Department
- **University study**: Riga Institute of Civil Aviation Engineers (1966–1971)
- Ph.D in Radiolocation and Radio-navigation (1980, Moscow Institute of Civil Aviation Engineers), Dr.sc.ing. (1992, Riga Aviation University)
- **Publications:** 73 scientific papers, 17 teaching books, 4 patents
- **Fields of research:** computer architecture, software engineering, aviation simulators, sensor networks, intelligent transportation systems

Victor Krebss (born in Riga, Latvia, October 1968)

- IT Director Complete Payment Systems Ltd. Riga, Latvia
- **Education:** Master of natural science in computer science.
- Doctorate student of Telematics and Logistics (Transport and Telecommunication Institute)
- **Fields of research:** Intelligent Transportation Systems, information technology applications, statistical data computer processing methods, sensor networks.

Sergey A. Orlov (born in Belaja Tcerkov, Ukraine)

- Head of the Chair of Software Engineering, Professor of Computer Science Department
- **Education:** the Perm High Engineering School, Kharkov Aviation Institute, Faculty of Control Systems of Flying Devices, Diploma of Electrical Engineer: control systems of flying devices and an electric equipment to them, 1970
- **Scientific and university degrees:** Candidate of Technical Science Degree (1984), Riga Aviation University, Dr.sc.ing. (1992)
- **Publications:** more than 100 scientific papers and teaching books
- **Fields of research:** software engineering, visual modelling, theory of programming languages, information technology applications, architecture of computer systems, theory of control systems

Andrei Vishnyakov (born in Rezekne, Latvia, February 12, 1982)

- Mg.sc.comp., Transport and Telecommunication Institute
- **University study**: Bachelor degree in computer science, Transport and Telecommunication Institute (2004); Master degree in computer science, Transport and Telecommunication Institute (2006)
- **Publications:** 3 scientific papers

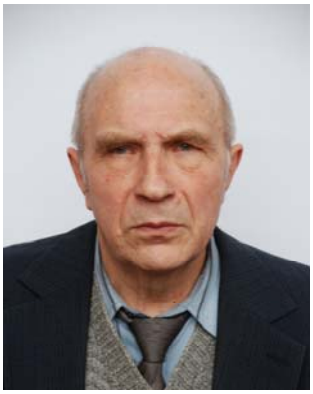

Yuri M. Paramonov (born in St.Petersburg, March 28, 1938)

- Head, Professor of Aircraft Theory and Structure Department of Aviation Institute of Riga Technical University
- Riga Aviation Engineering Military High School, Mechanical Engineering Diploma with golden Medal (1960). Dr. sc. ing. degree (1965). Dr.sc.habil. in Aviation (1992)
- **Fields of research:** Reliability of technical systems; loads, structure and strength analysis of transport vehicle
- **Publications:** 273 scientific papers, 11 monographs and textbooks

Maris Hauka (born in Talsi, Latvia, October 24, 1983)

- Aviation Institute of Riga Technical University, lecturer
- Riga Aviation University (former Riga Civil Aviation Engineering Institute), Faculty of Transport and Mechanical Engineering, Mg. sc. ing.
- **Publications:** 3 scientific papers
- **Fields of research:** computer modelling, reliability of technical systems

CUMULATIVE INDEX

TRANSPORT and TELECOMMUNICATION, Volume 11, No 4, 2010 (Abstracts)

Kopytov, E.A., Pavlov, A.N., Zelentsov, V.A. New Methods of Calculating the Genome of Structure and the Failure Criticality of the Complex Objects' Elements, *Transport and Telecommunication*, Vol. 11, No 4, 2010, pp. 4–13.

There are considered two new methods of analysing the contribution of separate elements into the efficiency of a complex object. The first one is based on the introduction of a new notion – "the genome of structure" applied for calculating the structural significance of the monotonous and non-monotonous systems. The second method allows estimation of a more general indicator – failure criticality of the element. This method is based on a combined method of a fuzzy logic conclusion and on the methods of the experiment planning theory. The failure criticality of the complex objects' elements is expressed by a vector property for which evaluating there is used a number of partial indicators, which may have both quantitative and qualitative character and for their measurement there may be used different types of scales. The resulting indicator of the element failure criticality is presented in the form of a polynomial which accounts both the influence of the separately taken indicators and the influence of the indicators' aggregations (of 2, 3, etc.). Calculation of the polynomial coefficients is made on the basis of processing the expert information and the corresponding linguistic variables quantitatively measured by fuzzy numbers.

Keywords: genome of structure, failure criticality, complex object, multi-criteria analysis, theory of experiment planning, linguistic variable

Krainyukov, A., Kutev, V., Opolchenov, D. Approach to Hardware Implementation of Genetic Algorithm for Inverse Problem of Roadway Coverage Subsurface Probing Solution, *Transport and Telecommunication*, Vol. 11, No 4, 2010, pp. 14–28.

This work has focused on the problem of approach to hardware implementation of genetic algorithm for inverse problem of roadway coverage subsurface radar probing solution. Iterative procedure to solve the inverse problem in frequency domain is used on base of aim function minimization. Genetic algorithm is used for search of global minimum of aim function.

For hardware implementation of genetic algorithm it is necessary correctly to choose the values of arguments for aim function and parameters of genetic algorithm. The authors investigated two different kinds of aim functions. Estimation of possibility for genetic algorithm hardware implementation on base of field-programmable gate array (FPGA) is discussed.

Keywords: roadway radar monitoring, inverse problem, genetic algorithm, field-programmable devices, hardware implementation

Krasnitsky, Yu. A. Some Features of the Hop Model of Earth-Ionosphere Waveguide, *Transport and Telecommunication*, Vol. 11, No 4, 2010, pp. 29–35.

The problem of electromagnetic pulse radiator location from single station observation is considered, based on the hop model of pulse propagation in spherical waveguide 'Earth-ionosphere'. Pulse characteristics both ground wave and hop (sky) waves of that waveguide are modelled as functions of the distance from radiation source. The waveguide parameters, namely, the distance from the radiator and the effective reflecting heights of the ionosphere, can be evaluated through the delays of the waves reflected by the ionosphere with respect to the ground wave. The errors in values of delays give rise to the errors in the waveguide parameters. These connections are investigated. It is demonstrated how the waveguide parameter errors depend on the distances and heights of reflections. A method to reinterpret the hop model features by using some equivalent antenna array conception is proposed.

Keywords: electromagnetic radiation, ionosphere, waveguide, hop model, distance, effective heights, delays, lightning discharge, atmospherics

Krebss, V, Tsilker, B. Coverage Estimation in Sinergic Networked Intelligent Transportation Systems with Non-Isotropic Nodes, *Transport and Telecommunication*, Vol. 11, No 4, 2010, pp. 36–45.

Safety of road travel is of the most considerable tasks solvable by intelligent transportation systems (ITS). It can be solved by mutual interaction of nodes equipped by sensors forming a sensor network. The wireless sensor networks can be integrated into ITS as vehicles through vehicle-to-vehicle or infrastructure-to-vehicle communication models to monitor the road condition, construction sites or obstacles for driving safety and to announce such road. Wireless sensor networks also pose a number of challenging optimisation problems. Coverage problem was and remains a fundamental issue in construction of wireless networks.

Most of known investigations, concerned with optimal (in sense of ensuring of necessary coverage level at every point in service area) deployment of networks' nodes, i.e., with optimal network topology, study the problem on the assumption that wireless network service area is free from obstacles, impeding normal propagation of information signals [1-3]. As a result, suggested network topologies become far from optimal at presence of obstacles within serviced area. More realistic solution presumes taking into account of obstacles within the serviced area.

Possible approaches for efficient placement of wireless network nodes on condition that service area contains obstacles are discussed at present work. Problem is examined from two points of view: as a probabilistic task, as well as a task of computational geometry. A probabilistic model is more realistic because the sensor design and environmental conditions are all stochastic in nature. Interference and noise in the environment can be modelled by stochastic processes. The investigation has resulted in some algorithms and considerations for near to optimal deployment of nodes within network service zone with obstacles.

Keywords: Intelligent Transportation System, anisotropic sensor, sensor network, coverage, service area

Orlov, S, Vishnyakov, A. Pattern-Oriented Decisions for Logistics and Transport Software, *Transport and Telecommunication*, Vol. 11, No 4, 2010, pp. 46–58.

Software architecture design and estimation play the key role for logistics and transport software development process. One of the design approaches is to reuse the architectural patterns, which express a fundamental structural organization of software systems and its behaviour. The usage of the proven and tested solutions allows us to increase the software quality and reduce potential risks.

In this paper, the most suitable architectural patterns are chosen for the typical logistics and transport software. For the evaluation of architectural patterns the metrics such as Functional Points, Coupling and Cohesion are used. Based on these metrics the criterion of efficiency has been obtained, which helps us to evaluate and select the optimal architectural patterns for specified logistics or transport software.

Keywords: software architecture, architectural patterns, logistics and transport software, coupling, cohesion, FP-metrics

Paramonov, Yu., Hauka, M. Reliability of Aircraft and Airline, *Transport and Telecommunication*, Vol. 11, No 4, 2010, pp. 59–65.

The reliability of aircraft (AC) and airline (AL) operation can be ensured by the implementation of a specific inspection program, which can be planned using full-scale fatigue test data and the theory of Markov Chains (MC) and a Semi-Markov process (SMP) with rewards. The process of the operation of aircraft is considered as absorbing MC with $(n+4)$ states. The states $E_1, E_2, ..., E_{n+1}$ correspond to AC operation in time intervals $[t_0, t_1), [t_1, t_2), ..., [t_n, t_{SL})$, where n is an inspection number, t_{SL} is specified life (SL), i.e. AC retirement time. States E_{n+2}, E_{n+3}, and E_{n+4} are absorbing states: AC is withdrawn from service when the SL is reached or fatigue failure (FF) or fatigue crack detection (CD) takes place. In the corresponding matrix for the operation processes of AL the states E_{n+2}, E_{n+3} and E_{n+4} are not absorbing, but correspond to the return of the MC to state E_1 (AL operation returns to first interval). The problem of inspection planning is the choice of the sequence $\{t_1, t_2, ..., t_n, t_{SL}\}$ (in case of equal inspection intervals and fixed t_{SL}, the choice of n)

corresponding to the maximum of airline gain taking into account the limitations imposed by the intensity of AL fatigue failure (or AC failure probability).

This paper considers the case when the parameters of the fatigue crack growth exponential model are known. Numerical examples are given.

Keywords: inspection program, Markov chains, reliability

Tsilker, B., Orlov, S. Computing Efficiency Metrics for Synergic Intelligent Transportation Systems, *Transport and Telecommunication*, Vol. 11, No 4, 2010, pp. 66–74.

Considerable progress in computing and telecommunications opened new approaches for solving of transportation problems, affected in the concept of intelligent transportation systems (ITS). Technically such systems represent a set of interacting computational nodes with various sensors, and can be considered as distributed computer systems. Distributed nature of the ITS implies parallelization of solvable transportation tasks in conjunction with their distributed realization.

Under efficiency of parallelized calculations we presuppose several aspects. Three of them are picked out in the work: calculation speed, efficiency of system scaling, and efficiency of parallel computations as compared to sequential ones. Typical metrics for numerical characterization of parallelized computations form three groups: index of parallelism and speedup (*PI* and *S*), efficiency and utilization (*E* and *U*), redundancy and compression (*R* and *C*).

The main peculiarity of synergic intelligent transportation systems shows up in bulk of intercommunications, substantially affecting the indexes of the system. Present work focuses on influence of these communication overheads on overall efficiency of the synergic ITS.

Keywords: intelligent transportation system, parallelization, distributed systems, efficiency, performance metrics

TRANSPORT and TELECOMMUNICATION, 11.sējums, Nr.4, 2010 (Anotācijas)

Kopitovs, E.A., Pavlovs, A.N., Zelencovs, V.A. Struktūras genoma aprēķina jaunās metodes un komplekso objektu elementu kritiskuma neveiksme. *TRANSPORT and TELECOMMUNICATION,* 11.sēj., Nr.4, 2010, 4.–13. lpp.

Tiek izskatītas divas metodes, analizējot atsevišķu elementu ieguldījumu kompleksa objekta efektivitātē. Pirmais tiek balstīts, ieviešot jaunu vīziju – „struktūras genoms", kas tiek pielietots monotonu un nemonotonu sistēmu strukturāla nozīmīguma aprēķinam. Otra metode ļauj izvērtēt vispārīgāku rādītāju – elementa kritiskuma neveiksmi. Šī metode ir balstīta uz fazi-loģiska nobeiguma kombinētu metodi un uz eksperimentālas plānošanas teorijas metodēm. Komplekso objektu elementu neveiksmes kritiskums tiek izteikts ar vektora īpašību, kuras noteikšanā tiek lietota vesela rinda parciālu rādītāju, kuriem var būt kā kvantitatīvas, tā arī kvalitatīvas īpašības, un to novērtēšanai var tikt lietoti dažādu tipi mērogi. Elementa kritiskuma neveiksmes iznākuma rādītājs tiek parādīts polinoma veidā, kurš izskata gan atsevišķi ņemtu rādītāju ietekmi, gan rādītāju agregācijas (no 2, 3 un vairāk) ietekmi. Polinomu koeficientu aprēķināšana tiek veikta eksperta informācijas apstrādes pamatā un pēc atbilstoša kvantitatīvi vērtēta ar fazi skaitļu palīdzību lingvistiska mainīgā lieluma.

Atslēgvārdi: struktūras genoms, neveiksmes kritiskums, komplekss objekts, multikritēriju analīze, eksperimenta plānošanas teorija, lingvistisks mainīgais lielums

Kraiņukovs, A., Kutevs, V., Opolčenovs, D. Pieeja ierīču ieviešanai ģenētiskajam algoritmam lielceļa pārklājuma zemvirsmas zondēšanas risinājuma inversai problēmai. *TRANSPORT and TELECOMMUNICATION,* 11.sēj., Nr.4, 2010, 14.–28. lpp.

Dotais pētījums ir fokusēts uz pieeju aparatūras ieviešanai ģenētiskajam algoritmam lielceļa pārklājuma zemvirsmas radara zondēšanas risinājuma problēmai. Iteratīvā procedūra, lai risinātu inverso problēmu frekvenču domēnā tiek lietota, balstoties uz mērķa funkcijas minimizāciju. Ģenētiskais algoritms tiek lietots mērķa funkcijas globālā minimuma meklēšanai.

Ģenētiskā algoritma aparatūras ieviešanai ir nepieciešams pareizi izvēlēties argumentu vērtības mērķa funkcijai un ģenētiskā algoritma parametrus. Autori izpētīja divus atšķirīgus mērķa funkciju veidus. Tiek diskutēta ģenētiskā algoritma ierīču ieviešanas iespējas novērtēšana, balstīta uz lauka-programmatisko aizsargbarjeras sakārtojumu.

Atslēgvārdi: lielceļa radara monitorings, inversā problēma, ģenētiskais algoritms, kauka-programmatiskās ierīces, aparatūras ieviešana

Krasņitskis, Ju. A. Dažas zemes jonosfēras viļņvada lēkuma modeļa iezīmes. *TRANSPORT and TELECOMMUNICATION,* 11.sēj., Nr.4, 2010, 29.–35. lpp.

Rakstā tiek izskatīts jautājums par elektromagnētiskā impulsa radiatora izvietojumu no vienas stacijas novērošanas, kas balstīts uz impulsa izplatīšanas lēkuma modeli sfēriskajā viļņvadā "Zeme-jonosfēra". Impulsa īpašības, kā zemes viļņa, tā arī lēkuma (debess) viļņu, no šī viļņvada tiek modelēti kā distances funkcijas no radiācijas avota. Viļņvada parametri, piemēram, attālums no radiatora un efektīvi atstarojoši jonosfēras augstumi, var tikt novērtēti caur viļņu aizkavēšanu, kas atstaroti no jonosfēras, attiecībā uz zemes vilni. Aizkavējumu vērtību kļūdas ir par iemeslu viļņvada parametru kļūdām. Šīs saiknes tiek izskatītas. Tiek parādīts, kā viļņvada parametra kļūdas ir atkarīgas no attālumiem un atstarošanas augstumiem. Tiek piedāvāta metode atkārtoti interpretēt lēkuma modeļa iezīmes, pielietojot ekvivalentu antenas sakārtojuma koncepciju.

Atslēgvārdi: elektromagnētiskā radiācija, jonosfēra, viļņvads, lēkuma modelis, distance, efektīvie augstumi, aizkavēšanas, zibens izlādēšanās, atmosfēras traucējumi

Krebss, V., Ciļkers, B. Pārklājuma novērtēšana sinerģiskajās tīklotajās inteliģentās transportēšanas sistēmās ar ne-izotropiskiem mezgliem. *TRANSPORT and TELECOMMUNICATION,* 11.sēj., Nr.4, 2010, 36.–45. lpp.

Auto ceļojumu drošība ir visvairāk vērā ņemams risināms uzdevums, kas jāsveic inteliģentām transportēšanas sistēmām (ITS). Tas var būt risināts ar savstarpēju mezglu sadarbību, apgādātu ar sensoru veidojošu sensoru tīklu. Bezvadu sensoru tīkli var būt integrēti ITS kā transporta līdzekļi caur transporta līdzeklis-transporta līdzeklim vai infrastruktūra-transporta līdzeklim komunikācijas modeļu veidā ceļu stāvokļa, celtniecības atrašanās vietas vai šķēršļu braukšanas drošības monitoringam un paziņošanai par šādiem ceļiem. Bezvadu sensoru tīkli arī izvirza veselu rindu izaicinājuma optimizācijas problēmas. Pārklājuma problēma bija un paliek fundamentāls jautājums bezvadu tīklu uzbūvē.

Vairākums zināmu pētījumu, kas skar optimālu tīklu mezglu izvēršanu, t.i., ar optimālu tīklu topoloģiju, problēmas izpēti ar pieņēmumu, ka bezvadu tīkla servisa sfēra ir brīva no šķēršļiem, kas traucē normālu informācijas signālu izplatīšanos [1-3].

Dotajā rakstā tiek diskutētas iespējamās pieejas bezvadu tīkla mezglu efektīvai izvietošanai ar nosacījumu, ka servisa lauks satur šķēršļus. Problēma tiek apskatīta no diviem viedokļiem: kā varbūtības uzdevums, kā arī kā skaitļošanas ģeometrijas uzdevums. Varbūtības modelis ir reālāks tāpēc, ka sensora dizains un vides apstākļi ir stohastiski pēc dabas. Iejaukšanās un troksnis vidē var būt modelēti ar stohastiskiem procesiem. Pētījuma rezultātā ir iegūti daži algoritmi un pieņēmumi tuvu optimālam mezglu izvietošanā tīkla servisa zonā ar šķēršļiem.

Atslēgvārdi: inteliģentā transportēšanas sistēma, anizotrops sensors, sensoru tīkls, pārklājums servisa sfēra

Orlovs, S., Višņakovs, A. Modelim piemēroti lēmumi loģistikas un transporta programmatūrai. *TRANSPORT and TELECOMMUNICATION,* 11.sēj., Nr.4, 2010, 46.–58. lpp.

Programmatūras arhitektūras projekts un novērtējums spēlē galveno lomu loģistikas un transporta programmatūras attīstības procesā. Viena no projekta pieejām ir atkārtoti lietot arhitektūras modeļus, kas izsaka programmatūras sistēmas fundamentālu strukturālu organizāciju, kā arī tās uzvedību. Pierādītu un testētu risinājumu lietošana atļauj mums palielināt programmatūras kvalitāti un samazināt potenciālos riskus.

Dotajā rakstā tiek izvēlēti vispiemērotākie arhitektoniskie modeļi tipiskai loģistikas un transporta programmatūrai. Arhitektonisko modeļu novērtēšanai tiek pielietota tāda metrika kā *Functional Points, Coupling* un *Cohesion*. Balstoties uz šīm metrikām, tiek iegūts efektivitātes kritērijs, kas mums palīdz novērtēt un izvēlēties optimālo arhitektonisko modeli specifiskai loģistikas un transporta programmatūrai.

Atslēgvārdi: programmatūras arhitektūra, arhitektoniskie modeļi, loģistikas un transporta programmatūra, savienojums, kohēzija, *FP*-metrika

Paramonovs, J. Hauka, M. Lidaparāta un aviolīnijas drošums. *TRANSPORT and TELECOMMUNICATION,* 11.sēj., Nr.4, 2010, 59.–65. lpp.

Lidaparāta drošums un aviolīnijas darbība var būt garantēta, ieviešot specifisku inspekcijas programmu, kas var būt plānota, lietojot pilna-mēroga noguruma testa datus un Markova ķēžu teoriju, kā arī *Semi*-Markova procesu ar atlīdzību.

Autori rakstā izskata gadījumu, kad eksponenciālā modeļa noguruma plaisas pieauguma parametri ir zināmi. Rakstā tiek doti arī skaitliskie piemēri.

Atslēgvārdi: inspekcijas programma, Markova ķēdes, drošums

Ciļkers, B., Orlovs, S. Efektivitātes metrikas skaitļošana sinerģiskām inteliģentām transporta sistēmām. *TRANSPORT and TELECOMMUNICATION,* 11.sēj., Nr.4, 2010, 66.–74. lpp.

Zināms progress skaitļošanas tehnikā un telekomunikācijās deva iespēju jaunām pieejām transporta problēmu risināšanā, ietekmējot inteliģentās transporta sistēmas (ITS) konceptu.. Tehniski šādas sistēmas pārstāv veselu rindu savstarpēji darbojošamies skaitļošanas mezglus ar dažādiem sensoriem un var tikt uzskatīti kā distributīvas skaitļošanas sistēmas. Distributīvs raksturs, kas piemīt ITS, diktē risināmo transportēšanas uzdevumu attēlošanu kā paralēlo plūsmu kopumu un šo plūsmu dalīto realizāciju.

Ar paralēlo aprēķinu efektivitāti mēs iepriekš pieņemam dažus aspektus. Trīs no tiek ir izcelti dotajā darbā: skaitļošanas ātrums, sistēmas mērogošanas efektivitāte, paralēlās skaitļošanas efektivitāte salīdzinājumā ar sekojošām.

Sinerģiskās inteliģentās transportēšanas galvenā īpatnība parādās savstarpējās komunikācijas apjomā, pamatīgi ietekmējot sistēmas indeksus. Dotais darbs fokusējas uz šo komunikāciju virstēriņiem pār vispārējo sinerģiskās ITS efektivitāti.

Atslēgvārdi: inteliģentās transportēšanas sistēmas, paralēlisms, sadalītās sistēmas, efektivitāte, izpildes metrika

TRANSPORT & TELECOMMUNICATION

ISSN 1407-6160 & ISSN 1407-6179 (on-line)

All articles are reviewed.
Articles can be presented in the journal in English.

EDITORIAL CORRESPONDENCE

Transporta un sakaru institūts (Transport and Telecommunication Institute)
Lomonosova iela 1, LV-1019, Riga, Latvia. Phone: (+371)67100594. Fax: (+371)67100535.
E-mail: kiv@tsi.lv, http:// www.tsi.lv

TRANSPORT and TELECOMMUNICATION, 2010, Vol. 11, No 4
ISSN 1407-6160
The journal of Transport and Telecommunication Institute (Riga, Latvia).
The journal is being published since 2000.

The papers published in Journal "Transport and Telecommunication" are included in **SCOPUS** (since 2008, Vol. 9, No 1), **Elsevier Database**
www.info.scopus.com
www.elsevier.com

PREPARATION OF CAMERA-READY TYPESCRIPT: COMPUTER MODELLING AND NEW TECHNOLOGIES

1. In order to format your manuscript correctly, see the Page Layout Guideline for A4 (21 cm x 29,7 cm) paper size. Page Layout should be as follows: Top – 3 cm, Bottom – 3 cm, Left – 3 cm, Right – 3 cm.
2. Maximum length for the article is **10 pages**.
3. **Using of other Styles with the exception of Normal is not to be allowed!**
4. ***Articles*** should be Times New Roman typeface, single-spaced.
5. The article should include:
   - title;
   - author's name(s) and information (institution, city, country, the present address, phones, and e-mail addresses);
   - abstract (100-150 words);
   - keywords (max. 6);
   - introduction – clear explanation of the essence of the problem, previous work, purpose of the research and contribution;
   - description of the research;
   - conclusion section (this is mandatory) – should clearly indicate on the advantages, limitations and possible applications;
   - references.

   Attention! First name, last name, the title of the article, abstract and keywords must be submitted in the English and Latvian languages (in Latvian it is only for Latvian authors) as well as in the language of the original (when an article is written in different language).
6. The text should be in clear, concise English (or other declared language). Please be consistent in punctuation, abbreviations, spelling (***British English***), headings and the style of referencing.
7. ***The title of the article*** – 14 point, UPPERCASE, style Bold and centred.
8. ***Author's names*** – centred, type size 12 point, Upper and lower case, style Bold Italic.
9. ***Author's information*** – 10 point, Upper and lower case, style Italic, centred.
10. ***Abstract and keywords*** – 8 point size, style Normal, alignment Justify.
11. ***The first level Headings*** – 11 point, Upper and lower case, style Bold, alignment Left. Use one line space before the first level Heading and one line space after the first level Heading.
12. ***The second level Headings*** – 10 point, Upper and lower case, style Bold, alignment Left. One line space should be used before the second level Heading and 1/2 line space after the second level Heading.
13. ***The third level Headings*** – 10 point, Upper and lower case, style Italic, alignment Left. One line space should be used before the second level Heading and 1/2 line space after the third level Heading.
14. ***Text*** of the article – 10 point, single-spaced, alignment Justify.
15. The set of ***formulas*** on application of fonts, signs and a way of design should be uniform throughout the text. The set of formulas is carried out with use of editors of formulas MS Equation 3.0 or MathType. The formula with a number – the formula itself should be located on the left edge of the text, but a number – on the right one. Font sizes for equations are the following: 11pt – full, 7pt – subscripts/superscripts, 5pt – sub- subscripts/superscripts, 16pt – symbols, 11pt – subsymbols.
16. All ***Figures*** – must be centred. Figure number and caption always appear below the Figure, type size 8 point.

Figure 1. This is figure caption

Diagrams, Figures and Photographs – must be of high quality, in format *.TIFF, *.JPG, *.BMP with resolution not less than 300 dpi. Also formats *.CDR, *.PSD are possible. Combination of Figures in format, for instance, *.TIFF with elements of the in-built Figure Editor in MS Word is prohibited.

17. ***Table Number and Title*** – always appear above the Table. Alignment Left. Type size 8 point. Use one line space before the Table Title, one line space after the Table Title and 1/2 line space after the Table.

Table 1. This is an example of a Table

Heading	**Heading**	**Heading**
Text	Text	Text
Text	Text	Text

18. ***References*** in the text should be indicated by a number in square brackets, e.g. [1].
References should be numbered in the order cited in the manuscript. The correct format for references is the following:

*Article***:** author, title, journal (in italics), volume and issue number, year, inclusive pages
Example: 1. Amrahamsson M., Wandel S. A Model of Tearing in Third – Party Logistics with a Service Parts Distribution Case Study, *Transport Logistics*, Vol. 1, No 3, 1998, pp. 181-194.

*Book***:** author, title (in Italics), location of publishers, publishers, year, whole pages
Example: 2. Kayston M. and Fried W. R. *Avionic Navigation Systems.* New York: John Wiley and Sons Inc, 1969. 356 p.

Conference Proceedings: author; title of an article; proceedings (in italics); title of a conference, date and place of a conference; publishing house, year, concrete pages
Example: 3. Canales Romero J. A First Step to Consolidate the European Association of Aerospace Students in Latvia (Presented by the Munich Local Group). In: *Research and Technology – Step into the Future: Programme and Abstracts. Research and Academic Conference, Riga, Latvia, April 7–11, 2003, Transport and Telecommunication Institute.* Riga: TTI, 2003, p. 20.

19. ***Authors Index***
Editors form the author's index of a whole Volume. Thus, all contributors are expected to present personal colour photos with the short information on the education, scientific titles and activities.
20. ***Acknowledgements***
Acknowledgements (if present) mention some specialists, grants and foundations connected with the presented paper. The first page of the contribution should start on page 1 (right-hand, upper, without computer page numbering). Please paginate the contributions, in the order they are to be published. Use simple pencil only.
21. **Articles poorly produced or incorrectly formatted may not be included in the proceedings**.